Journal for ImmunoTherapy of Cancer

Immunosuppressive lncRNA LINC00624 promotes tumor progression and therapy resistance through ADAR1 stabilization

Qi Zhang,[1,2] Bingqiu Xiu,[1,2] Liyi Zhang,[1,2] Ming Chen,[1,2] Weiru Chi,[1,2] Lun Li,[1,3] Rong Guo,[1,4] Jingyan Xue,[1,2] Benlong Yang,[1] Xiaoyan Huang,[1] Zhi-Ming Shao,[1,2] Shenglin Huang,[2,5] Yayun Chi,[1,2] Jiong Wu [1,2,6]

To cite: Zhang Q, Xiu B, Zhang L, *et al*. Immunosuppressive lncRNA LINC00624 promotes tumor progression and therapy resistance through ADAR1 stabilization. *Journal for ImmunoTherapy of Cancer* 2022;**10**:e004666. doi:10.1136/jitc-2022-004666

► Additional supplemental material is published online only. To view, please visit the journal online (http://dx.doi.org/10.1136/jitc-2022-004666).

QZ, BX, LZ and MC contributed equally.

Accepted 22 September 2022

For numbered affiliations see end of article.

Correspondence to
Professor Jiong Wu;
wujiong1122@vip.sina.com

Professor Yayun Chi;
yychi@126.com

Dr Bingqiu Xiu;
oswaldshiu@gmail.com

ABSTRACT

Background Despite the success of HER2-targeted therapy in achieving prolonged survival in approximately 50% of treated individuals, treatment resistance is still an important challenge for HER2+ breast cancer (BC) patients. The influence of both adaptive and innate immune responses on the therapeutic outcomes of HER2+BC patients has been extensively demonstrated.

Methods Long non-coding RNAs expressed in non-pathological complete response (pCR) HER2 positive BC were screened and validated by RNA-seq. Survival analysis were made by Kaplan-Meier method. Cell death assay and proliferation assay were performed to confirm the phenotype of LINC00624. RT-qPCR and western blot were used to assay the IFN response. Xenograft mouse model were used for in vivo confirmation of anti-neu treatment resistance. RNA pull-down and immunoblot were used to confirm the interaction of ADAR1 and LINC00624. ADAR1 recombinant protein were purified from baculovirus expression system. B16-OVA cells were used to study antigen presentation both in vitro and in vivo. Flow cytometry was used to determine the tumor infiltrated immune cells of xenograft model. Antisense oligonucleotides (ASOs) were used for in vivo treatment.

Results In this study, we found that LINC00624 blocked the antitumor effect of HER2- targeted therapy both in vitro and in vivo by inhibiting type I interferon (IFN) pathway activation. The double-stranded RNA-like structure of LINC00624 can bind and be edited by the adenosine (A) to inosine (I) RNA-editing enzyme adenosine deaminase RNA specific 1 (ADAR1), and this editing has been shown to release the growth inhibition and attenuate the innate immune response caused by the IFN response. Notably, LINC00624 promoted the stabilization of ADAR1 by inhibiting its ubiquitination-induced degradation triggered by β-TrCP. In contrast, LINC00624 inhibited major histocompatibility complex (MHC) class I antigen presentation and limited CD8+T cell infiltration in the cancer microenvironment, resulting in immune checkpoint blockade inhibition and anti-HER2 treatment resistance mediated through ADAR1.

Conclusions In summary, these results suggest that LINC00624 is a cancer immunosuppressive lncRNA and targeting LINC00624 through ASOs in tumors expressing high levels of LINC00624 has great therapeutic potential in future clinical applications.

WHAT IS ALREADY KNOWN ON THIS TOPIC

⇒ The efficacy of antitumor treatment relies on IFN response. ADAR1 inhibits the overactivation of double-stranded RNA sensors such as RIG-I and MDA5, therefore mitigate the alert system and thus shape a 'cold' tumor microenvironment.

WHAT THIS STUDY ADDS

⇒ We found an immunosuppressive lncRNA LINC00624 restrains the activation of IFN pathway through stabilizing ADAR1. LINC00624 also relies on the A-to-I RNA editing ability of ADAR1 to inhibit MHC class I antigen presentation and limited CD8+T cell infiltration in the cancer microenvironment, resulting in immune checkpoint blockade inhibition and anti-HER2 treatment resistance.

HOW THIS STUDY MIGHT AFFECT RESEARCH, PRACTICE OR POLICY

⇒ LINC00624 could be a biomarker for anti-HER2 and immune therapy. Targeting LINC00624 through antisense oligonucleotides could show great therapeutic potential for future clinical use.

INTRODUCTION

The human innate immune system has evolved a well-designed mechanism for providing the first line of defense against viral infection. When viral double-stranded RNAs (dsRNAs) are sensed by cytosolic pattern recognition receptors, such as RIG-I and MDA5,[1] IFNs are secreted by most human cells, and they trigger the expression of IFN stimulated genes (ISGs). ISGs stimulate antigen presentation pathways, which lead to the recruitment of immune cells and facilitate antiviral responses.[1 2] In addition, immune systems are well adapted to avoid eliciting damage in normal tissue[3 4] when mistranscribed RNAs are expressed by cells or released after physiological cell death.[5] Tumors can evade T cell-mediated antitumor immunity by decreasing

IFN or MHC class I antigen induction triggered by the dsRNA or cytoplasmic DNA products of aberrant transcription or mitosis.[6 7] Therefore, the efficacy of antitumor treatment also relies on autonomous autocrine of type I IFN in tumor cells.[8] In addition to traditional cytotoxic drugs, tyrosine kinase inhibitors (TKIs) and humanized antibodies can enhance type I IFN and antigen presentation pathway activation.[9–11] Therefore, the regulation of the innate immune response is critical for therapeutic efficacy in breast cancer (BC).

Adenosine deaminase RNA specific 1 (ADAR1) is a regulator of the innate immune response. ADAR1 catalyzes the conversion of adenosine (A) to inosine (I) in a dsRNA substrate and destroys the dsRNA structure, and therefore, ADAR1 inhibits the overactivation of dsRNA sensors such as RIG-I and MDA5.[7 12 13] The involvement of ADAR1 RNA-editing in cancer development and immune therapy failure has been established.[7 12 13] Loss of ADAR1 in melanoma promotes antigen presentation and reverses cellular resistance to immune checkpoint blockade.[14] Therefore, ADAR1 can mitigate the alert system and thus shape a 'cold' tumor microenvironment.

Human epidermal growth factor receptor 2 (HER2, also known as ErbB-2 or Neu) is an oncogene overexpressed in 20%–30% of BCs.[15] Humanized monoclonal antibodies such as trastuzumab and TKIs such as lapatinib can prolong the survival of BC patients. However, treatment resistance is still an important issue for at least 50% of patients.[16 17] It has been reported that HER2 suppresses the innate immune response and antitumor immunity.[9 11] BC cell lines from transgenic mice expressing HER2 express low levels of MHC class I antigens.[18] Blocking IFN receptor 1 (IFNAR1) weakens the therapeutic efficacy of anti-HER2 monoclonal antibodies.[19] Interestingly, HER2-positive (HER2+) BC patients with higher ISG scores or more tumor-infiltrating lymphocytes have a better outcome after anti-HER2 treatment.[20 21] These findings suggest that the activation of the innate immune response, particularly with respect to IFNs and the antigen presentation pathway, can enhance HER2+BC treatment, and the underlying mechanisms should be further clarified.

To discover new regulators that can affect HER2+BC treatment outcomes, we focused on long non-coding RNAs (lncRNAs), which might be involved in disease progression and therapeutic resistance. We compared lncRNA expression in tumors before neoadjuvant chemotherapy between HER2+BC patients in the pathological complete response (pCR) and non-pCR groups and found that LINC00624 was enriched in the non-pCR group. Overexpression of LINC00624 inhibited the IFN-related innate immune response and MHC class I antigen presentation, which subsequently induced cancer cell proliferation and blocked the antitumor effect of lapatinib and trastuzumab. We found that the ADAR1 Editing Region (AER) of LINC00624 could be edited in which adenosine was modified to inosine by ADAR. The edited LINC00624 stabilized ADAR1 and further suppressed the IFN induced expression of ISGs. Our data support the supposition that LINC00624 plays a critical role in ADAR regulation and may serve as an antitumor target in future BC combination treatments.

METHODS

Detailed methods have been described in online supplemental files.

RESULTS

LINC00624 promotes treatment resistance in HER2+ BC

To screen for lncRNAs involved in the modulation of the HER2-targeted treatment response, 20 core needle biopsy specimens taken from primary tumors in patients with HER2+BC before neoadjuvant therapy were retrospectively collected and subjected to RNA sequencing. The cohort was classified into the pCR and non-pCR groups based on the outcomes determined on pathological evaluation. We analyzed the expression profiles and found that LINC00624 was the most significantly increased long non-coding gene in the non-pCR group after the exclusion of pseudogenes (figure 1A,B). When the sample size was expanded to 100, LINC00624 was still significantly higher in non-pCR group (figure 1C). To further determine the potential function of LINC00624 in BC pathogenesis, we analyzed two independent clinical patient datasets. In early-stage BC patient samples in The Cancer Genome Atlas database and a cohort of 319 RNA samples in our center, high LINC00624 expression was significantly correlated with poor disease-free survival and overall survival (figure 1D, online supplemental figure 1B, and online supplemental tables 1 and 2). Among the patients characterized by molecular subtype, patients with HER2+or luminal A BC with high LINC00624 expression showed worse outcomes than those with low LINC00624 expression (figure 1D, online supplemental figure 1A, B), suggesting that LINC00624 may be involved in the progression of BC. Based on the expression difference in the HER2+BC pCR and non-pCR groups, we focused on the role of LINC00624 in HER2+BC.

To further characterize LINC00624, rapid amplification of cDNA ends was performed to obtain the full-length sequence of LINC00624. We found that LINC00624 was transcribed from chromosome 1q21.1-1q21.2 as four isoforms, all of which carrying intergenic regions between BCL9 and CHD1L in BC cell lines (online supplemental file 1). In contrast to full-length isoform 1, isoform-specific internal deletions in exon 4 were found in isoforms 2, 3, and 4 (online supplemental figure 1C,D). However, we did not observe the 3088 nt transcript (RefSeq Accession: NR_038423) annotated in the National Center for Bioinformation database; the 3088 nt sequence overlaps with the CHD1L gene locus. Full-length isoform 1 (RefSeq Accession: NR_038423) was the most abundant among all isoforms, and the other three isoforms were expressed in low abundance in the examined BC cell lines (online

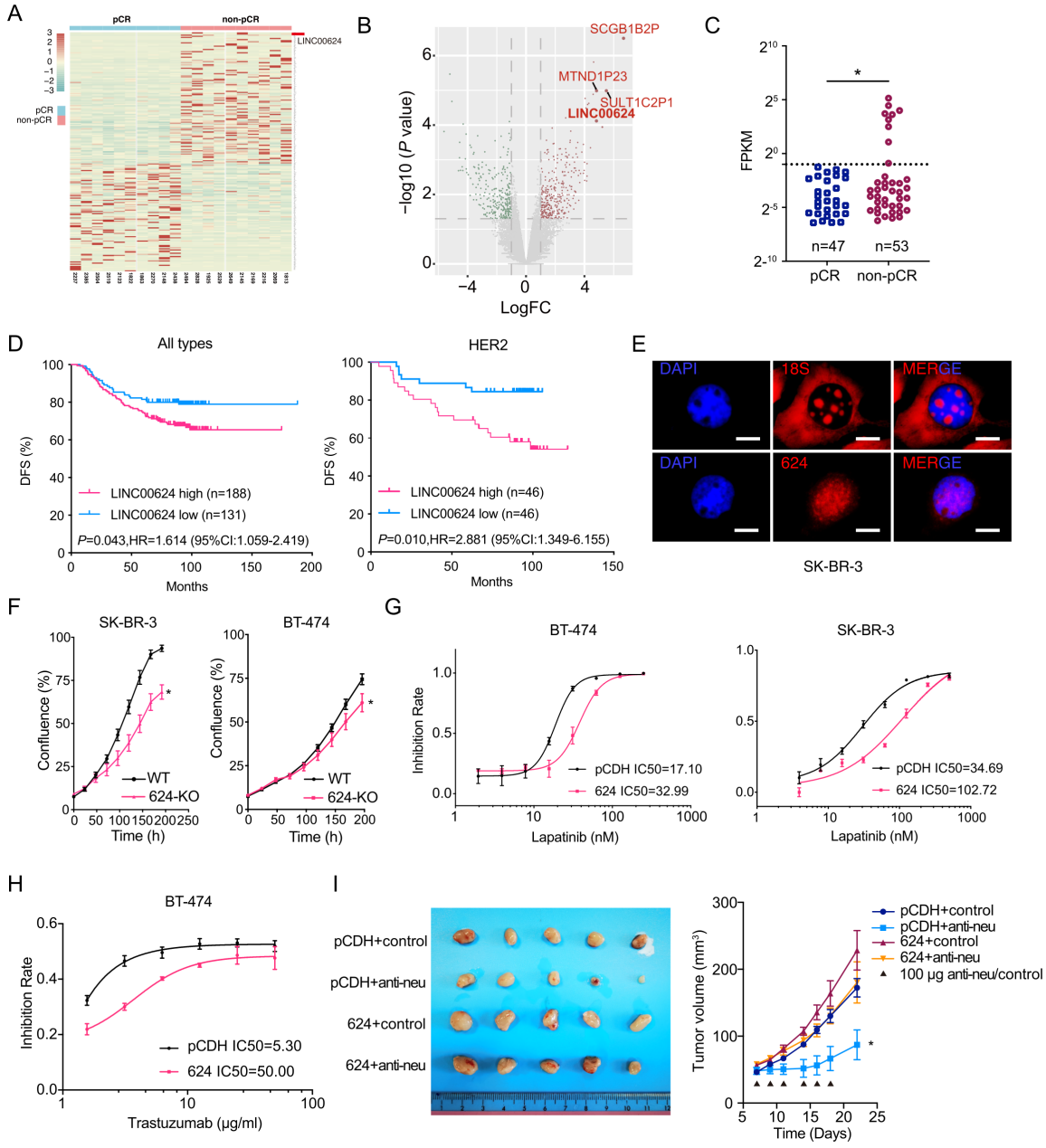

Figure 1 LINC00624 promotes treatment resistance in HER2+BC. (A) HER2+BC patients core needle biopsy specimen before neoadjuvant treatment were divided into pCR (n=10) and non-pCR (n=10) groups according to pathology evaluation after surgery. The heatmap summarizes differentially expressed RNAs between pCR and non-pCR group. (B) The volcano plots showed the fold changes (FC) and p values in non-pCR tumors versus pCR tumors. The most differentially expressed lncRNAs were shown. (C) Fragments per kb of transcript per million mapped reads (FPKM) of LINC00624 in HER2+BC neoadjuvant treatment cohort. Patients were divided in to pCR or non-pCR group according to the pathological evaluation after surgery. The expression of LINC00624 were divided into high or low expression group with the cut-off value FPKM=0.5, separated by the dotted line. Statistical analysis was performed using Fisher's exact tests. (D) Disease-free survival (DFS) plot of BC patients in a consecutive cohort receiving adjuvant treatment. Patients were divided into high and low LINC00624 groups according to RNA expression in the primary tumor. Statistical analysis was performed using two-sided log-rank tests. Left, all the molecular subtypes were pooled and shown. Right, HER2 enrichment subtype were shown. (E) RNA FISH with LINC00624 probe showed LINC00624 was mainly located in the cell nucleus of SK-BR-3 cells. Cell nucleus was stained with DAPI. 18S RNA was probed as positive control. (F) Cell proliferation assay of WT and LINC00624 KO cells in SK-BR-3 and BT-474 cells. n=6 for each time point. Statistical analysis was performed using two-sided t-test at the end point. (G) Inhibition rate of WT and LINC00624 KO SK-BR-3 and BT-474 cells in response to lapatinib. (H) Inhibition rate of pCDH and LINC00624 overexpression BT-474 cells in response to trastuzumab. (I) Tumor growth curve and tumor size of BT-474 pCDH or LINC00624 cells receiving anti-neu or isotype control in nude mice. n=5 animals in each group. Statistical analysis was performed using two-sided t-test for the tumor volume at the end point. *p<0.05. All data are mean±SE. (F–H) n=3 biological independent samples, similar results were obtained from two more independent experiments. BC, breast cancer; FISH, fluorescence in situ hybridization; KO, knockout; pCR, pathological complete response; WT, wild type.

supplemental figure 1E). According to phylogenetic codon substitution frequencies and Coding Potential Assessing Tool,[22 23] LINC00624 showed no coding ability (online supplemental figure 1F,G).

Fluorescence in situ hybridization assays showed that LINC00624 was mainly located in the cell nucleus of HER2+BC cell lines (figure 1E). Cytoplasmic and nuclear RNA purification also confirmed that the four isoforms were mainly located in the cell nucleus (online supplemental figure 2A). The BT-474 and SK-BR-3 ectopic overexpression cell lines were constructed with isoform 1 of LINC00624 by lentiviral infection, and knockout (KO) cells were generated by using CRISPR-cas9 to delete part of the promoter region and exons 1–2, which abolished the expression of all the isoforms (online supplemental figure 2B,C).

To illustrate the biological function of LINC00624, we found overexpressed LINC00624 accelerated cell growth (figure 1F and online supplemental figure 2D). Furthermore, cells with LINC00624 overexpression were resistant to lapatinib and trastuzumab treatment (figure 1G,H), while KO cells were more sensitive (online supplemental figure 2E). We also employed a BT-474 xenograft tumor model to evaluate the oncogenic functions of LINC00624 in vivo. We found LINC00624 promoted tumor growth and the resistantance to anti-HER2/neu treatment (figure 1I). In summary, these data suggest that LINC00624 may promote the treatment resistance of HER2+BC.

LINC00624 inhibits the innate immune response by inhibiting type I IFN signaling

To further investigate the mechanism involved in LINC00624 signaling in BC, we performed RNA-seq with pCDH/LINC00624-expressing cells and WT/LINC00624-KO cells and analyzed candidate genes and pathways regulated by LINC00624. Interestingly, we found that LINC00624 expression was negatively correlated with the interferon α response, TNFα via NF-κB, and the innate immune response (figure 2A), and hallmarks related to IFN pathways were enriched in LINC00624-KO cells (online supplemental figure 3A), implying a role for LINC00624 in regulating the type I IFN response and antigen presentation. Then, we analyzed the involvement of LINC00624 in immune reactions with ImmLnc, a public database used for investigating the immune-related function of lncRNAs.[24] In this analysis, LINC00624 exhibited a strong negative correlation with antigen processing and presentation (figure 2B). Consistently, RT-qPCR detection also showed the induction of ISGs by IFNα was increased significantly in LINC00624-KO SK-BR-3 cells, as well as MHC class I pathway-related genes (figure 2C). Then, we used polyinosinic:polycytidylic acid (poly(I:C)), a synthetic analog of dsRNA that can activate cytosolic RNA sensors to stimulate inflammatory signaling pathways.[25] We found that LINC00624 inhibited the induction of ISGs by dsRNAs (figure 2C, online supplemental figure 3B), and the phosphorylation of STAT1 was inhibited on LINC00624 overexpression (online supplemental figure 3C). Then, we evaluated the signaling pathway in the dsRNA-triggered IFN response. We found that the phosphorylation of TBK1/IRF3/STAT1 was increased in LINC00624-KO cells (figure 2D). A previous study has reported that the type I IFN-generated antiviral response causes cell growth arrest and apoptosis.[3] We found that overexpression of LINC00624 attenuated the cell apoptosis caused by the stimulation of dsRNA sensors (figure 2E, online supplemental figure 3D,E). Thus, we believe LINC00624 is a potential immunosuppressive lncRNA. Furthermore, treatment with poly(I:C) or IFNα induced the expression of LINC00624 (online supplemental figure 3F), indicating that LINC00624 is an ISG and can serve as a negative feedback regulator in the IFN signaling pathway.

Previous studies have reported that HER2 amplification leads to the impairment of IFN pathway activation and antitumor immune responses through inhibition of TBK1 phosphorylation.[9] Moreover, HER-2/neu overexpression is associated with a reduction in MHC class I molecules at the cell surface, possibly induced through IFN response inhibition.[18 26] In our study, treatment with the anti-HER2 antibody trastuzumab markedly induced ISG and antigen presentation-related gene expression in a HER2-driven BC cell line while has little effect in HER2 negative cell lines (online supplemental figure 3G,H). In addition, the LINC00624 level was increased (online supplemental figure 3H), suggesting that LINC00624 was possibly elevated by treatment-induced IFN activation. To determine whether LINC00624 could inhibit the induction of the type I IFN response after anti-HER2 treatment, we compared the expression of ISGs and antigen presentation-related genes after trastuzumab treatment of wild-type and LINC00624-KO cells. In the LINC00624-depleted cells, the number of ISG transcripts increased significantly in response to HER2 blockade compared with that in the wild-type cells (figure 2F,G). These results indicate that LINC00624 inhibits the anti-HER2-induced cell inflammatory response, which further contributes to treatment resistance.

LINC00624 is bound to and edited by ADAR1

To understand the underlying mechanism of LINC00624 in innate immune response blockade, we performed an RNA pull-down assay to explore its potential protein partners (figure 3A). We found that LINC00624 bound several RNA-binding proteins (online supplemental table 3). Among them, ADAR1, an A-to-I RNA-editing protein that can inhibit the innate immune response and is related to type I IFN response regulation, attracted our attention. ADAR1 has two isoforms: the longer ADAR1 p150 is expressed from an interferon (IFN)-inducible promoter and both nuclear and cytoplasmic, while the shorter p110 is constitutively expressed and mainly nuclear. The p110 could be translated from an alternative ATG start codon within the transcript of p150.[12 27] We first confirmed the interaction between ADAR1 and LINC00624 (online

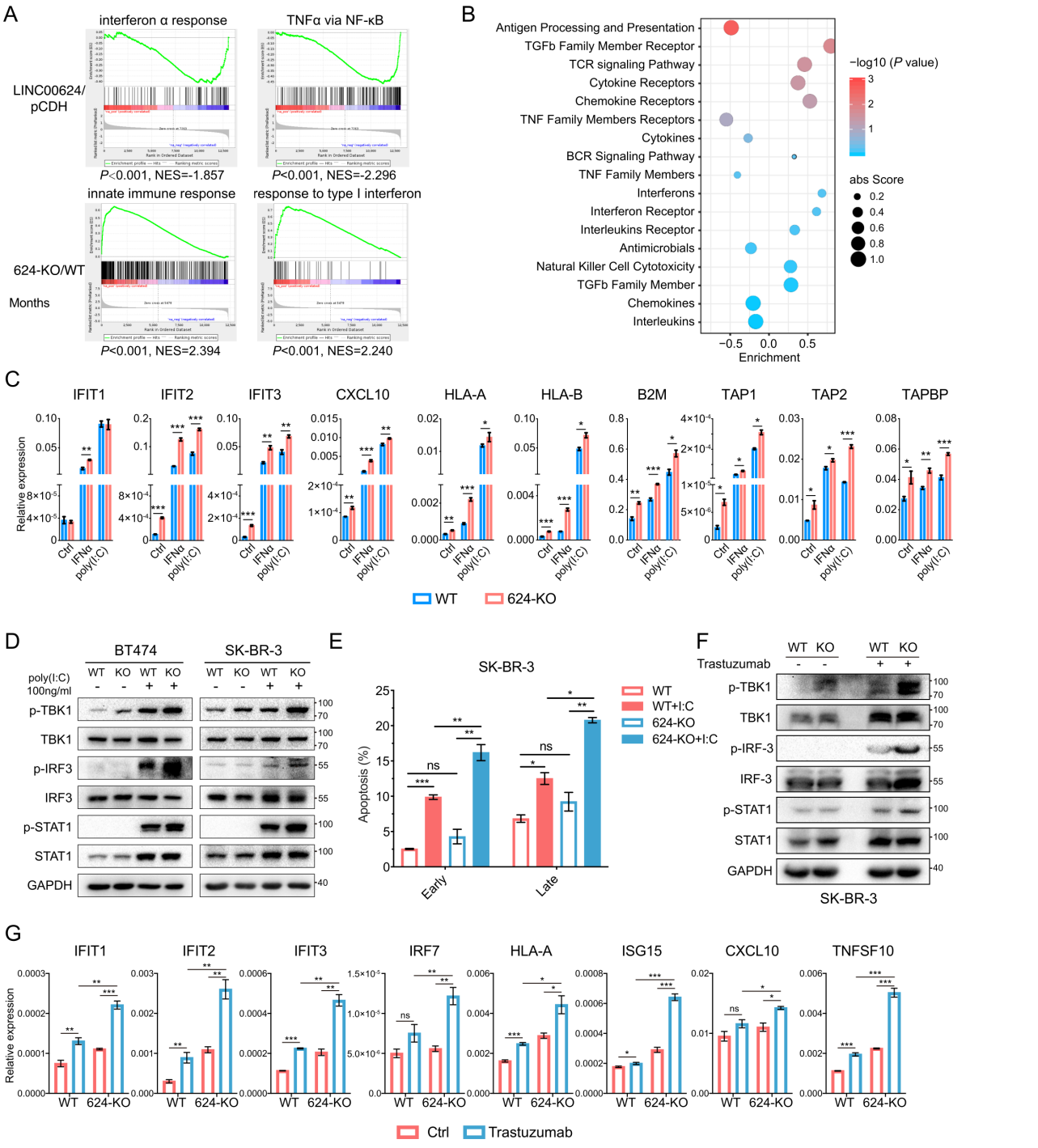

Figure 2 LINC00624 inhibits the innate immune response by inhibiting type I IFN signaling. (A) GSEA analysis showed the indicated gene signatures in different LINC00624 expression SK-BR-3 cells. Top, LINC00624 overexpression versus pCDH; Bottom, LINC00624-KO vs WT. (B) LINC00624 related immune pathways were analyzed by ImmLnc Database. Enrichment score and p value were used for graphing. (C) WT or LINC00624-KO BT-474 cells were treated with 5 ng/mL IFNα for 4 hours or transfected poly(I:C) for 24 hours. RNA levels of ISGs and antigen presentation related genes were analyzed by RT-qPCR. GAPDH was used as reference gene. (D) WT or LINC00624 KO cells were treated with transfected poly(I:C) for 24 hours with indicated concentration. The levels of the indicated proteins were determined by immunoblot. The experiment was performed twice with similar results. (E) The percentage of early and late apoptosis were determined after 1 µg/mL transfected poly(I:C) in SK-BR-3 WT and LINC00624-KO cells. Statistical analysis was performed using two-sided t-test. (F, G) WT or LINC00624-KO SK-BR-3 cells were treated with 20 µg/mL trastuzumab for 3 days. (F) The levels of the indicated proteins were determined by immunoblot. The experiment was performed twice with similar results. (G) RNA levels of ISGs and antigen presentation related genes were analyzed by RT-qPCR. GAPDH antibodies were used as reference gene. (C, E, G) n=3 biological independent samples. Statistical analyses were performed using two-sided t-test. *p<0.05, **p<0.01, ***p<0.001. Data are shown as mean±SE. GSEA, Gene Set Enrichment Analysis; ISGs, IFN stimulated genes; NES, Normalized Enrichment Score; KO, knockout; WT, wild type.

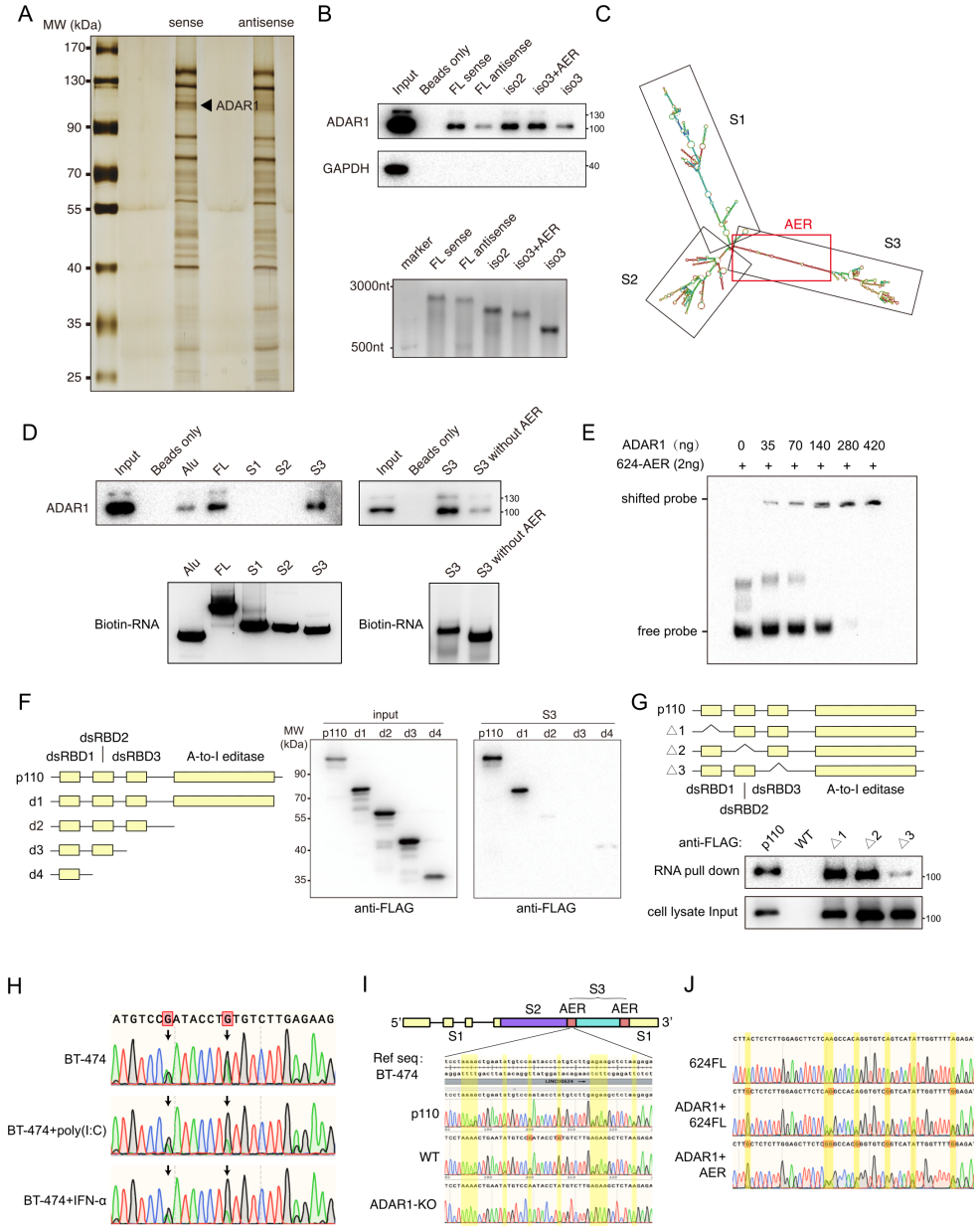

Figure 3 LINC00624 is bound to and edited by ADAR1. (A) Silver staining of RNA pull-down proteins followed by SDS-PAGE. Biotin-labeled LINC00624 sense and antisense full-length (FL) RNA were incubated with SK-BR-3 whole cell lysates. ADAR1 was identified a specific band. (B) RNA pull-down assay with FL LINC00624 sense, antisense, iso 2 of LINC00624 (iso2), isoform3 with additional AER region (iso3+AER), and isoform 3 only (iso3) biotin labeled RNAs in 293T cells. Top, immunoblot of ADAR1 and GAPDH antibodies were shown. Bottom, the input RNAs was confirmed by electrophoresis. The experiment was performed twice with similar results. (C) Predicted secondary structure of full length LINC00624 by RNAfold Web server. Three segments were truncated and annotated as S1, S2 and S3. The AER region was in S3. (D) Left, RNA pull-down assay was performed with Alu (a positive control that ADAR1 bound cloned from an Alu located in PHACTR4), LINC00624 FL, and the three segments. Right, S3, and S3 without AER (S3-AER) biotin labeled RNA was used. Immunoblot of ADAR1 was shown on the top. The input RNAs were confirmed by electrophoresis. The experiment was performed twice with similar results. (E) RNA electrophoretic mobility shift assay (EMSA) was performed with recombinant ADAR1 and in vitro transcribed biotin labeled AER sequence was used. (F) Left, Schematic view of ADAR1 p110 truncations with 3xFLAG tag used for RNA pull-down with S3 biotin labeled RNA. Right, Immunoblot of FLAG. Input of cell lysates expressing ADAR1 p110 truncations and RNA pull-down elutes were immunoblotted by FLAG antibody. (G) RNA pull-down of ADAR1 p110 truncations with S3 biotin labeled RNA. Up, Schematic view of ADAR p110 truncations with dsRBDs deletion. Down, Immunoblot of FLAG. Input of cell lysates expressing ADAR1 truncations and RNA pull-down elutes were shown. (H, I) LINC00624 AER was edited by ADAR1 in vivo. (H) AER was A-to-I edited in BT-474 cells. The editing ratio was increased after poly(I:C) treatment for 24 hours or IFNα treatment for 4 hours. (I) Up, schematic view of LINC00624 region domain. Down, Sanger sequencing data of AER region were shown. ADAR1 p110 overexpressed, WT, and ADAR1-KO cells of BT-474 were compared. (J) Recombinant ADAR1 could edit in vitro transcribed (IVT) LINC00624. Recombinant ADAR1 was incubated with IVT LINC00624 FL or AER. Sanger sequencing results were shown. For (A, B, D–J, the experiment was performed twice with similar results. dsRBD, double-stranded RNA-binding domains.

supplemental figure 4A). As the expression of p150 isoform is relatively low under normal conditions, we found LINC00624 mainly binds p110 in BC cells. It has been reported that ADAR1 is a major RNA editor, catalyzing the deamination of A to generate I, which is prevalent across the whole transcriptome.[13] By disrupting the secondary structure of self-generated or virus-produced dsRNAs through RNA editing, ADAR1 hinders the innate immune response, especially the type I IFN pathway-related response, which is activated by multiple RNA sensors in the presence of dsRNAs.[13 28] Therefore, we speculated that the interaction between ADAR1 and LINC00624 might contribute to tumor progression and innate immune response repression.

Next, we investigated the binding affinity between ADAR1 and different isoforms of LINC00624. Isoform 1 and isoform 2 showed a high affinity for ADAR1, while isoform 3 negligibly bound ADAR1, which suggested that isoform 3 missed a structure critical for LINC00624 and ADAR1 binding (figure 3B). To further elaborate the ADAR1-binding sequence on LINC00624, we employed the RNAfold tool to predict the secondary structure of LINC00624.[29] We found a folded dsRNA-like structure (an AER) transcribed from inverted repeats on both sides of the S3 segment of LINC00624 (figure 3C); this fragment in full-length LINC00624 was absent in isoform 3. Then, we truncated LINC00624 according to its secondary structure and found that only S3 binds ADAR1 in human BC cells, and that the AER region-deletion mutation in S3 caused isoform 3 to lose its ADAR1-binding ability, suggesting that the AER region is the major domain contributing to ADAR1 binding (figure 3D). This hypothesis was confirmed through RNA electrophoretic mobility shift assay showing that the AER domain was shifted after incubation with recombinant ADAR1 protein (figure 3E and online supplemental figure 4B).

As reported, ADAR1 contains three dsRNA-binding domains (dsRBDs) that are involved in RNA binding under different circumstances (figure 3F).[30 31] The A-to-I editase is located in the C-terminus and is the functional group for RNA editing.[13 30–32] Therefore, we truncated the three dsRBDs and editase separately to map the ADAR1 domains involved in LINC00624 binding. The RNA pull-down assay showed that dsRBD3 of ADAR1 was essential to ADAR1 interaction with LINC00624 (figure 3G). As dsRBD3 domain is shared between ADAR1 p110 and p150,[13] LINC00624 could be bound by both of the isoforms. As previously reported, the KKxxK motif in the dsRBD region is critical for dsRNA binding.[33] We mutated KKxxK to EExxA in dsRBD3. Consistently, LINC00624 failed to bind the ADAR1 mutant with EExxA in dsRBD3 (online supplemental figure 4C).

As A-to-I RNA editing can be catalyzed by ADAR enzymes, which converted 'A's in dsRNA structures into 'I's via hydrolytic deamination, we asked whether LINC00624 could be edited by ADAR1. As expected, we found that the AER structure of LINC00624, which was bound by ADAR1, was edited in BC cell lines, and the portion that was edited was further increased after poly(I:C) or IFNα treatment (figure 3H). This finding was consistent with observations of BC tissues (online supplemental figure 4D). In addition, the frequency of AER region editing events was reduced in ADAR1-KO BT-474 cells, confirming that ADAR1 is the major editase involved in LINC00624 A-to-I substitution (figure 3I). This discovery also explained the multiple inconsistent A-to-G mutations found in the cDNA of LINC00624 when we cloned LINC00624 extracted from human cell lines. To confirm the A-to-I editing ability of ADAR1 on LINC00624, we incubated recombinant ADAR1 with transcribed LINC00624 in vitro. The AER region was also edited at the same sites as those in the regions examined in vivo (figure 3J). These data demonstrated that LINC00624 could be bound and edited by ADAR1.

LINC00624 promotes ADAR1 stabilization

As LINC00624 interacted with ADAR1, we hypothesized that LINC00624 might affect ADAR1 function. First, to determine whether the RNA-editing events of ADAR1 were affected by LINC00624 in BC cells, the Alu-Editing Index (AEI) score, a normalized measure based on hyper-editing of Alu elements that allows comparison of editing activity across tissues and tumors, was used to evaluate the editase activity in cancer cells.[34 35] The AEI score has been validated with experimental data obtained with both clinical samples and cell lines, and an increased AEI score is correlated with higher ADAR1 activity.[34 35] We first validated the correlation between the AEI score and ADAR1 expression by assessing the AEI score in ADAR1-WT and ADAR1-KO cells. The AEI score was indeed higher in the ADAR1-WT cells than in the ADAR1-KO cells, as we expected (online supplemental figure 4E). Interestingly, the AEI score was decreased in LINC00624-depleted SK-BR-3 cells compared with that in wild-type cells (figure 4A), supporting the idea that LINC00624 can enhance the RNA-editing ability of ADAR1.

We next sought to determine whether LINC00624 promoted ADAR1 RNA-editing ability by regulating ADAR1 expression. The mRNA level of ADAR1 was stable on exposure to different LINC00624 levels (online supplemental figure 4F). However, the protein expression of ADAR1 was correlated with the level of LINC00624 in BT474 and SK-BR-3 cells (figure 4B). In SK-BR-3 cells, the half-life of ADAR1 was prolonged significantly after LINC00624 overexpression, indicating that LINC00624 could stabilize the ADAR1 protein (figure 4C,D). KO of LINC00624 promoted the degradation of ADAR1 (figure 4C,D). As LINC00624 isoform 3 binds only weakly to ADAR1, we reconstituted either LINC00624 (isoform 1) or isoform 3 in LINC00624-KO cells. As expected, LINC00624 isoform 1, but not isoform 3, restored ADAR1 protein expression (online supplemental figure 4G). In addition, ectopic overexpression of LINC00624 in 293 T cells promoted the stability of coexpressed ADAR1, while the half-life of ADAR1 with EExxA (EAA) mutation in dsRBD3 remained unchanged with or

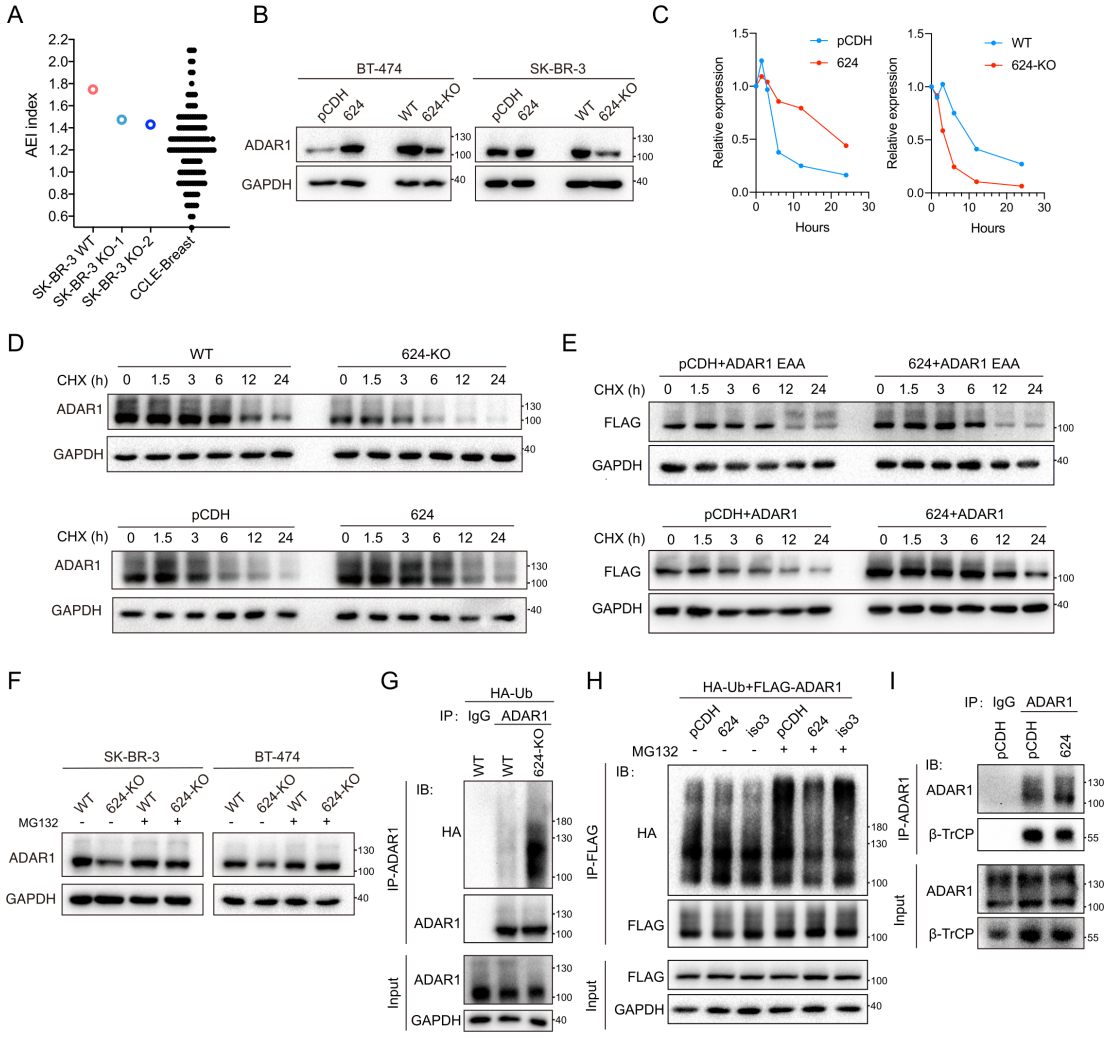

Figure 4 LINC00624 promotes ADAR1 expression. (A) AEI score represents A-to-I RNA editing in cells. The AEI score of WT and LINC00624 KO SK-BR-3 cells were shown. AEI score of breast cancer cell lines from CCLE was used as reference control. (B), ADAR1 protein expression in LINC00624 overexpression and 624-KO cells was examined by immunoblot. (C, D) Expression kinetics of ADAR1 with differentially expressed LINC00624 in SK-BR-3 cells. (C) Relative expression of ADAR1 normalized to GAPDH from (D) was shown. (D) Immunoblot was carried out in cells treated with the transcription inhibitor CHX (200 µg/mL). (E) Expression kinetics of ADAR1-p110-FLAG, and ADAR1-p110-FLAG with EAA mutation in 293 T cells. Cells were treated with CHX and collected at the time points as indicated. (F) WT or LINC00624-KO SK-BR-3 and BT-474 cells were treated with MG132 as indicated. The expression of ADAR1 was determined. (G) WT and LINC00624-KO SK-BR-3 cells were transfected with HA-Ubiquitin (HA-Ub). ADAR1 were immunoprecipitated (IP) with anti-ADAR1 antibody. IgG isotype control antibody was used. Immunoblot of the HA, ADAR1 and GAPDH was shown as indicated. (H) 293 T cells were transfected with FLAG-ADAR1-p110, HA-Ub, and LINC00624 isoforms as indicated (pCDH control vector, LINC00624, or isoform3 (iso3)). Treated with or without MG132 for 4 hours, cells were harvested and immunoprecipitated (IP) with anti-FLAG. Immunoblot (IB) of HA, FLAG, and GAPDH was shown. (I) SK-BR-3 cells with pCDH control or LINC00624 overexpression were immunoprecipitated (IP) with anti-ADAR1 or IgG isotype control. ADAR1 and β-TrCP were detected by immunoblot (IB). For (B–I) the experiments were performed twice with similar results. AEI, Alu-Editing Index; KO, knockout; WT, wild type.

without LINC00624 (figure 4E). These results confirmed the stability of ADAR1 depended on LINC00624 binding.

A previous study has showed that ADAR1 is degraded through the ubiquitin-proteasome pathway in human cells.[36] Similarly, we found that the proteasomal degradation of ADAR1 enhanced by on LINC00624-KO was blocked by MG132 (figure 4F). To evaluate the role of LINC00624 in ADAR1 ubiquitination, we transfected hemagglutinin (HA)-ubiquitin into WT and LINC00624-KO SK-BR-3 cells. We found that LINC00624-KO promoted the ubiquitination-related degradation of ADAR1 (figure 4G). To verify that the binding of ADAR1 by LINC00624 is critical for ADAR1 ubiquitination inhibition, we coexpressed LINC00624 (isoform 1 or 3), HA-ubiquitin, and FLAG-ADAR1 in 293 T cells. Overexpression of LINC00624, but not the AER region-deleted isoform 3, inhibited the ubiquitination of ADAR1 (figure 4H). The E3 ligase β-TrCP has been demonstrated to be involved in ADAR1 ubiquitination. We found that ADAR1 bound to β-TrCP in BC

cells and that overexpression of LINC00624 inhibited the binding of β-TrCP with ADAR1 (figure 4I). These results suggest that LINC00624 stabilizes ADAR1 by inhibiting ADAR1 ubiquitination-related degradation by blocking the interaction of the ubiquitin ligase β-TrCP and ADAR1.

LINC00624 inhibits the immune response and promotes treatment resistance through ADAR1

Although our data confirmed that LINC00624 was A-to-I edited both in vitro and in vivo, we found that overexpression or knockdown of ADAR1 did not affect the RNA expression of LINC00624 (online supplemental figure 5A,B). Next, we questioned whether immune response inhibition by LINC00624 was mediated through ADAR1. To answer this question, we overexpressed LINC00624 with ADAR1 knocked down in SK-BR-3 and BT-474 cells. Antigen presentation-related gene and ISG expression was recovered after ADAR1 knockdown (figure 5A, online supplemental figure 5C), suggesting that ADAR1 was involved in IFN response inhibition by LINC00624. In addition, we found that ADAR1-depleted cells were more sensitive to lapatinib (figure 5B). Overexpression of LINC00624 in ADAR1-KO cells failed to enhance the survival of SK-BR-3 cells treated with lapatinib (figure 5C), indicating that the molecular mechanism of LINC00624 in anti-HER2 treatment resistance depends on ADAR1.

Next, we questioned whether the function of LINC00624 was dependent on editing by ADAR1. When ADAR1 was constitutively expressed, LINC00624 was spontaneously edited in BC cell lines and clinical samples (figure 3H and online supplemental figure 4D). To generate an unedited isoform of LINC00624, we artificially mutated ADAR1-sensitive bases to render them uneditable. RNAfold was used to simulate the secondary structure of LINC00624 with or without edits (figure 5D). When we substituted editable A bases with C bases, the structure and free energy of the mutant S3 region were found to be similar to those of the natural A-to-I edited isoform, while mutating the bases from A to G rendered the mutant S3 similar to that of the unedited wild type (figure 5D). RNA pull-down assays showed that ADAR1 could bind to all three isoforms (figure 5E). Interestingly, ADAR1 bound even more tightly to the spontaneously edited WT or artificially edited A-to-C isoform than to the A-to-G isoform. In addition, we found that in the simulated A-to-C isoform (representing edited LINC00624) and WT isoform, the half-maximal inhibitory concentration (IC50) of lapatinib was higher than that in the A-to-G isoform (representing unedited LINC00624) (figure 5F). These results indicate that LINC00624 relies on ADAR1 A-to-I RNA editing to function. Then, we overexpressed the A-to-C isoform in ADAR1-KO cells. We found that the A-to-C isoform failed to inhibit the lapatinib response (figure 5G), an outcome similar to that of WT LINC00624 in ADAR1-KO cells, indicating that edited LINC00624 cannot function without ADAR1.

LINC00624 inhibits tumor antigen presentation

To further investigate the immune inhibition phenotype of LINC00624 in vivo, mouse cell lines and immunocompetent xenograft mouse model were then used. First, through Pipeline for lncRNA annotation from RNA-seq data (PLAR),[37] we did not find orthologs or 'synteny with sequence conservation' of LINC00624 in mouse. LINC00624 has orthologs in rhesus and dog only (online supplemental table 5). Therefore, we overexpressed human LINC00624 in mouse cell lines. We found that LINC00624 could inhibit the type I IFN response induced by poly(I:C) in B16-OVA and NF639 cells, which was consistent with the phenotype of human cell lines (figure 6A and online supplemental figure 6A–C). Furthermore, LINC00624 promoted cell proliferation and inhibited the lapatinib response in NF639 cells, a neu-positive cell line derived from MMTV-neu tumors (online supplemental figure 6D-E). Next, we validated that the function of LINC00624 relied on ADAR1 in mouse cells. RNA pull-down confirmed the interaction between ADAR1 and LINC00624 (online supplemental figure 7A). we reconfirmed that LINC00624 could decrease mouse ADAR1 degradation in NF639 cells through ubiquitination inhibition and the blockade of ADAR1-β-TrCP interaction (online supplemental figure 7B–E). Furthermore, KO of ADAR1 in NF639 cells inhibited their proliferation (online supplemental figure 7F). Similar to their human cell counterparts, ADAR1-depleted cells were more sensitive to lapatinib in mouse cells(online supplemental figure 7G). Moreover, overexpression of LINC00624 in WT cells, but not in ADAR1-KO cells, decreased cell sensitivity to lapatinib (online supplemental figure 7G), supporting the idea that the function of LINC00624 was dependent on ADAR1 in mouse cells.

We also evaluated the role of LINC00624 in antigen presentation in mouse model. LINC00624 decreased the levels of major histocompatibility complex (MHC) class I-bound SIINFEKL, an eight-amino-acid peptide derived from OVA, in B16-OVA cells treated with IFNα and IFNγ (figure 6B,C). Coculture of tumor cells overexpressing LINC00624 with CD8+T cells from OT-I mice significantly inhibited IFNγ production (figure 6D), confirming the inhibitory effect of LINC00624 on antigen processing and presentation.

To determine whether LINC00624 can render tumor cells immunotolerant in vivo, we inoculated B16-OVA cells with or without LINC00624 overexpressing vectors into the flanks of immunocompetent C57BL/6J mice. First, LINC00624 overexpression increased B16-OVA xenograft tumor growth, compared with the control group (figure 6E). The MHC class I-bound SIINFEKL level was also lower in LINC00624-overexpressing tumors (figure 6F). Transcription of antigen presentation-related genes and ISGs was inhibited by LINC00624 in vivo, confirming the in vitro results (figure 6G). These results indicate the antigen presentation process of tumor cells were inhibit by LINC00624.

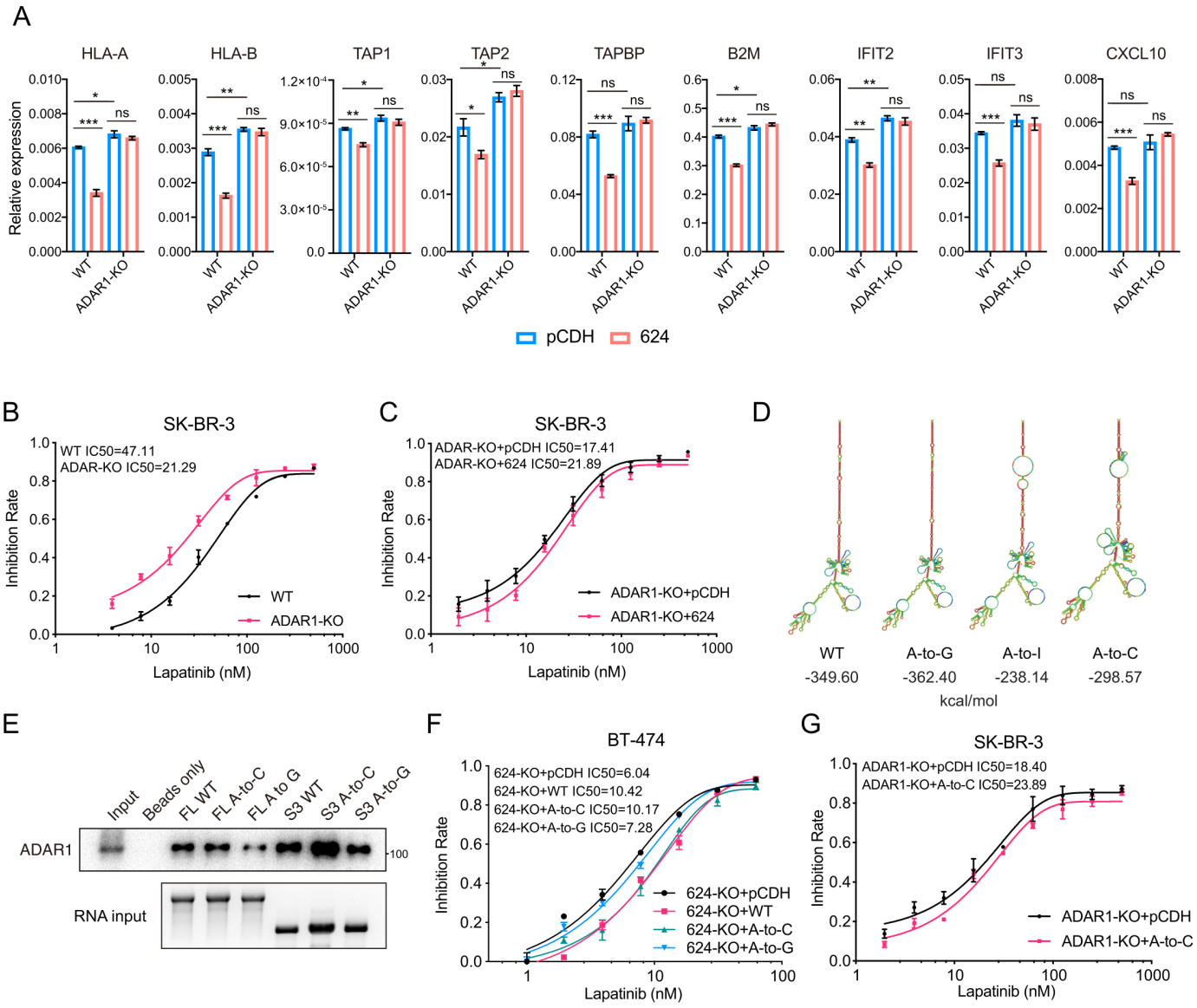

Figure 5 LINC00624 inhibits the immune response and promotes treatment resistance through ADAR1. (A) WT or ADAR1-KO SK-BR-3 cells were overexpressed with pCDH control or LINC00624. After poly(I:C) transfection for 24 hours, RNA levels of ISGs and antigen presentation related genes were analyzed by RT-qPCR. GAPDH were used as reference gene. n=3 biological independent samples. Statistical analysis was performed using two-sided t-test. *p<0.05, **p<0.01, ***p<0.001. Data are shown as mean±SE. (B) Inhibition rate of cells in response to lapatinib. (B) WT compared with ADAR1-KO in SK-BR-3. (C) ADAR1-KO pCDH compared with ADAR1-KO LINC00624 in SK-BR-3. (D) The secondary structure of S3 was predicted by RNAfold web server. The edited base in AER region by ADAR1 was substituted with guanine (G), inosine (I), or cytidine (C) as indicated. Free energy was shown below. (E) Binding of ADAR1 with LINC00624 WT, A-to-C or A-to-G isoforms. Immunoblot of ADAR1 was shown after RNA pull-down. IVT RNA was loaded with same quantity. (F) Recovery assay of LINC00624 in BT474 624-KO cells. pCDH, LINC00624, artificially mutated A-to-C, or A-to-G isoforms were overexpressed. Inhibition rate to lapatinib was plotted. (G) Recovery assay of LINC00624 in SK-BR-3 ADAR1-KO cells. pCDH or A-to-C mutated LINC00624 were overexpressed in ADAR1-KO cells. Inhibition rate to lapatinib was plotted. (B, C, E–G) the experiments were performed twice with similar results. AER, ADAR1 Editing Region; ISGs, IFN stimulated genes; KO, knockout; ns, no significance.

LINC00624 inhibits antitumor immunity and immunotherapy response *in vivo*

To further analyze whether LINC00624 inhibits antitumor immunity, we first investigated the infiltrated immune cells in mouse tumors. Xenograft tumors from B16-OVA cells with or without LINC00624 were dissected and digested to single cells. Flow cytometry analyses indicated a decrease in CD8+T cells, CD45+immune cells, CD3+T cells, CD4+T cells, CD8+T cells, and CD49f+ monocytes in the immune microenvironment of tumors with high LINC00624 levels, while the population of myeloid-derived suppressor cells was increased significantly (figure 6H–J, online supplemental figure 8A,B). Through immunohistochemical (IHC) staining, we confirmed a significant decrease in the infiltration of CD8+T cells in the immune microenvironment of tumors with high LINC00624 levels (figure 6K).

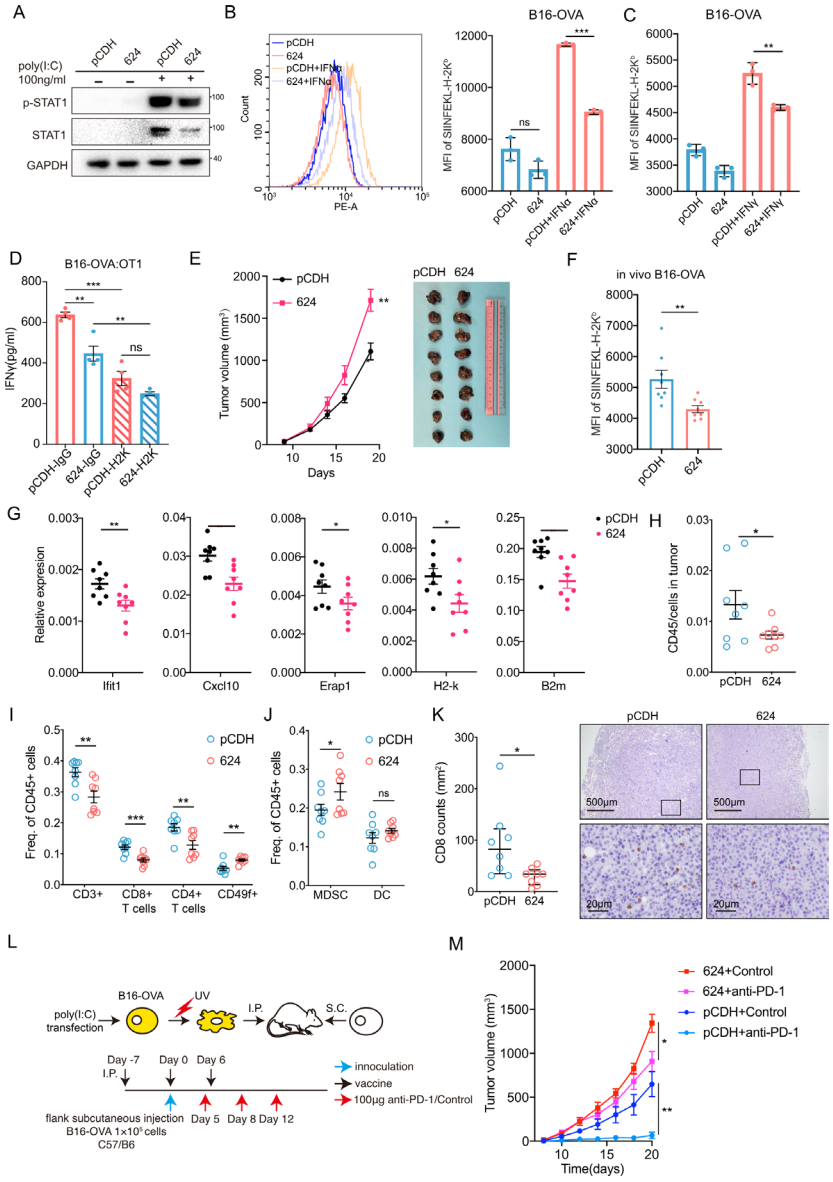

Figure 6 LINC00624 inhibits antitumor immunity and immunotherapy response in vitro and in vivo. (A) pCDH and LINC00624 KO B16-OVA cells were transfected with poly(I:C) for 24 hours with indicated concentration. The levels of the indicated proteins were determined by immunoblot. The experiments were performed twice with similar results. (B, C) Quantitative analysis of SIINFEKL-H-2K^b levels in pCDH and LINC00624 B16-OVA cells with or without (B) IFNα and (C) IFNγ treatment. (B) Left, representative flow cytometry image. Right, statistical analysis. n=3 biologically independent samples. (D) IFNγ released by OT-I CD8+T cells cocultured with isotype IgG or anti-SIINFEKL-H-2K^b pretreated pCDH control or LINC00624 overexpressing B16-OVA cells. n=4 biological independent samples. (E) Tumor growth curve and tumor size of B16-OVA pCDH or LINC00624 cells in C57/B6J. n=8 animals in each group. The experiment was performed twice with similar results. Statistical analysis was performed using two-sided t-test for the tumor volume at the end point. (F) Quantitative analysis of SIINFEKL-H-2K^b levels in pCDH and LINC00624 B16-OVA tumors (n=8 tumors each group). The experiment was performed twice with similar results. (G) RNA expression of ISGs and antigen presentation genes expressed in the B16-OVA tumors quantified by RT-qPCR (n=8 tumors each group). GAPDH were used as reference gene. (H–J) Flow cytometry of immune populations from pCDH control and LINC00624 overexpression B16-OVA tumors (n=8 tumors each group). (H) Percentage of CD45+cells in tumors. (I) The proportion of CD3+, CD8+T, CD4+T, CD49f+, (J) myeloid-derived suppressor cells (MDSCs) and dendritic cells (DCs) in CD45+ cells in tumor. The experiment was performed twice with similar results. Statistical analyses were performed using two-sided t-test. (K), B16-OVA tumor infiltrated CD8+cells were determined by immunohistochemistry. Left, statistical analysis (n=8 tumors each group). Right, representative images. Statistical analyses were performed using two-sided t-test. (L,M) C57/B6J were vaccinated intraperitoneally (I.P.) with poly(I:C) transfected and ultraviolet treated B16-OVA cells as indicated. B16-OVA pCDH or LINC00624 cells were inoculated subcutaneously (S.C.). Mice were treated with anti-PD-1 or IgG isotype control as indicated. (L) Schematic view of treatment protocol. (M) Tumor growth curve of each group. n=6 animals in each group. For (B–D, F–G) statistical analysis was performed using two-sided t-test for the tumor volume at the end point. The experiment was performed twice with similar results. *p<0.05, **p<0.01, ***p<0.001. Data are shown as mean±SE. ISGs, IFN stimulated genes; ns, no significance.

A previous study showed that loss of ADAR1 sensitized tumors to the innate immune response.[14] Type I or type II IFNs led to growth arrest and death of ADAR1-KO B16-OVA cells, indicating that ADAR1 was involved in the modulation of the innate immune response.[12] In addition, ADAR1 also promoted the blockade of immune checkpoint inhibitors. Loss of ADAR1 reversed cell resistance to immune therapy. As LINC00624 can inhibit the degradation of ADAR1, we hypothesized that LINC00624 caused resistance to immune checkpoint blockers. To test this, a B16-OVA murine model was used to investigate the role of LINC00624 in immune checkpoint blockade in vivo with a whole tumor cell vaccine loaded with poly(I:C) and anti-PD-1 (figure 6L). We found that LINC00624 significantly inhibited the tumor response to the anti-PD-1 treatment compared with the control group (figure 6M). To investigate whether the inhibition of immune therapy was dependent on ADAR1, ADAR1-KO B16 cells with different LINC0624 expression were used to address this issue. After ADAR1 knocked out, the growth of B16 tumors were significantly reduced (online supplemental figure 9A,B). Overexpression of LINC00624 could not promote tumor growth in ADAR1 null tumors. In addition, tumors were regressed after the treatment of PD-1 in ADAR1 null tumors without the vaccination process, consistent with previous study[14] (online supplemental figure 9B). Overexpression of LINC00624 could not further cause treatment resistance of PD-1 (online supplemental figure 9B). Furthermore, we found tumor-infiltrating CD8+cells were significantly increased after ADAR1 KO, while LINC00624 could not inhibit CD8+cells infiltration in ADAR1 null tumors (online supplemental figure 9C), confirming the function of LINC00624 was dependent on ADAR1. All these in vivo data confirmed that LINC00624 inhibited antitumor immunity and promoted immune checkpoint inhibitor blockade.

Translational exploration of LINC00624-targeted treatments with antisense oligonucleotides

To investigate the potential therapeutic target of LINC00624 in BC, we designed five independent antisense oligonucleotides (ASOs) complementary to the LINC00624 S3 region (figure 7A). An ASO with a scrambled sequence in BC was used as the negative control. Transfection with each of the 5 ASOs reduced LINC00624 RNA levels in BT-474 cells, while ASO-2 and ASO-3 showed the highest knockdown efficiency (figure 7B). Consistently, the expression of ADAR1 was reduced, similar to the in vitro results (figure 7C). Next, we synthesized cholesterol-conjugated locked nucleic acid-modified ASOs for in vivo use. Free uptake assay results showed the downregulation of LINC00624 (figure 7D). To determine the potential clinical application of ASOs in treating BC, we generated an orthotopic mammary tumor model with BT-474 WT cells in nude mice, and the mice were treated with either control (ASO-Ctrl) or ASO-2 and ASO-3 mixtures (ASO-2/3) 10 days after inoculation (figure 7E). Although this model did not present with an adaptive immune response, we found that targeting LINC00624 significantly inhibited the proliferation of BT474 tumor cells (figure 7F,G). Indeed, xenograft tumors treated with ASOs exhibited decreased ADAR expression compared with the control, as determined by IHC (figure 7H). Moreover, the expression levels of ISGs and innate immune response genes were significantly increased in the ASO-treated xenograft tumors (figure 7I).

Altogether, these data strongly support the supposition that LINC00624 promotes therapy resistance and tumor progression by inhibiting the immune response in BC cells exposed to HER2-targeted treatment. Therefore, LINC00624 can serve as a future therapeutic target in HER2+BC.

DISCUSSION

Tumors can escape elimination by immune cells at the initiation stage. By decreasing the expression of mutated or fusion proteins, reducing antigen presentation of neoantigens, or secreting immune suppressive signals, tumor cells can evade recognition by the immune system.[38] The underlying mechanisms that tumors shape the immunosuppressive microenvironment have attracted considerable attention in recent years. Among them, the suppression of the innate immune response that prevents tumors from turning from 'cold' to 'hot' has been demonstrated.[38–40]

Type I IFNs recently re-entered the focus of investigation in tumor biology.[1 8] Induced by the activation of nucleic sensors through transductors such as TBK1 and IRF3, type I IFNs activate the phosphorylation of STAT1, leading to increased transcription of ISGs.[1 41 42] Hundreds of genes have been identified as ISGs under transcriptional regulation, and they are elevated 3- to 100-fold after type I IFN stimulation.[42 43] The protein products of ISGs play different roles in antitumor biology, including immune regulation, protein synthesis suppression and apoptosis induction.[43–45] Even without the involvement of immune cells, the proliferation of cancer cells were found to be inhibited when the IFN pathway was stimulated,[3] consistent with our results showing that proliferation was inhibited and apoptosis was induced in LINC00624-KO cells on IFN signaling activation. In addition, upregulation of the expression of ISGs such as MHC class I proteins enhances antigen presentation to infiltrated T and B cells, eliciting an adaptive immune response.[1] As we shown in our work, LINC00624 inhibits antitumor responses both in tumor cells and in the tumor microenvironment.

The tumor cell response to conventional treatments is modulated by the activation of the type I IFN pathway. In addition to cytotoxic drugs, the blockade of growth signaling pathways such as the EGFR and HER2 pathways relies on IFN signaling. Previous studies have shown that PI3K-AKT, a signaling axis downstream of the EGFR and HER2 pathways, can suppress the expression of MHC class I proteins.[46 47] HER2 amplification also reduces TBK1/NAK phosphorylation, leading to the inhibition

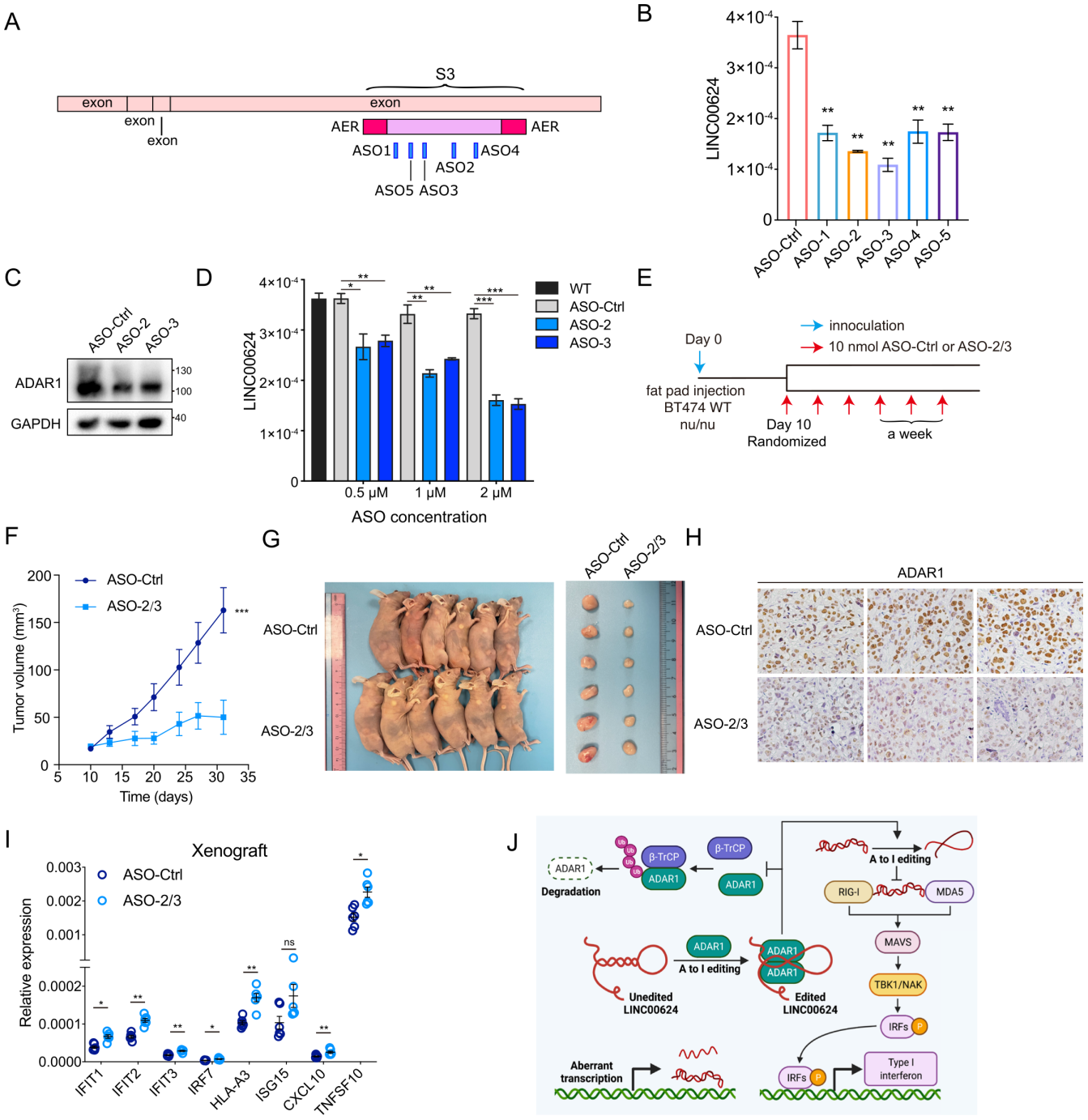

Figure 7 Translational exploration of LINC00624-targeted treatments with ASOs. (A) Schematic view of ASOs designed in the S3 segment of LINC00624. (B) Relative expression of LINC00624 48 hours after ASOs transfection in SK-BR-3 were determined by RT-qPCR, normalized to GAPDH. For each ASO, statistical analysis was performed using two-sided t-test compared with Ctrl, n=3 biological replicates. (C) Immunoblot of ADAR1 expression after ASOs transfection in SK-BR-3 cells. The experiment was performed twice with similar results. (D) LINC00624 expression after cholesterol modified ASOs delivery without transfect reagents. ASOs were added into SK-BR-3 wild type cells at the concentration as indicated. After 48 hours, RNA was extracted, and RT-qPCR was performed. Normalized to GAPDH. For each ASO, statistical analysis was performed using two-sided t-test compared with ASO-Ctrl, n=3 biological replicates. (E–G) BT-474 WT cells were inoculated in nude mice and treated with cholesterol modified ASOs through tail vein injection. (E) Schematic view of treatment plan. (F) Tumor growth curve of each group. (G) Left, mice with tumors after sacrifice were shown. Right, tumors were dissected as shown. n=6 animals in each group. The experiment was performed twice with similar results. Statistical analysis was performed using two-sided t-test for the tumor volume at the end point. ***p<0.001. (H) ADAR1 expression determined by IHC. Representative images were shown. (I) RNA expression of ISGs and antigen presentation genes expressed in the BT474 tumors after ASO treatment quantified by RT-qPCR (n=6 tumors each group), normalized to GAPDH. The experiment was performed twice with similar results. (J) Schematic view of this study. For, (B, C, and I), statistical analyses were performed using two-sided t-test. *p<0.05, **p<0.01, ***p<0.001. Data are shown as mean±SE. ASOs, antisense oligonucleotides; IHC, immunohistochemical; WT, wild type.

of STING pathway activation, reduction of MHC class I protein expression, and compromise of antitumor immune response.[9 18]

A previous study has showed that loss of ADAR1 in tumor cells enhances tumor inflammation, increases infiltrated immune cells, and sensitizes tumor cells to the blockade of immune checkpoints.[7 13 14] Several researchers are exploring ADAR1 inhibitors.[48 49] However, ADAR1 plays immunoregulatory roles in normal cells, inhibition of ADAR1 editase activity may raise concerns about autoimmune reactions. In our study, we found targeting LINC00624 through ASOs can significantly inhibit tumor cell proliferation, suppress ADAR1 activity and promote the type I IFN response. Through the regulation of LINC00624, we can possibly modulate ADAR1 function in tumor cells.

As LINC00624 is evolutionarily new and expressed only in human cells, the experimental models are limited and sometimes artificial models are used, especially in immune research. To tackle this issue, we overexpressed LINC00624 in mammary mouse cell lines and its effectiveness has been proven to be the same as it is in human cells. In addition, B16-OVA contains a model antigen OVA. In our study, it was used to investigate antigen presentation process as many other studies did.[14 50] Through this model, we illustrated how LINC00624 regulates antigen presentation, antitumor immunity and immunotherapy response in vivo, confirming the immune suppression role of LINC00624 in immunocompetent model. Bitransgenic mice with LINC00624 overexpression in MMTV/neu mice could be used in further study to confirm how LINC00624 inhibits tumor immunity and the immunotherapy response with anti-HER2 therapy.

In conclusion, our findings demonstrate that LINC00624 plays an important role in inhibiting the IFN response and results in anti-HER2 treatment resistance. Targeting LINC00624 through ASOs shows great therapeutic potential for future clinical use.

Author affiliations
[1]Department of Breast Surgery, Key Laboratory of Breast Cancer in Shanghai, Fudan University Shanghai Cancer Center, Shanghai, China
[2]Department of Oncology, Shanghai Medical College, Fudan University, Shanghai, China
[3]Department of General Surgery, The Second Xiangya Hospital, Central South University, Changsha, Hunan, China
[4]Department of Breast Surgery, The Third Affiliated Hospital of Kunming Medical University, Kunming, Yunnan, China
[5]Department of Integrative Oncology, Fudan University Shanghai Cancer Center, and Shanghai Key Laboratory of Medical Epigenetics, International Co-laboratory of Medical Epigenetics and Metabolism (Ministry of Science and Technology), Institutes of Biomedical Sciences, Fudan University, Shanghai, China
[6]Collaborative Innovation Center for Cancer Medicine, Shanghai Medical College, Fudan University, Shanghai, China

Contributors QZ and BX designed and performed most of the experiments, analyzed the data, and wrote the manuscript with help from all co-authors. LZ and MC carried out all in vivo experiments and the revision of the manuscript. MC and WC maintained cell culture. LL analyzed clinical data. RG and JX collected and prepared the clinical samples for RNA-seq. XH and BY provided advice on clinical evaluation. SH analyzed the RNA-seq data and AEI index. Z-MS provided assistance in this study. JW, YC and BX initiated the study and provided funding and study supervision. JW is the guarantor for this study.

Funding This work was supported by the National Natural Science Foundation of China (81874115, 82002795, 82072919, and 82173274) and Natural Science Foundation of Shanghai (21ZR1414300).

Competing interests None declared.

Patient consent for publication Not applicable.

Ethics approval The present study was approved by the Medical Ethics Committee of Fudan University Shanghai Cancer CenterID:2018FUSCC-JS-025. Patients signed the informed consent forms before biosample collection through the central biosample bank of Fudan University Shanghai Cancer Center. The ID number is:050432-4-1212B and 050432-4-1911D. Participants gave informed consent to participate in the study before taking part.

Provenance and peer review Not commissioned; externally peer reviewed.

Data availability statement Data relevant to the study are included in the article or uploaded as online supplemental information. Original data are available on reasonable request.

ORCID iD
Jiong Wu http://orcid.org/0000-0002-8103-0505

REFERENCES

1 Borden EC. Interferons α and β in cancer: therapeutic opportunities from new insights. *Nat Rev Drug Discov* 2019;18:219–34.
2 Mogensen TH. Pathogen recognition and inflammatory signaling in innate immune defenses. *Clin Microbiol Rev* 2009;22:240–73.
3 Chung H, Calis JJA, Wu X, *et al*. Human ADAR1 prevents endogenous RNA from triggering translational shutdown. *Cell* 2018;172:811–24.
4 Ivashkiv LB, Donlin LT. Regulation of type I interferon responses. *Nat Rev Immunol* 2014;14:36–49.
5 Schlee M, Hartmann G. Discriminating self from non-self in nucleic acid sensing. *Nat Rev Immunol* 2016;16:566–80.
6 Jansz N, Faulkner GJ. Endogenous retroviruses in the origins and treatment of cancer. *Genome Biol* 2021;22:147.
7 Herbert A. ADAR and immune silencing in cancer. *Trends Cancer* 2019;5:272–82.
8 Sistigu A, Yamazaki T, Vacchelli E, *et al*. Cancer cell-autonomous contribution of type I interferon signaling to the efficacy of chemotherapy. *Nat Med* 2014;20:1301–9.
9 Wu S, Zhang Q, Zhang F, *et al*. HER2 recruits Akt1 to disrupt sting signalling and suppress antiviral defence and antitumour immunity. *Nat Cell Biol* 2019;21:1027–40.
10 Brea EJ, Oh CY, Manchado E, *et al*. Kinase regulation of human MHC class I molecule expression on cancer cells. *Cancer Immunol Res* 2016;4:936–47.
11 Kumagai S, Koyama S, Nishikawa H. Antitumour immunity regulated by aberrant ERBB family signalling. *Nat Rev Cancer* 2021;21:181–97.
12 Fritzell K, Xu L-D, Lagergren J, *et al*. ADARs and editing: the role of A-to-I RNA modification in cancer progression. *Semin Cell Dev Biol* 2018;79:123–30.
13 Samuel CE. Adenosine deaminase acting on RNA (ADAR1), a suppressor of double-stranded RNA-triggered innate immune responses. *J Biol Chem* 2019;294:1710–20.
14 Ishizuka JJ, Manguso RT, Cheruiyot CK, *et al*. Loss of ADAR1 in tumours overcomes resistance to immune checkpoint blockade. *Nature* 2019;565:43–8.

15 Meric-Bernstam F, Hung M-C. Advances in targeting human epidermal growth factor receptor-2 signaling for cancer therapy. *Clin Cancer Res* 2006;12:6326–30.
16 Scaltriti M, Rojo F, Ocaña A, *et al*. Expression of p95HER2, a truncated form of the HER2 receptor, and response to anti-HER2 therapies in breast cancer. *J Natl Cancer Inst* 2007;99:628–38.
17 Le Du F, Diéras V, Curigliano G. The role of tyrosine kinase inhibitors in the treatment of HER2+ metastatic breast cancer. *Eur J Cancer* 2021;154:175–89.
18 Herrmann F, Lehr H-A, Drexler I, *et al*. HER-2/neu-mediated regulation of components of the MHC class I antigen-processing pathway. *Cancer Res* 2004;64:215–20.
19 Park S, Jiang Z, Mortenson ED, *et al*. The therapeutic effect of anti-HER2/neu antibody depends on both innate and adaptive immunity. *Cancer Cell* 2010;18:160–70.
20 Yamaguchi R, Tanaka M, Yano A, *et al*. Tumor-infiltrating lymphocytes are important pathologic predictors for neoadjuvant chemotherapy in patients with breast cancer. *Hum Pathol* 2012;43:1688–94.
21 Luen SJ, Salgado R, Fox S, *et al*. Tumour-infiltrating lymphocytes in advanced HER2-positive breast cancer treated with pertuzumab or placebo in addition to trastuzumab and docetaxel: a retrospective analysis of the CLEOPATRA study. *Lancet Oncol* 2017;18:52–62.
22 Lin MF, Jungreis I, Kellis M. PhyloCSF: a comparative genomics method to distinguish protein coding and non-coding regions. *Bioinformatics* 2011;27:i275–82.
23 Wang L, Park HJ, Dasari S, *et al*. CPAT: Coding-Potential assessment tool using an alignment-free logistic regression model. *Nucleic Acids Res* 2013;41:e74.
24 Li Y, Jiang T, Zhou W, *et al*. Pan-cancer characterization of immune-related lncRNAs identifies potential oncogenic biomarkers. *Nat Commun* 2020;11:1000.
25 Kato H, Takeuchi O, Sato S, *et al*. Differential roles of MDA5 and RIG-I helicases in the recognition of RNA viruses. *Nature* 2006;441:101–5.
26 Pollack BP, Sapkota B, Cartee TV. Epidermal growth factor receptor inhibition augments the expression of MHC class I and II genes. *Clin Cancer Res* 2011;17:4400–13.
27 Tan MH, Li Q, Shanmugam R, *et al*. Dynamic landscape and regulation of RNA editing in mammals. *Nature* 2017;550:249–54.
28 Li Z, Lu X, Liu Y, *et al*. Gain of LINC00624 enhances liver cancer progression by disrupting the histone deacetylase 6/Tripartite motif containing 28/Zinc finger protein 354C corepressor complex. *Hepatology* 2021;73:1764–82.
29 Gruber AR, Lorenz R, Bernhart SH, *et al*. The Vienna RNA websuite. *Nucleic Acids Res* 2008;36:W70–4.
30 Valente L, Nishikura K. RNA binding-independent dimerization of adenosine deaminases acting on RNA and dominant negative effects of nonfunctional subunits on dimer functions. *J Biol Chem* 2007;282:16054–61.
31 Liu Y, Samuel CE. Mechanism of interferon action: functionally distinct RNA-binding and catalytic domains in the interferon-inducible, double-stranded RNA-specific adenosine deaminase. *J Virol* 1996;70:1961–8.
32 Thuy-Boun AS, Thomas JM, Grajo HL, *et al*. Asymmetric dimerization of adenosine deaminase acting on RNA facilitates substrate recognition. *Nucleic Acids Res* 2020;48:7958–72.
33 Rajendren S, Manning AC, Al-Awadi H, *et al*. A protein-protein interaction underlies the molecular basis for substrate recognition by an adenosine-to-inosine RNA-editing enzyme. *Nucleic Acids Res* 2018;46:9647–59.
34 Roth SH, Levanon EY, Eisenberg E. Genome-wide quantification of ADAR adenosine-to-inosine RNA editing activity. *Nat Methods* 2019;16:1131–8.
35 Schaffer AA, Kopel E, Hendel A, *et al*. The cell line A-to-I RNA editing catalogue. *Nucleic Acids Res* 2020;48:5849–58.
36 Li L, Qian G, Zuo Y, *et al*. Ubiquitin-Dependent turnover of adenosine deaminase acting on RNA 1 (ADAR1) is required for efficient antiviral activity of type I interferon. *J Biol Chem* 2016;291:24974–85.
37 Hezroni H, Koppstein D, Schwartz MG, *et al*. Principles of long noncoding RNA evolution derived from direct comparison of transcriptomes in 17 species. *Cell Rep* 2015;11:1110–22.
38 Vinay DS, Ryan EP, Pawelec G, *et al*. Immune evasion in cancer: mechanistic basis and therapeutic strategies. *Semin Cancer Biol* 2015;35 Suppl:S185–98.
39 Wang H, Li S, Wang Q, *et al*. Tumor immunological phenotype signature-based high-throughput screening for the discovery of combination immunotherapy compounds. *Sci Adv* 2021;7. doi:10.1126/sciadv.abd7851. [Epub ahead of print: 22 01 2021].
40 Liu X, Bao X, Hu M, *et al*. Inhibition of PCSK9 potentiates immune checkpoint therapy for cancer. *Nature* 2020;588:693–8.
41 Liu S, Cai X, Wu J, *et al*. Phosphorylation of innate immune adaptor proteins MAVS, STING, and TRIF induces IRF3 activation. *Science* 2015;347:aaa2630.
42 Stark GR, Cheon H, Wang Y. Responses to cytokines and interferons that depend upon JAKs and STATs. *Cold Spring Harb Perspect Biol* 2018;10. doi:10.1101/cshperspect.a028555. [Epub ahead of print: 02 01 2018].
43 Schneider WM, Chevillotte MD, Rice CM. Interferon-stimulated genes: a complex web of host defenses. *Annu Rev Immunol* 2014;32:513–45.
44 Hertzog PJ, Williams BRG. Fine tuning type I interferon responses. *Cytokine Growth Factor Rev* 2013;24:217–25.
45 Ortiz A, Fuchs SY. Anti-metastatic functions of type 1 interferons: foundation for the adjuvant therapy of cancer. *Cytokine* 2017;89:4–11.
46 Chandrasekaran S, Sasaki M, Scharer CD, *et al*. Phosphoinositide 3-kinase signaling can modulate MHC class I and II expression. *Mol Cancer Res* 2019;17:2395–409.
47 Sivaram N, McLaughlin PA, Han HV, *et al*. Tumor-intrinsic PIK3CA represses tumor immunogenecity in a model of pancreatic cancer. *J Clin Invest* 2019;129:3264–76.
48 Fritzell K, Xu L-D, Otrocka M, *et al*. Sensitive ADAR editing reporter in cancer cells enables high-throughput screening of small molecule libraries. *Nucleic Acids Res* 2019;47:e22.
49 Wang L, Sun Y, Song X, *et al*. Hepatitis B virus evades immune recognition via RNA adenosine deaminase ADAR1-mediated viral RNA editing in hepatocytes. *Cell Mol Immunol* 2021;18:1871–82.
50 Goel S, DeCristo MJ, Watt AC, *et al*. CDK4/6 inhibition triggers anti-tumour immunity. *Nature* 2017;548:471–5.

Supplementary Fig. 1

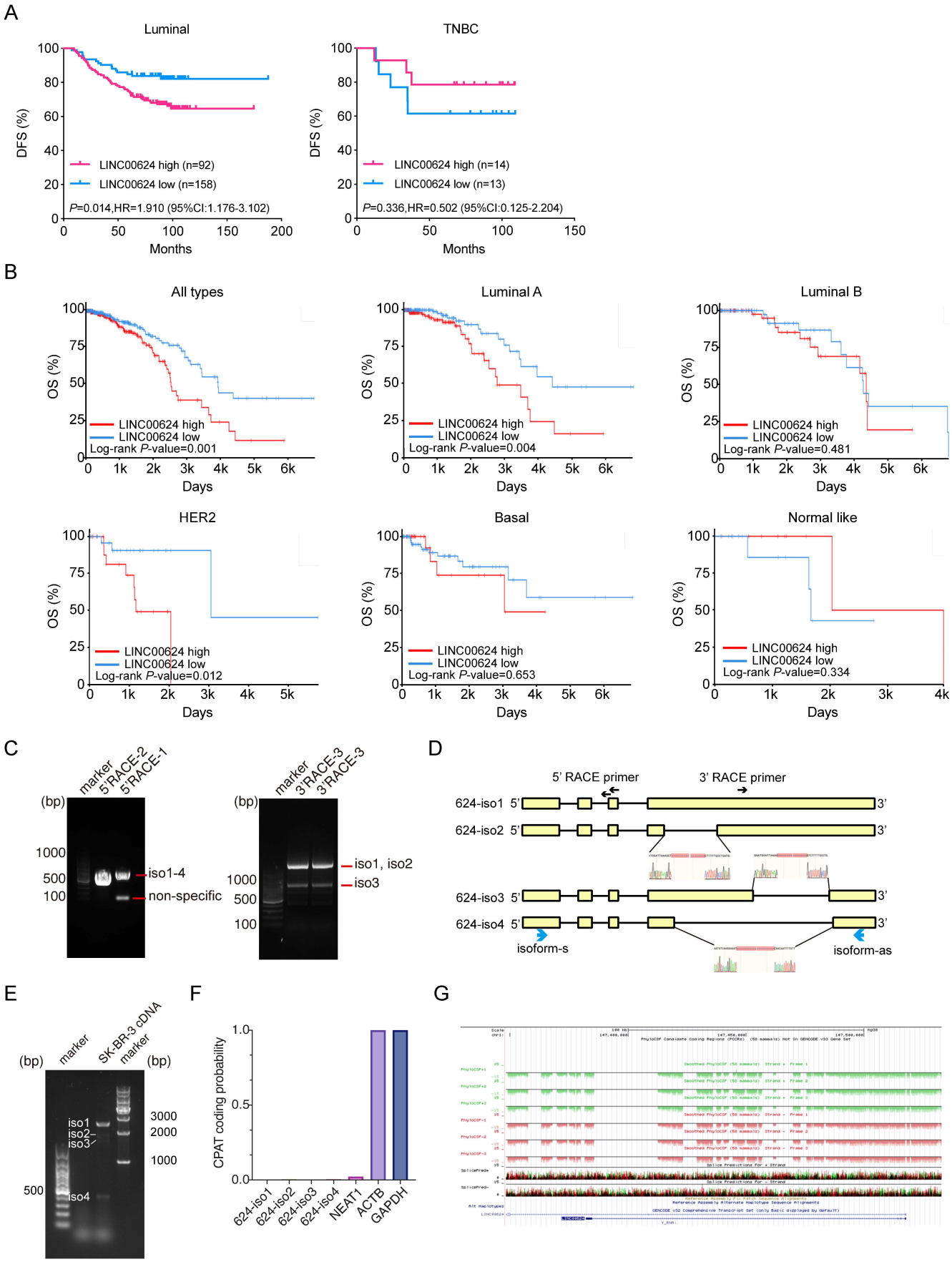

Supplementary Fig. 1 LINC00624 promotes treatment resistance in HER2+ BC. A, Disease-free survival plot (DFS) of patients in a consecutive cohort receiving adjuvant treatment. Patients were divided into high and low LINC00624 groups. Statistical analysis was performed using two-sided log-rank tests. HR, hazardous ratio. TNBC, triple negative breast cancer. CI: confidential interval. HR: hazardous ratio. **B**, TCGA-BRCA expression data were used for survival analysis. Overall survival (OS) was shown as indicated. **C-D**, RACE-PCR was performed. (**C**) Representative image of RACE-PCR electrophoresis. isoform 1-4 were verified. (**D**) Schematic view of LINC00624 isoforms and sanger sequencing at the junctions of exon 4. **E**, The abundance of LINC00624 isoforms were analyzed by PCR with SK-BR-3 cDNA. Normalized to GAPDH. Representative image was shown. **F**, CPAT coding probability of LINC00624 isoforms were shown. NEAT1, ACTB, and GAPDH were used as positive or negative control. **G**, PhyloCSF coding score were demonstrated at the LINC00624 region from UCSC genome browser. For **C-E**, the experiments were performed twice with similar results.

Supplementary Fig. 2

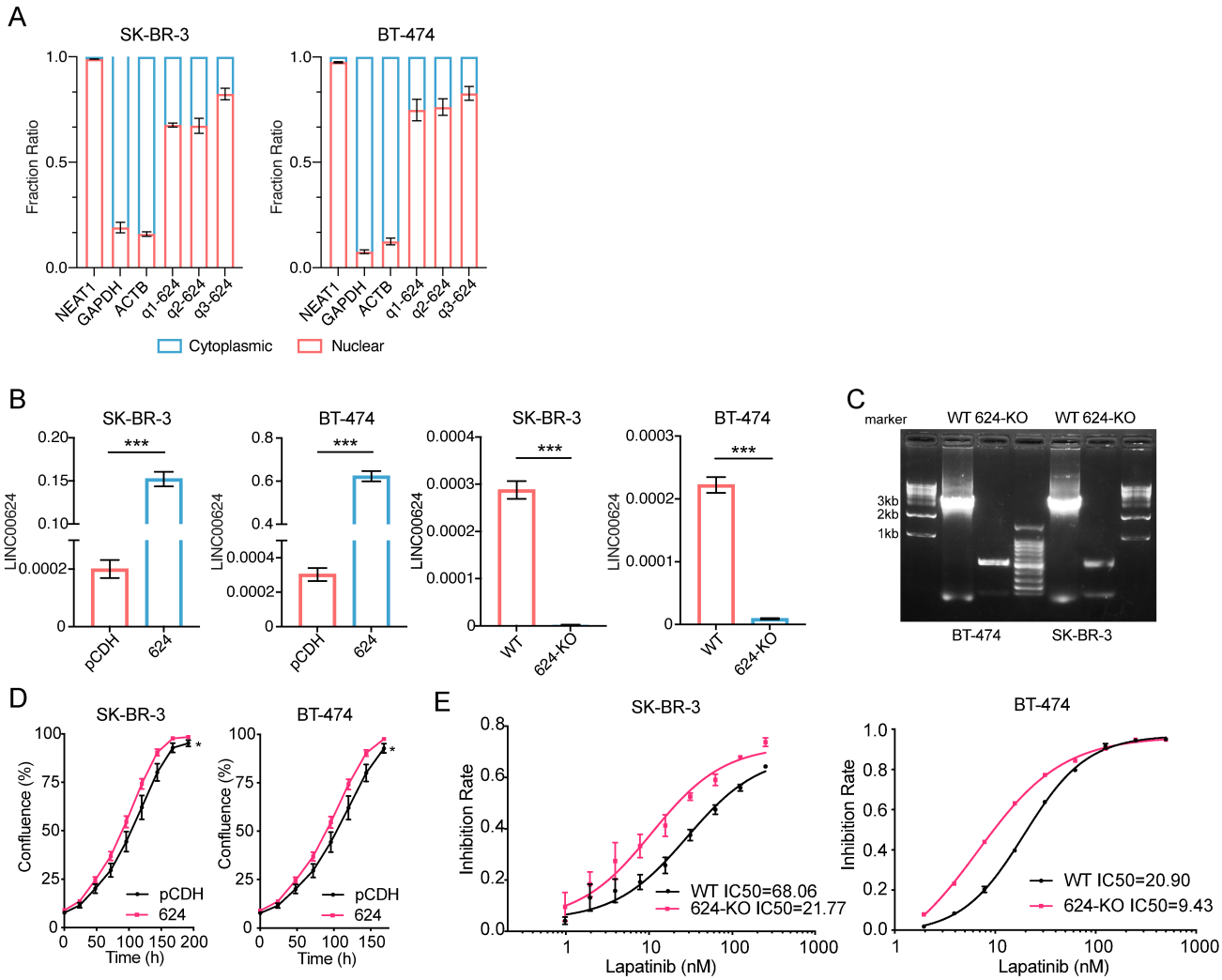

Supplementary Fig. 2 LINC00624 promotes treatment resistance in HER2+ BC. A LINC00624 mainly located in the cell nucleus of SK-BR-3 and BT-474. Cytoplasmic and nuclear fractions were extracted from SK-BR-3 and BT-474 cells. LINC00624, GAPDH and NEAT1 expression was analyzed by RT-qPCR. n=3 biological replicates. **B**, The overexpressed and KO strains of LINC00624 in SK-BR-3 and BT-474 was constructed and verified by RT-qPCR. n=3 biological replicates. **C**, LINC00624-KO strains were verified by PCR with genome DNA. Representative images were shown. The experiment was performed twice with similar results. **D**, Cell proliferation assay of pCDH and LINC00624 cells in SK-BR-3 and BT-474 cells. n=6 for each time point. Statistical analysis was performed using two-sided t-test at the end point. The experiments were performed twice with similar results. **E**, Inhibition rate of WT and LINC00624-KO SK-BR-3 and BT-474 cells in response to lapatinib. n=3 biological replicates. The experiments were performed twice with similar results. * P<0.05, ** P<0.01, *** P<0.001. Data are shown as mean ± s.e.m.

Supplementary Fig. 3

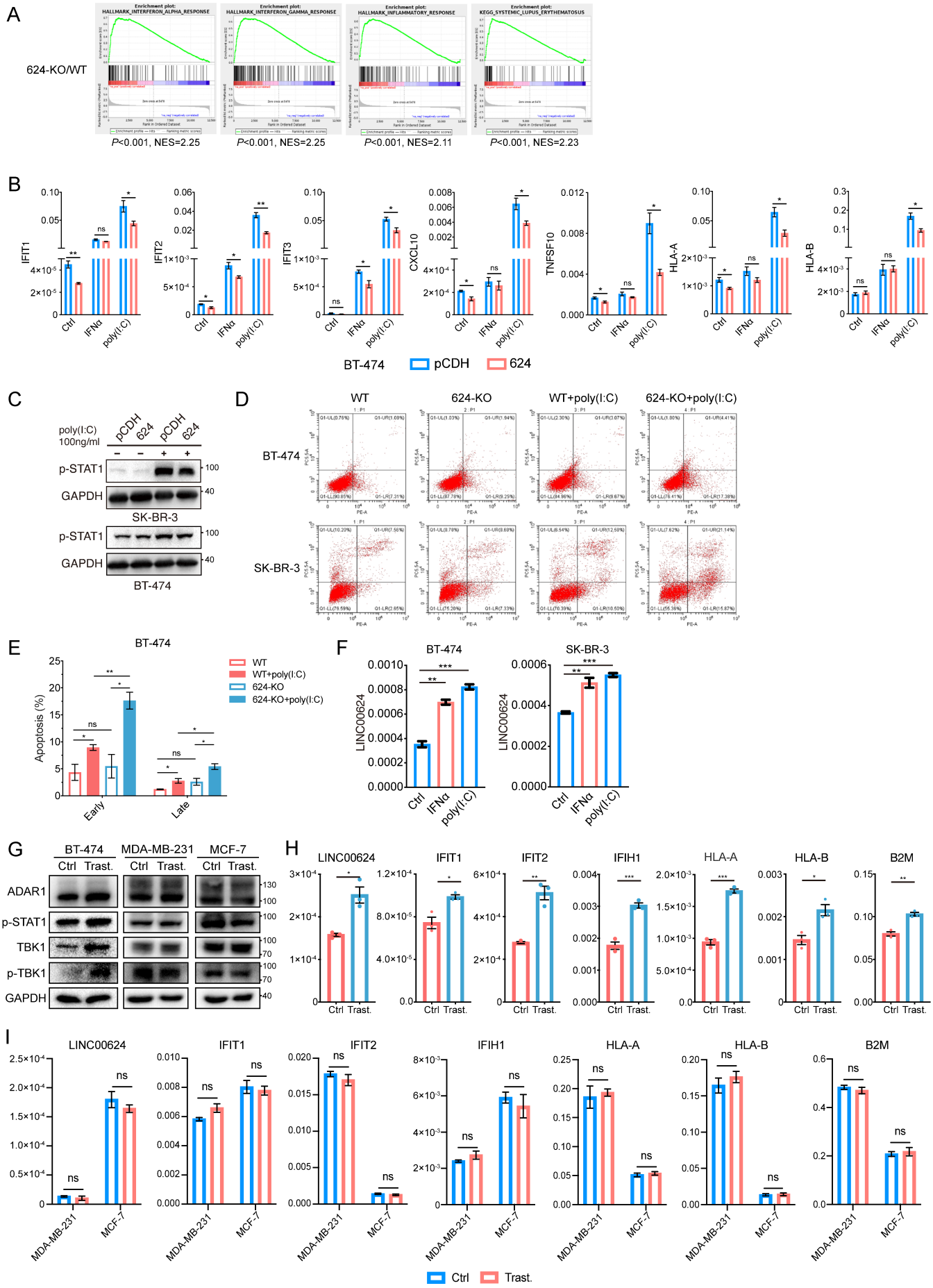

Supplementary Fig. 3 LINC00624 inhibits the innate immune response by inhibiting type I IFN signaling. A, GSEA analysis showed the indicated gene signatures comparing different LINC00624 expression SK-BR-3 cells. NES, normalized enrichment score. **B**, pCDH or LINC00624 BT-474 cells were treated with 5 ng/ml IFNα for 4 h or transfected poly(I:C) for 24h. RNA levels of ISGs and antigen presentation related genes were analyzed by RT-qPCR, normalized to GAPDH. **C**, pCDH or LINC00624 cells were treated with transfected poly(I:C) for 24h with indicated concentration. The levels of the indicated proteins were determined by immunoblot. **D**-**E**, Apoptosis of WT and LINC00624 BT-474 cells and SK-BR-3 cells were determined by flow cytometry with or without transfected poly(I:C). (**D**) Representative images of flow cytometry were shown. (**E**) The percentage of early and late apoptosis were determined after 1 μg/ml transfected poly(I:C) in BT-474 WT and LINC00624 KO cells. n=3 biological replicates. Statistical analysis was performed using two-sided t-test. **F**, RNA expression of LINC00624 in SK-BR-3 and BT-474 cells with the treatment of 5 ng/ml IFNα or 1 μg/ml poly(I:C) for 24h were analyzed by RT-qPCR, normalized to GAPDH. **G-I**, BT-474, MCF7 and MDA-MB-231 cells were treated with 20 μg/ml trastuzumab for 3 days. (**G**) The levels of the indicated proteins were determined by immunoblot. The experiment was performed twice with similar results. (**H**) RNA levels of LINC00624, ISGs and antigen presentation related genes were analyzed by RT-qPCR in BT474, (**I**) MDA-MB-231 and MCF-7 cells, normalized to GAPDH. For **B**, **E**-**F**, and **H-I**, n=3 biological replicates. Statistical analysis was performed using two-sided t-test. For **C**-**E** and **G**, the experiment was performed twice with similar results. * P<0.05, ** P<0.01, *** P<0.001. ns, no significance. Data are shown as mean ± s.e.m.

Supplementary Fig. 4

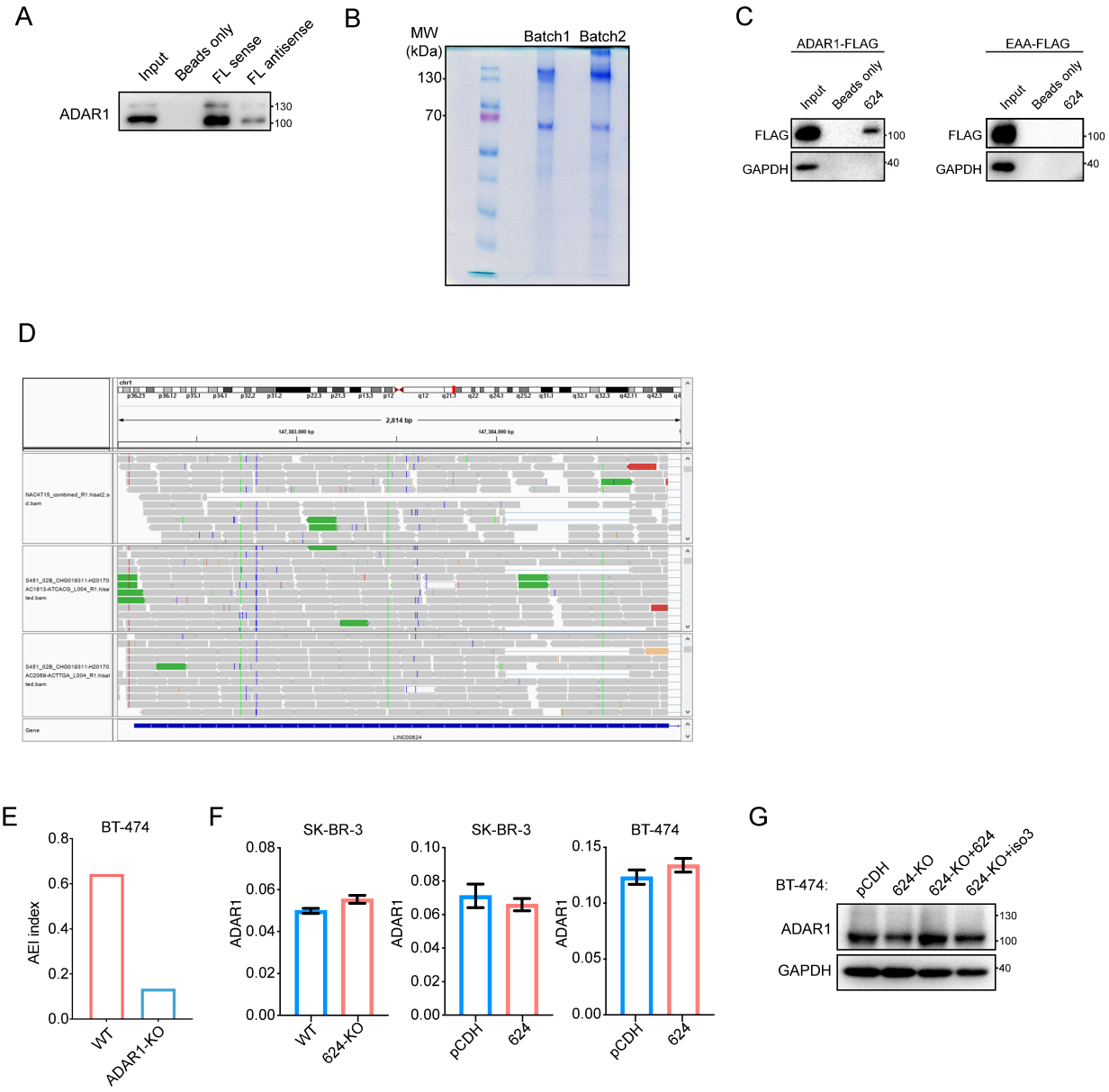

Supplementary Fig. 4 LINC00624 is bound to and edited by ADAR1. **A**, Biotin-labeled LINC00624 sense and antisense full-length (FL) RNA were incubated with SK-BR-3 whole cell lysates. ADAR1 was pull-down and verified by immunoblot. The experiment was performed twice with similar results. **B**, Recombinant ADAR1-p150 was purified and verified by SDS-PAGE and Coomassie blue staining. The Batch 1 and Batch 2 were two experiments. Batch 2 protein were used for subsequent experiments. **C**, ADAR1-FLAG or ADAR1-FLAG with EAA mutation was overexpressed in 293T cells. Cell lysates and biotin-labeled LINC00624 were used for RNA pull-down. immunoblot of FLAG and GAPDH antibodies were shown. **D**, RNA-seq results of HER2+BC core needle biopsy before neoadjuvant treatment was shown. The exon 4 of LINC00624 was illustrated. The blue dashes represent mutations where adenosines were changed to guanines. Representative images of RNA-seq results were shown. **E**, AEI score of WT or ADAR1-KO BT-474 cells were shown. **F**, The RNA expression of ADAR1 was determined by RT-qPCR in LINC00624 overexpression or KO cells, normalized to GAPDH. n=3 biological replicates. Statistical analysis was performed using two-sided t-test. There was no statistical significance found. **G**, Recovery assay of LINC00624 WT and isoform3 (iso3) in LINC00624-KO cells. The levels of the indicated proteins were determined by immunoblot. For **A**-**C,** and **F-G,** the experiment was performed twice with similar results. Data are shown as mean ± s.e.m.

Supplementary Fig. 5

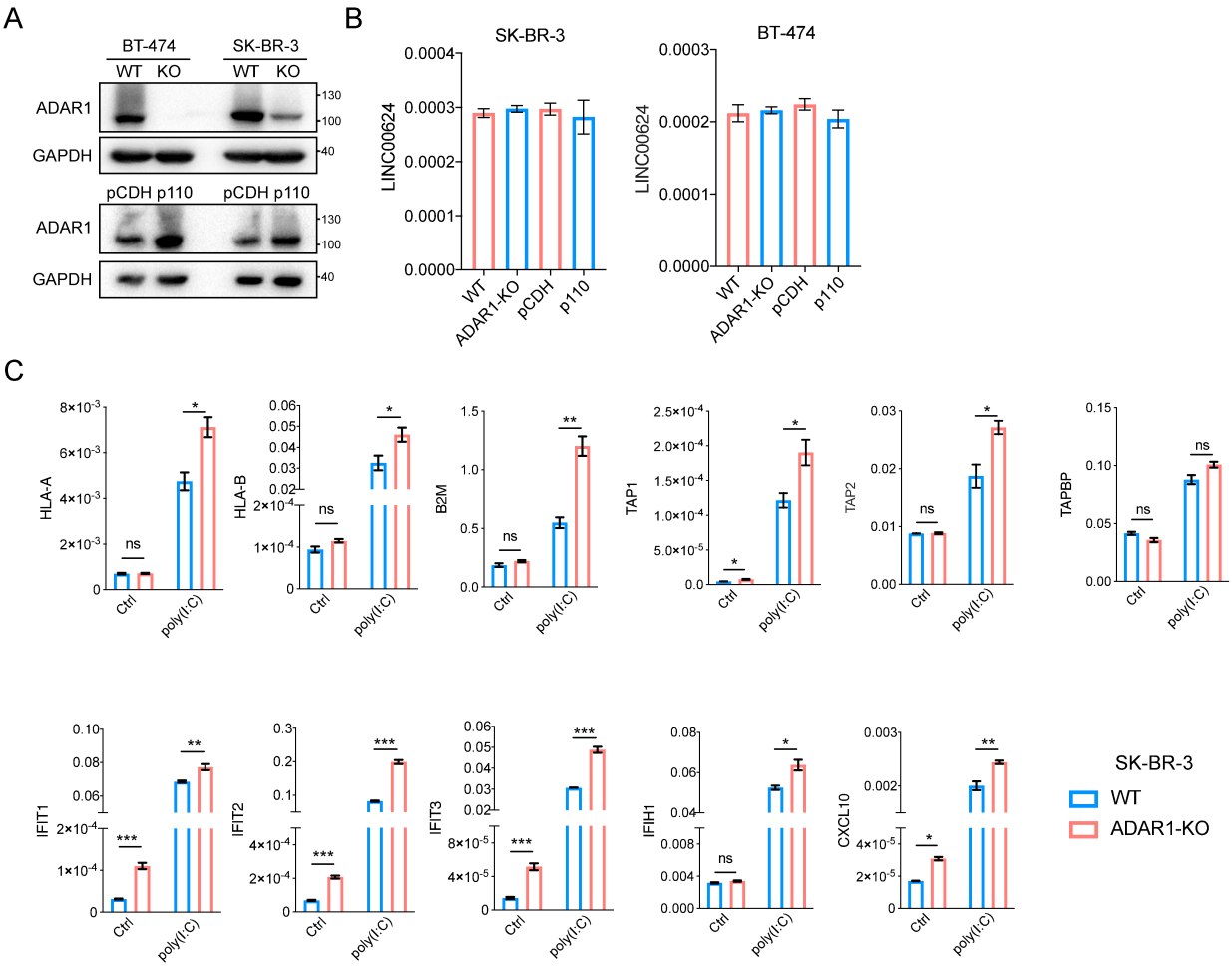

Supplementary Fig. 5 LINC00624 inhibits the immune response and promotes treatment resistance through ADAR1. A, ADAR1-KO or p110 overexpression in SK-BR-3 and BT-474 cells were verified by immunoblot. The experiment was performed twice with similar results. **B**, RNA levels of LINC00624 with ADAR1 KO or overexpression were analyzed by RT-qPCR**.** Normalized to GAPDH. **C**, RNA levels of ISGs and antigen presentation related genes were analyzed by RT-qPCR in WT and ADAR1 KO SK-BR-3 cells, normalized to GAPDH. Cells were transfected with mock or 100 ng/ml poly(I:C) for 24h before RNA extraction. For **B**-**C**, statistical analyses were performed using two-sided t-test. n=3 biological replicates. * P<0.05, ** P<0.01, *** P<0.001. ns, no significance. Data are shown as mean ± s.e.m.

Supplementary Fig. 6

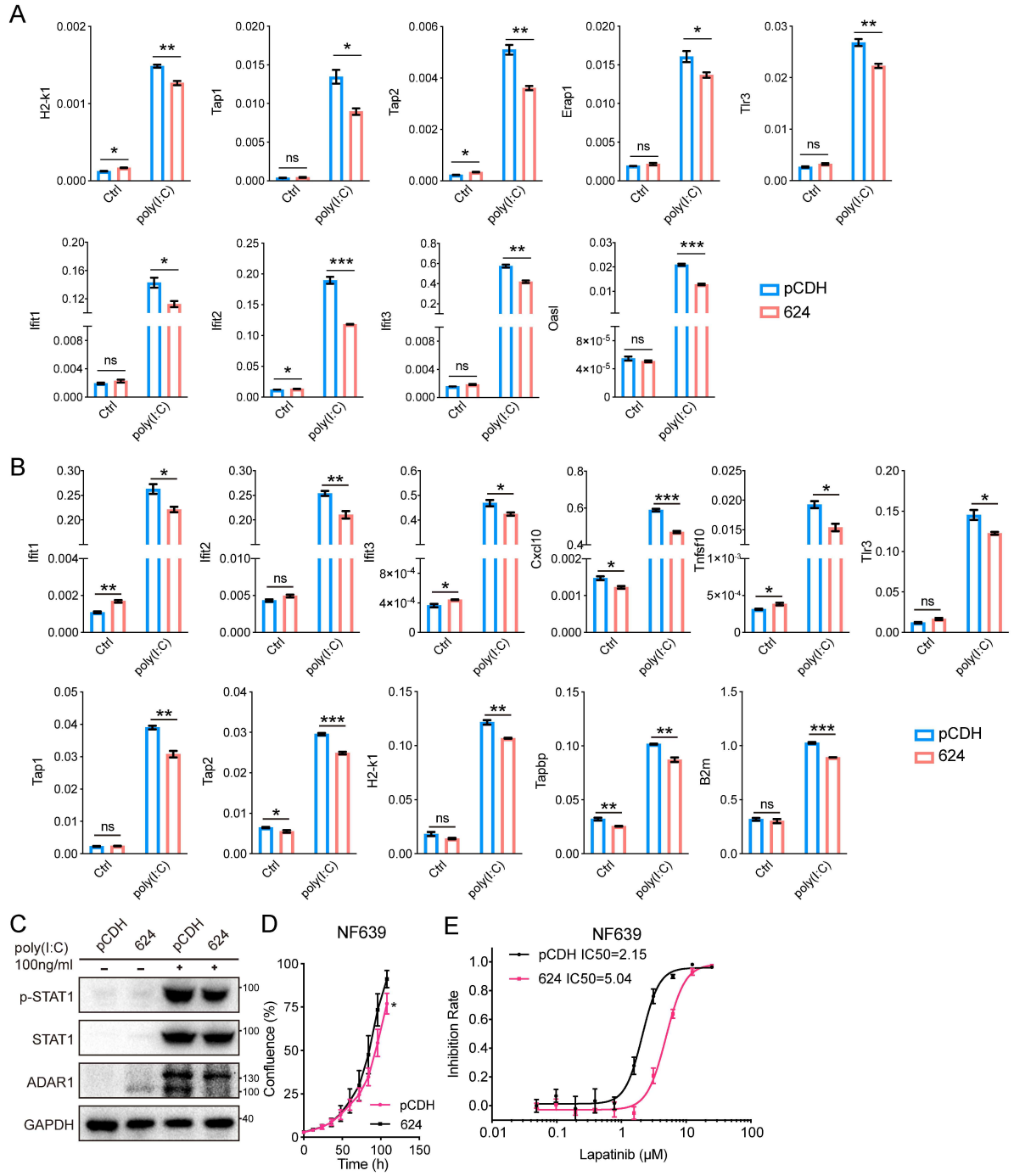

Supplementary Fig. 6 LINC00624 inhibits tumor immunity and immunotherapy response *in vivo*. A-**C**, pCDH or LINC00624 were treated with transfected poly(I:C) for 24h. RNA levels of ISGs and antigen presentation related genes were analyzed by RT-qPCR in B16-OVA (**A**) and NF639 cells (**B**). Normalized to mouse GAPDH. n=3 biological replicates. (**C**) The levels of the indicated proteins were determined by immunoblot. **D**, Cell proliferation assay of pCDH and LINC00624 cells in NF639. n=6 for each time point. Statistical analysis was performed using two-sided t-test at the end point. **E**, Inhibition rate of pCDH and LINC00624 NF639 cells in response to lapatinib. For **C**-**E**, the experiments were performed twice with similar results. For **A**-**B**, statistical analyses were performed using two-sided t-test. * P<0.05, ** P<0.01, *** P<0.001. ns, no significance. Data are shown as mean ± s.e.m.

Supplementary Fig. 7

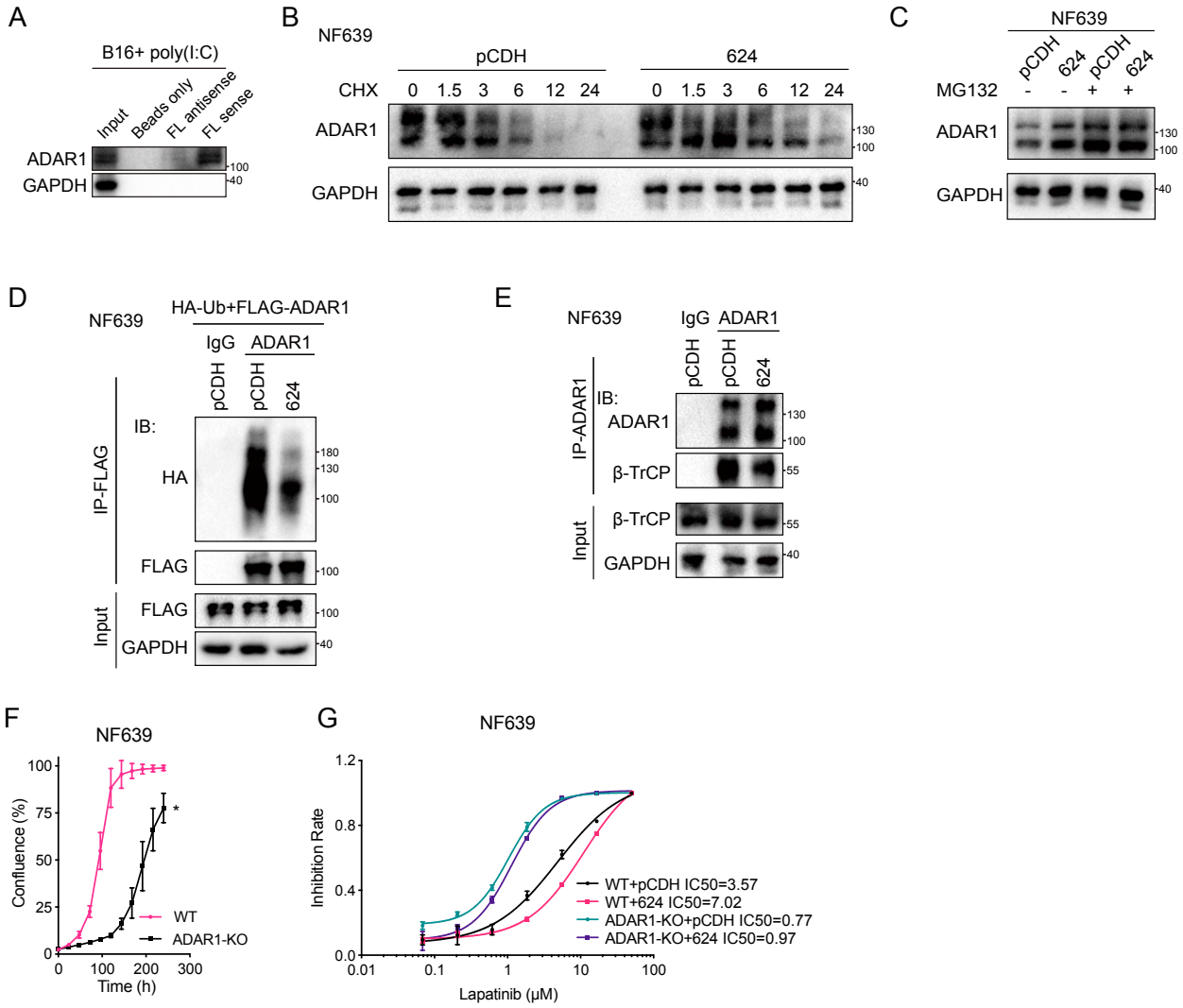

Supplementary Fig. 7

A, B16 cells were transfected with 1 μg/ml poly(I:C) for 24h. Cells were lysed and incubated with biotin-labeled in vitro transcribed RNAs. LINC00624 full-length (FL) sense or antisense RNAs were used. Beads only serving as blank control. Immunoblot of ADAR and GAPDH were shown as indicated. **B**, Expression kinetics of endogenous mouse ADAR1 in NF639 pCDH and LINC00624 overexpression cells. Cells were treated with CHX and collected at the time points as indicated. **C**, NF639 pCDH or LINC00624 cells were treated with MG132 as indicated. The expression of mouse ADAR1 was determined. **D**, pCDH and LINC00624 overexpression NF639 cells were transfected with HA-Ub and mouse ADAR1-p110-FLAG. Cells were treated with MG132 before collection. ADAR1 were immunoprecipitated (IP) with anti-FLAG antibody. IgG isotype control antibody was used. Immunoblot of the HA, FLAG and GAPDH was shown as indicated. **E**, NF639 cells with pCDH control or LINC00624 overexpression were immunoprecipitated (IP) with anti-ADAR1 (Santa Cruz) or IgG isotype control. Mouse ADAR1 and β-TrCP were detected by immunoblot (IB). **F**, Cell proliferation assay of WT and ADAR1-KO cells in NF639. n=6 for each time point. Statistical analysis was performed using two-sided t-test at the end point. **G**, Inhibition rate of WT or ADAR1 KO cells with pCDH or LINC00624 in response to lapatinib. For **A**-**G**, the experiments were performed twice with similar results.

Supplementary Fig. 8

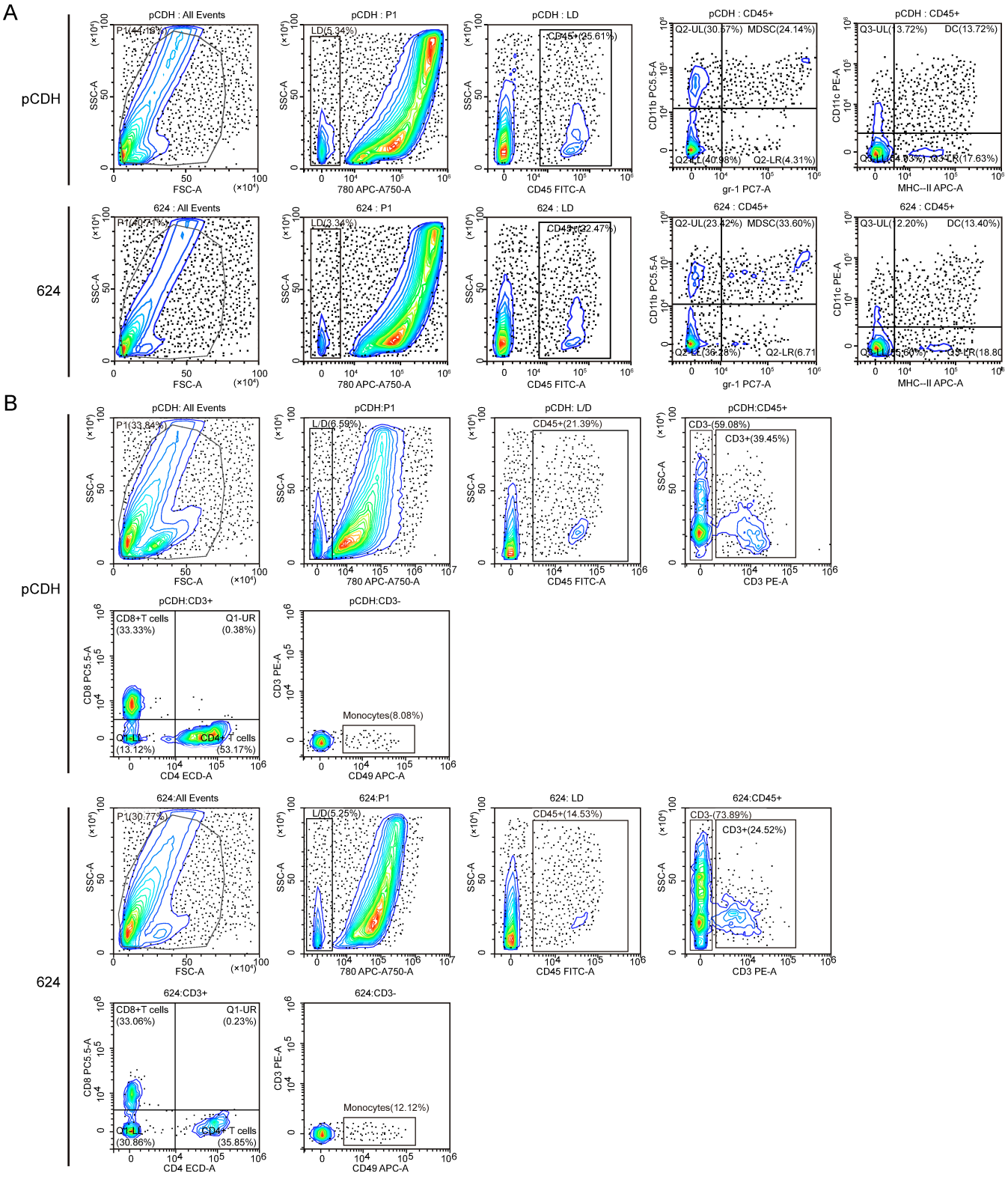

Supplementary Fig. 8 Flow cytometry gating strategies and representative plots. A, Gating strategy and representative flow cytometry plots for the assessment of DCs and MDSCs in pCDH and LINC00624 B16-OVA tumors. **B**, Gating strategy and representative flow cytometry plots for the assessment of CD4+ T cells, CD8+ T cells and CD49f+ cells in pCDH and LINC00624 B16-OVA tumors.

Supplementary Fig. 9

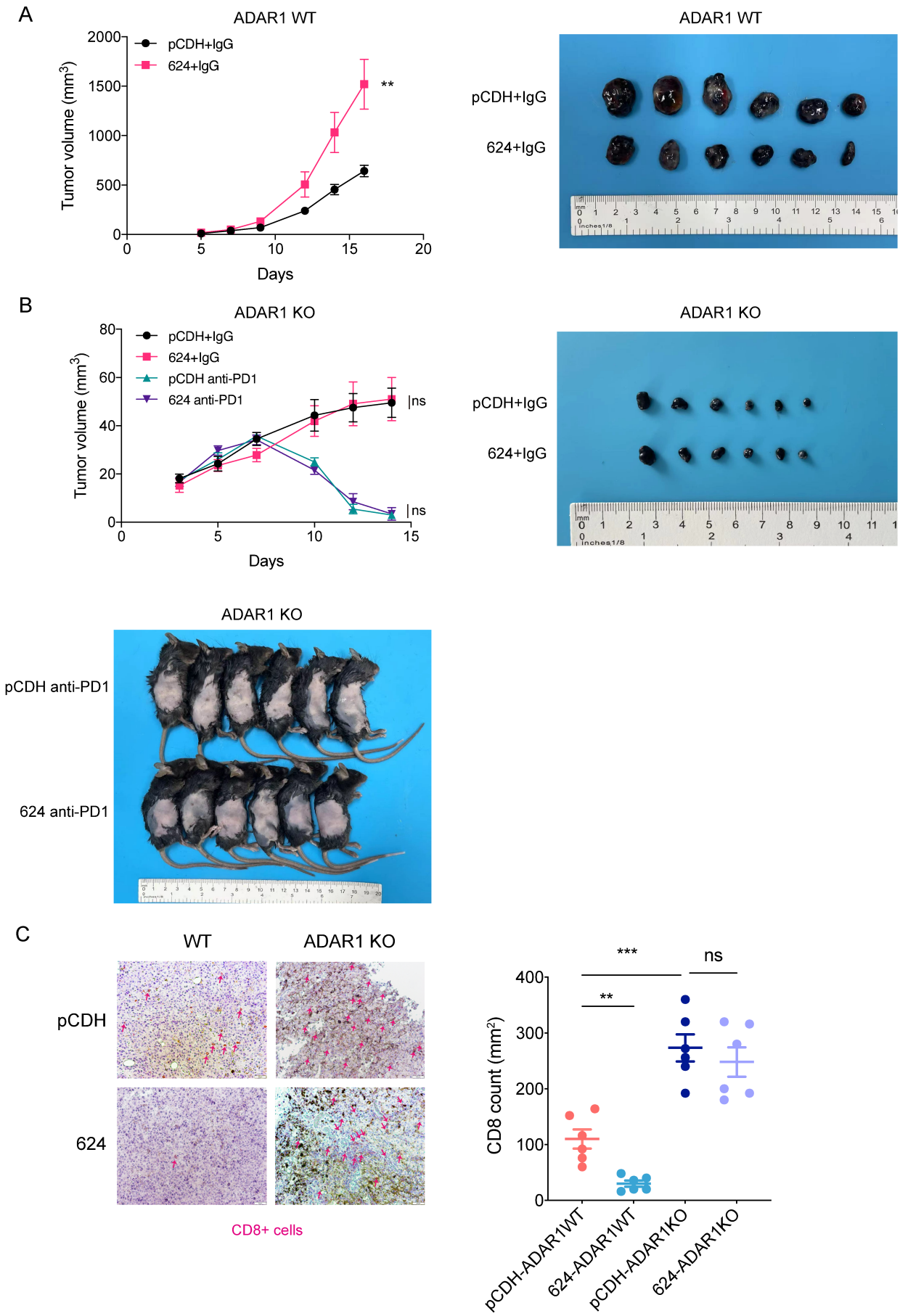

Supplementary Fig. 9 LINC00624 is ADAR1-dependent in suppressing immune responses and promoting treatment resistance *in vivo*. A, Tumor growth curve (left) and tumor size (right) of B16-OVA pCDH or LINC00624 cells with wild-type ADAR1 in C57/B6J. Mice were not vaccinated. Mice were treated with IgG isotype control with 100ug/mice on day 3, 5, 7, 10. n = 6 animals in each group. **B**, Tumor growth curve and tumor size of B16-OVA pCDH or LINC00624 cells with ADAR1-KO in C57/B6J. Mice were not vaccinated. Mice were treated with anti-PD-1 or IgG isotype control as indicated with 100ug/mice on day 3, 5, 7, 10. n = 6 animals in each group. Upper right, representative image of tumor size in IgG control group. Lower left, tumors were regressed in anti-PD-1 groups. **C**, Tumor infiltrated CD8+ cells from pCDH/ADAR1-WT, pCDH/ADAR1-KO, 624/ADAR1-WT, 624 ADAR1-KO tumors with IgG treatment were determined by immunohistochemistry. AEC staining (red) was used in this assay. Left, representative images. Right, statistical analysis (n = 6 tumors each group). Statistical analyses were performed using two-sided t-test. For **A**-**B**, statistical analysis was performed using two-sided t-test for the tumor volume at the end point.

Table S1 Baseline clinicopathological characteristics of patients according to LINC00624 expression

Characteristics		Low expression	High expression	*P* value
Age at diagnosis	<40	9	10	0.565
	≥40	122	178	
BMI at diagnosis	<18.5	5	3	0.352
	18.5-24	85	117	
	>24	40	66	
Subtype	ER+/PR+	73	137	**0.005****
	HER2 positive	29	18	
	TNBC	19	21	
ER	Negative	54	38	**0.000****
	Positive	76	150	
PR	Negative	41	38	**0.007****
	Positive	77	148	
HER2	Negative	76	130	**0.041***
	Positive	46	46	
Ki-67	Low	50	67	0.389
	High	41	42	
Tumor grade	I & II	71	119	0.151
	III	52	62	
pT	pT1	52	68	0.714
	pT2	74	112	
	pT3	4	8	
pN	pN0	58	75	0.898
	pN1	37	56	
	pN2	16	26	
	pN3	20	30	
LVI	Negative	63	108	0.106
	Positive	65	76	

Abbreviations: BR: Breast Cancer; HR: hazard ratio; CI: confidence interval; BMI, body mass index; ER, estrogen receptor; PR, progesterone receptor; HER2, human epidermal growth factor receptor 2; LVI: lymphovascular invasion. Fisher exact test was used. Statistically significant (*P<0.05 and **P<0.01).

Table S2 Univariate COX regression analyses of DFS in BC patients

Characteristics		No of Patients	No of Events	*P* value	HR (95%CI)
Age at diagnosis	<40	19	6		
	≥40	300	84	0.888	0.942 (0.412-2.157)
BMI at diagnosis	<18.5	8	3		
	18.5-24	202	56	0.519	0.682 (0.214-2.179)
	>24	106	30	0.594	0.724 (0.221-2.373)
Subtype	ER+/PR+	250	67		
	HER2 positive	92	11	0.748	0.901 (0.476-1.705)
	TNBC	27	10	0.437	1.302 (0.67-2.531)
ER	Negative	92	25		
	Positive	226	64	0.842	1.049 (0.656-1.677)
PR	Negative	79	23		
	Positive	225	67	0.842	1.049 (0.656-1.677)
HER2	Negative	206	50		
	Positive	92	28	0.217	1.339 (0.842-2.131)
Ki-67	<14%	117	31		
	≥14%	83	29	0.135	1.472 (0.887-2.443)
Tumor grade	I & II	190	47		
	III	114	36	0.139	1.388 (0.899-2.144)
pT	pT1	120	29		
	pT2	186	57	0.18	1.357 (0.868-2.123)
	pT3	12	4	0.406	1.558 (0.548-4.432)
pN	pN0	133	21		
	pN1	93	28	**0.013***	2.053 (1.166-3.615)
	pN2	42	14	**0.015***	2.321 (1.18-4.566)
	pN3	50	26	**0.000****	4.355 (2.447-7.75)
LVI	Negative	171	40		
	Positive	141	45	0.079	1.465 (0.957-2.244)
LINC00624	Low	131	28		
	High	188	62	**0.037***	1.602 (1.025-2.503)

Abbreviations: BR: Breast Cancer; HR: hazard ratio; CI: confidence interval;BMI, body mass index; ER, estrogen receptor; PR, progesterone receptor; HER2, human epidermal growth factor receptor 2; LVI: lymphovascular invasion. Statistically significant (**P*<0.05 and ***P*<0.01).

Table S3 MS result of LINC00624 RNA pull down

gene name	protein score	MW	Cover (%)
NONO	2570	54311	56.3
PTBP1	2158	57357	60.6
PTBP3	1630	59937	50.9
ALB	1574	71317	53.2
TUBA1B	455	50804	34.6
TUBA1C	439	50548	34.7
HNRNPL	433	64720	34.6
FUBP3	415	61944	27.6
MCCC2	376	61808	33.6
ADAR	372	137178	15.6
STAU1	288	63428	22.9
SFPQ	267	76216	11.2
CPNE3	246	60947	19.7
HNRNPM	242	77749	15.1
PTBP2	240	57569	6.2
MCCC1	236	80935	13.2
ILF3	221	95678	8.5
CCT2	206	57794	22.6
DDX5	192	69618	14.8
SERBP1	189	44995	13.5
YBX3	183	40066	25.8
CCT4	172	58401	23.6
HNRNPU	171	91269	6.3
HRNR	168	283140	0.8
EIF2AK2	167	62512	10.7
ACTC1	163	42334	26.5
ACTA1	163	42366	26.5
STAU2	161	62829	17.7
G6PD	154	59675	14
HIST2H2BF	140	13912	24.6

Abbreviations: MS: mass spectrometry; MW: molecular weight;

Table S4 Primers and sequences

Primers for RT-qPCR	
LINC00624-F	CCAGGTTTGCCTTCCTGTTGA
LINC00624-R	GATGCTCCTGTGATGTGCCTC
q2-624-F	CTGTGGCGATGAGAGAGAGAGG
q2-624-R	ACCCAGTACAGTGAAGACAAACC
q3-624-F	GAATACCTACCTTGGGCACAGAA
q3-624-R	CACATTGTCTCTCTAGGTTGCCT
h-NEAT1-F	CTTCCTCCCTTTAACTTATCCATTCAC
h-NEAT1-R	CTCTTCCTCCACCATTACCAACAATAC
h-GAPDH-F	AACGGGAAGCTTGTCATCAA
h-GAPDH-R	TGGACTCCACGACGTACTCA
h-ACTB-F	GCCAACCGCGAGAAGATGA
h-ACTB-R	CATCACGATGCCAGTGGTA
h-IFIT1-F	CGCTATAGAATGGAGTGTCCA
h-IFIT1-R	TTTCCTCCACACTTCAGCA
h-IFIT2-F	CTAAAGCACCTCAAAGGGCA
h-IFIT2-R	GCATAGTTTCCCCAGGTGAC
h-IFIT3-F	AGTCTAGTCACTTGGGGAAAC
h-IFIT3-R	ATAAATCTGAGCATCTGAGAGTC
h-CXCL10-F	TGACTCTAAGTGGCATTCAAGGAG
h-CXCL10-R	TTTTTCTAAAGACCTTGGATTAACAGG
h-B2M-F	AGCAGCATCATGGAGGTTTG
h-B2M-R	TCAAACATGGAGACAGCACTCAA
h-TAPBP-F	CCTGGAGGTAGCAGGTCTTTC
h-TAPBP-R	ATCCTTGCAGGTGGACAGGTA
h-TAP1-F	TGCCCCGCATATTCTCCCT
h-TAP1-R	CACCTGCGTTTTCGCTCTTG
h-TAP2-F	AATCCCTCACTATTCTGGTCGT
h-TAP2-R	TCGAGACATGGTGTAGGTGAAG
h-ERAP1-F	AGAGCACTGAAGCATCTCCAA
h-ERAP1-R	AACTGGGATGACGTACTCAGG
h-NLRC5-F	AACGAGACCTTGGACCCTGAA
h-NLRC5-R	GCTGGTGAACCCATCATCATAG
m-H-2K1-k-F	GAGACACAGGTCGCCAAGAAC
m-H-2K1-k-R	CGCTGGTAAGTGTGAGAGCC
m-OASL-F	CAGGAGCTGTACGGCTTCC
m-OASL-R	CCTACCTTGAGTACCTTGAGCAC
m-TLR3-F	GTGAGATACAACGTAGCTGACTG
m-TLR3-R	TCCTGCATCCAAGATAGCAAGT
m-B2M-F	TTCTGGTGCTTGTCTCACTGA
m-B2M-R	CAGTATGTTCGGCTTCCCATTC
m-ACTB-F	GTGACGTTGACATCCGTAAAGA
m-ACTB-R	GCCGGACTCATCGTACTCC
m-TNFSF10-F	GCTTGCAGGTTAAGAGGCAAC
m-TNFSF10-R	GCTTCTCCGAGTGATCCCAG
m-CXCL10-F	CCAAGTGCTGCCGTCATTTTC
m-CXCL10-R	GGCTCGCAGGGATGATTTCAA

m-IFIT1-F	CTGAGATGTCACTTCACATGGAA
m-IFIT1-R	GTGCATCCCCAATGGGTTCT
m-IFIT2-F	AGTACAACGAGTAAGGAGTCACT
m-IFIT2-R	AGGCCAGTATGTTGCACATGG
m-IFIT3-F	GCCGTTACAGGGAAATACTGGA
m-IFIT3-R	TAGGAGTTCAAAGGACTTCGCC
m-Adar-F	TGAGCATAGCAAGTGGAGATACC
m-Adar-R	GCCGCCCTTTGAGAAACTCT
m-Tap1-F	GGACTTGCCTTGTTCCGAGAG
m-Tap1-R	GCTGCCACATAACTGATAGCGA
m-Tap2-F	CTGGCGGACATGGCTTTACTT
m-Tap2-R	CTCCCACTTTTAGCAGTCCCC
m-Tapbp-F	GGCCTGTCTAAGAAACCTGCC
m-Tapbp-R	CCACCTTGAAGTATAGCTTTGGG
m-Erap1-F	TAATGGAGACTCATTCCCTTGGA
m-Erap1-R	AAAGTCAGAGTGCTGAGGTTTG

Primers for RACE

5'624-1	GTAAGCCCCCACTGACTAAGGTAGC
5'624-2	CTTTCATGCATCAGGTGGCAGTGTT
3'624-1	TAATGTCTCTCTTCTCTGGGGTGTC
isoform-F	CTGCTGTGGGAGCTTTGTTCTTTC
isoform-R	TATGCGTGCTGTAACAAGGTGC

Primers for CRISPR verification

624-KO-F	TTCAGAAGATTCATGGTGCTCTGGG
624-KO-R	GAGTGACCTCCAAGGATTATTCAGGG
h-ADARKO-F	AGCAACTCCACATCTGCCTTGG
h-ADARKO-R	TGTTCGTATTTCTCTTGATTTGCATCC
m-ADARKO-F	AGCTTCAGCAGATAGAGTTTCTCAAAGGG
m-ADARKO-R	GCAGTCTCATTGGTCCTGGTCTGG

Primers for IVT

T7-624/SEG1-F	TAATACGACTCACTATAGGGAGAAGCTGCTG CAACCCG
624/SEG1-R	GTTAATTATTTTATTGATACATAATAGATGTA CATATTTTGAGGG
T7-SEG2-F	TAATACGACTCACTATAGGGATTCATCAGAA TTGCTGGAGAGTCC
SEG2-R	TAAAATCAGTATCTTTGGATACTCGTGTAATT ATTC
T7-SEG3-F	TAATACGACTCACTATAGGGATACTGATTTTA GGAGAACAAGGTTGTTGG
SEG3-R	CATTTCTAGTTTCAGGAAAACAAAATTGTTG GG
T7-Alu-PHACTR4-F	TAATACGACTCACTATAGGGATGTGGACTTG CTGAAGAAACAGAATATC

Alu-PHACTR4-R	TTGTCACTTCTCTTCCCTCAGTTATCCC

ASOs	
ASO-LINC00624-1	GCCTATTTATTCACACCAAG
ASO-LINC00624-2	TGTTTCCTGCAGTATGCACC
ASO-LINC00624-3	GCAGAAGTAGGCCACATCTT
ASO-LINC00624-4	GAATACCTACCTTGGGCACA
ASO-LINC00624-5	CAACTTGCCTGGTACGGAGG

CRISPR Target sequence	
624-F1	GGGTATAAAAGCTGGCCACG
624-F2	GGAGGACACATGATAAGGAG
624-R1	GCAGAACTTTGTGCAGTACT
624-R2	GACCTGCTGCTCCTTGAAGG
h-ADAR-1	CTGCAGGGGTATTCCCTCAG
h-ADAR-2	TTAGAACCACCACCTTCAAC
m-ADAR-1	TTCCAAGTCAATCAGCACTG
m-ADAR-2	TGTGACTCTCAGAAATCAG

Table S5 Conservation Analysis of LINC00624 by PLAR database

Symbol	Transcripts With Conservation	Non-redundant Exons	Species With Seq Orthologs	Species With BLAST	Species With WGA	Species With Synteny	Species With Sequence And Synteny	Mouse BLAST	Mouse WGA	Mouse Synteny	Mouse Sequence+Synteny
NEAT1	ENST00000499732.3_2, ENST00000501122.2_1, ENST00000601801.3_2, ENST00000612303.2_2, ENST00000616315.2_2, ENST00000642367.1_1, ENST00000645023.1_1, ENST00000646243.1_1	1	Mouse, Dog, Ferret, Marmoset, Opossum, Rabbit	Mouse, Dog, Ferret, Marmoset, Opossum, Rabbit	Mouse, Dog, Ferret, Marmoset	Mouse, Dog, Ferret, Gar, Lizard, Marmoset, Opossum	Mouse, Dog, Ferret, Marmoset, Opossum	ENSMUST00000173672.1, ENSMUST00000174287.1, ENSMUST00000174829.1, ENSMUST00000232969.1	ENSMUST00000173672.1, ENSMUST00000174287.1, ENSMUST00000174829.1	ENSMUST00000172812.2, ENSMUST00000173314.1, ENSMUST00000173499.1, ENSMUST00000173672.1, ENSMUST00000174287.1, ENSMUST00000174808.1, ENSMUST00000174829.1, ENSMUST00000232969.1	ENSMUST00000173672.1, ENSMUST00000174287.1, ENSMUST00000174829.1, ENSMUST00000232969.1
LINC00624	ENST00000619867.4_1, ENST00000621316.1_1	7	Dog, Rhesus	Rhesus	Dog, Rhesus	Mouse, Dog, Gar, Rabbit, Rhesus	Dog, Rhesus	-	-	ENSMUST00000198613.1, ENSMUST00000199972.1	-

Data were extracted from PLAR database. BLAST: Basic Local Alignment Search Tool. WGA: Whole-Genome Amplification. NEAT1 were shown as control.

Supplementary File 1

Sequences

1.LINC00624-isoform1 full-length (FL, 3372nt)

AGCTGCTGCAACCCGCTGCCCTCTGGTGTCCTGCTGTGGGAGCTTTGTTCTTTCAC
TCTCGTAATAAGTCTTGCTGCTGCTCACTCTTTGGGTCCGCACTGTCTCTGTGAGCT
GTAACACTCACCGCGAGGTTCTGTGCCTTCGTTCTTTAAGTCAGGGAGACCACGAAC
CCACCGGGAGGAACAAACAACTGTGATGCGCCATCTTTAAGAGCTGTAACATTCACC
GCCGGGGTCTGCGGCTTCATTCCTGGAGTGAGTGAGACCACGAACCCACCAGAAG
GAAGAAACTCTGGACCCATCTGAACAGCTGAAGGAACAAACTCCGGACACACCATC
TTTAAGAACTGTAACACTCACCGGGAGTCTCCGTGGCTTCATTCTTGAAGACAGCGA
GACCAAGAACCCACCAGAAGGAATGAATTCCGCACACAGCAACAGCACAAAGTTAAA
CCAGGAAGTCCCTCTGCCTTGCTAGGGATCCAGGTTTGCCTTCCTGTTGAGGTATCC
CATTTCATTACAGTTGACCTAAGTTTGAACAAACACTGCCACCTGATGCATGAAAGCT
CTACTGTGACCTACGTTAAAAGGAGCTGACACTCCCTCAGGCTACCTTAGTCAGTGG
GGGCTTACTGCAGCATACCTGTGGCGATGAGAGAGAGAGGCACATCACAGGAGCAT
CTGGCACCAGTGGCATCCTGAATTTAAGATGAAACAATAGAGAAAGAACCAAGAAGT
TACATACATTCATCAGAATTGCTGGAGAGTCCTGACCTCTGGCCATCGATCAAAGGGA
AGCGTTCACTACTGAAGGTTTGTCTTCACTGTACTGGGTATTCAACTTCCTTGAAATT
AAAAGGAAGAAGGATAAAAAGTGGTATGCTGAATGGATTAAAGGTAATATTTTGATTAT
ATCAATAGTTTTCAAACTTTTATAACTCATGAGCTGTTTGGGAATATTTGAGCATATGGT
CAATCCACATCTGAATTATCCTGCCCACAAAAATGTCAAGGAAATACTTCTACTGCCC
CTTCTGAAGCCATCTTAATTCCAGGAGTTGAATCAATTTCAAAGTCATTGATAACTGCA
TCAGCCAAAATTTGTCCAAATGTTTTGAAATGCATTTCTATTTCCTGTCACACCTACCT
CTTTGGCTAATGCATTCATTTTATGAGTTTCAAAAATTACCATCTCCCTGTCCCAGGTC
TTTAAAGTTGTTGAATAAGCAAATCTCTGTTCACTTTATTTGTACTATTTATGGTTATATA
GATTTAATTACTTCTAATTAGATTTCCATATTGGAAGTACAAATCTAACCTTAAACAAAAA
ATTCTTTTTATAATTCTCAATATCTCCAATTATTTTGAGCTTGTGCTCTCTGGATCTTTTC
AAGTTATGGCAAACTTGGTTTTGAGGCATAGCAGCAAGAACTACATAAATCTTTTCAAA
CAGAGATATACCAGTATAAAGCTTGCTTTCCAGTATAGTCCTTAATGATTTTCTTCATTT
TCTAGGTCTTTTTGCCTGATGCAGAATATTGGTACATATGCTGGGGTCAACATTTAATG
ACTCTGGGTCTTTTTCTTGAGCAGAATCTAAGGGATAGTCTTTCATTTTATAGATGTGT
TTTAGATTACTCATAAATTCATTACTTTTTCCTCACACACATTATAACATCTCTTAAGGCT
CTGCCCATTGACACGAATCTCAGGATTATTCTATAATGTCTCTCTTCTCTGGGGTGTCT
TCTTTCTGGGGAGATTTGTATATCTTGGAGTCTGAGACTTCACTATGTACTCCTTCCTT
ATCATCATTTATAAACCTATTCAACAGACTCTGCCCCAGAATGGATTCTTGAGCAATCT
TGAATAATTACACGAGTATCCAAAGATACTGATTTTAGGAGAACAAGGTTGTTGGGTAC
AGGTAGTTAATTATTCCTAAAACTGAATATGTCCAATACCTATGTCTTGAGAAGCTCTAA
GAGAGTAACAGAAGAGCAACAATGGAATGTGACAATTGCCTGCACTGTCTTTCTAGG
TTGAAAATCCAAGAAATTTACATGCACTGAATTTTATTTCCTTTATTTGCCTATTTATTCA
CACCAAGAATTCAGGGTCCATGTTGCTGTAGTGGAAATTGGTTATTTCTGTTTTAGTC
TTGAATTGTCTAATTTTGTTCAACTTGCCTGGTACGGAGGGGAGATTCACCAGTGGG
CCTCACCTGTAAGTGAGGGTCACATCTGTAATTCTCTGATCTCGTGATGCAGAAGTAG
GCCACATCTTCCATTTTCATCCTTGGATTCCTGTGGAATTTACAGATGCACAGATAGAA

GTCATTTAGTCTTAGATAGATACCTTCATCTGCTTTGTCAATTGATGATGAATAAGACTG
AGTTGAATGTATTTAGAATGTCTTGGCTATAAATTCCTCCATATAGCTTAACCCACTGTT
TCCTGCAGTATGCACCCCTTTACCAAGAGAGAGAAAGAGAGAAAGAATTTCATGTTTC
TGTGGGTTTTAGAAGGCTATAGGAAGGGATTTTTGTTTGCTCATTTTCAGAACTTATTA
ATAGACAGTTATTGAATACCTACCTTGGGCACAGAAATAATCACATTCTCTCCTGAGAA
TTTTCAACCCACAGCCAAGTACAGGTGTGGAAATTTGATGATAGAATTAATACCAATG
GAAAAAGGGGCCCACAGAACTGAAAAAGTGGCCACTGGTGATGACAGTGACCTGG
GAGGGAGCGAGGCAACCTAGAGAGACAATGTGGGGAATCATCACGTTCCATTACAG
CGCCCTTCTCTTACTCTCTTGGAGCTTCTCAAGCCACAGGTGTCAGTCATATTGGTTT
TAGAGATTATTAGTAACTACCCAAACCCAACAATTTTGTTTTCCTGAAACTAGAAATGT
CCTGTTTCCAACTTTATATTTTCATCAACTTCTTTTTCTATGATGTGTGAGAAACTAGAA
TATTCAGTGTGCTTTCTTGAATACCAGCCTTGTTTCAACTCTTTAATGAGTGGACTATT
CTCTGAAGCTGGCCCTCAGTCTTACTCTGGGTTCATCAACCAAGGTCAAGATCTGTC
CACATGCACGTAACAGGAGCACTTTTCCGAGAATTGTAAAGGAGCCACGGTGCAAA
GCCTTCTGGACCTGGGTCTCATGTGAAAACTCAGCAATGAGCCTCCTGGCCTGAGA
TGAGCCTGCGGAGCACCTTGTTACAGCACGCATATGATGTATATAAAAAATGAACACA
TGTATTCCAATTACACTGATTTGATCTTTACAAACTATATGGATGTATTAAATTGTCACAT
GTACCCTCAAAATATGTACATCTATTATGTATCAATAAAATAATTAACA

* Segment 1 Uncolored; Segment 2 Green ; Segment 3 Yellow

2. LINC00624-isoform2 (2754nt)

AGCTGCTGCAACCCGCTGCCCTCTGGTGTCCTGCTGTGGGAGCTTTGTTCTTTCAC
TCTCGTAATAAGTCTTGCTGCTGCTCACTCTTTGGGTCCGCACTGTCTCTGTGAGCT
GTAACACTCACCGCGAGGTTCTGTGCCTTCGTTCTTTAAGTCAGGGAGACCACGAAC
CCACCGGGAGGAACAAACAACTGTGATGCGCCATCTTTAAGAGCTGTAACATTCACC
GCCGGGGTCTGCGGCTTCATTCCTGGAGTGAGTGAGACCACGAACCCACCAGAAG
GAAGAAACTCTGGACCCATCTGAACAGCTGAAGGAACAAACTCCGGACACACCATC
TTTAAGAACTGTAACACTCACCGGGAGTCTCCGTGGCTTCATTCTTGAAGACAGCGA
GACCAAGAACCCACCAGAAGGAATGAATTCCGCACACAGCAACAGCACAAAGTTAAA
CCAGGAAGTCCCTCTGCCTTGCTAGGGATCCAGGTTTGCCTTCCTGTTGAGGTATCC
CATTTCATTACAGTTGACCTAAGTTTGAACAAACACTGCCACCTGATGCATGAAAGCT
CTACTGTGACCTACGTTAAAAGGAGCTGACACTCCCTCAGGCTACCTTAGTCAGTGG
GGGCTTACTGCAGCATACCTGTGGCGATGAGAGAGAGAGGCACATCACAGGAGCAT
CTGGCACCAGTGGCATCCTGAATTTAAGATGAAACAATAGAGAAAGAACCAAGAAGT
TACATACATTCATCAGAATTGCTGGAGAGTCCTGACCTCTGGCCATCGATCAAAGGGA
AGCGTTCACTACTGAAGGTTTGTCTTCACTGTACTGGGTATTCAACTTCCTTGAAATT
AAAAGGAAGAAGGATAAAAAGTGGTATGCTGAATGGATTAAAGGTCTTTTTGCCTGAT
GCAGAATATTGGTACATATGCTGGGGTCAACATTTAATGACTCTGGGTCTTTTTCTTGA
GCAGAATCTAAGGGATAGTCTTTCATTTTATAGATGTGTTTTAGATTACTCATAAATTCA
TTACTTTTTCCTCACACACATTATAACATCTCTTAAGGCTCTGCCCATTGACACGAATC
TCAGGATTATTCTATAATGTCTCTCTTCTCTGGGGTGTCTTCTTTCTGGGGAGATTTGT
ATATCTTGGAGTCTGAGACTTCACTATGTACTCCTTCCTTATCATCATTTATAAACCTAT

TCAACAGACTCTGCCCCAGAATGGATTCTTGAGCAATCTTGAATAATTACACGAGTAT
CCAAAGATACTGATTTTAGGAGAACAAGGTTGTTGGGTACAGGTAGTTAATTATTCCTA
AAACTGAATATGTCCAATACCTATGTCTTGAGAAGCTCTAAGAGAGTAACAGAAGAGC
AACAATGGAATGTGACAATTGCCTGCACTGTCTTTCTAGGTTGAAAATCCAAGAAATT
TACATGCACTGAATTTTATTTCCTTTATTTGCCTATTTATTCACACCAAGAATTCAGGGT
CCATGTTGCTGTAGTGGAAATTGGTTATTTCTGTTTTAGTCTTGAATTGTCTAATTTTGT
TCAACTTGCCTGGTACGGAGGGGAGATTCACCAGTGGGCCTCACCTGTAAGTGAGG
GTCACATCTGTAATTCTCTGATCTCGTGATGCAGAAGTAGGCCACATCTTCCATTTTC
ATCCTTGGATTCCTGTGGAATTTACAGATGCACAGATAGAAGTCATTTAGTCTTAGATA
GATACCTTCATCTGCTTTGTCAATTGATGATGAATAAGACTGAGTTGAATGTATTTAGA
ATGTCTTGGCTATAAATTCCTCCATATAGCTTAACCCACTGTTTCCTGCAGTATGCACC
CCTTTACCAAGAGAGAGAAAGAGAGAAAGAATTTCATGTTTCTGTGGGTTTTAGAAG
GCTATAGGAAGGGATTTTTGTTTGCTCATTTTCAGAACTTATTAATAGACAGTTATTGAA
TACCTACCTTGGGCACAGAAATAATCACATTCTCTCCTGAGAATTTTCAACCCACAGC
CAAGTACAGGTGTGGAAATTTGATGATAGAATTAATACCAATGGAAAAAGGGGCCCAC
AGAACTGAAAAAGTGGCCACTGGTGATGACAGTGACCTGGGAGGGAGCGAGGCAA
CCTAGAGAGACAATGTGGGGAATCATCACGTTCCATTACAGCGCCCTTCTCTTACTCT
CTTGGAGCTTCTCAAGCCACAGGTGTCAGTCATATTGGTTTTAGAGATTATTAGTAACT
ACCCAAACCCAACAATTTTGTTTTCCTGAAACTAGAAATGTCCTGTTTCCAACTTTATA
TTTTCATCAACTTCTTTTTCTATGATGTGTGAGAAACTAGAATATTCAGTGTGCTTTCTT
GAATACCAGCCTTGTTTCAACTCTTTAATGAGTGGACTATTCTCTGAAGCTGGCCCTC
AGTCTTACTCTGGGTTCATCAACCAAGGTCAAGATCTGTCCACATGCACGTAACAGG
AGCACTTTTCCGAGAATTGTAAAGGAGCCACGGTGCAAAGCCTTCTGGACCTGGGT
CTCATGTGAAAACTCAGCAATGAGCCTCCTGGCCTGAGATGAGCCTGCGGAGCACC
TTGTTACAGCACGCATATGATGTATATAAAAAATGAACACATGTATTCCAATTACACTGA
TTTGATCTTTACAAACTATATGGATGTATTAAATTGTCACATGTACCCTCAAAATATGTAC
ATCTATTATGTATCAATAAAATAATTAACA

3. LINC00624-isoform3 (2363nt)

AGCTGCTGCAACCCGCTGCCCTCTGGTGTCCTGCTGTGGGAGCTTTGTTCTTTCAC
TCTCGTAATAAGTCTTGCTGCTGCTCACTCTTTGGGTCCGCACTGTCTCTGTGAGCT
GTAACACTCACCGCGAGGTTCTGTGCCTTCGTTCTTTAAGTCAGGGAGACCACGAAC
CCACCGGGAGGAACAAACAACTGTGATGCGCCATCTTTAAGAGCTGTAACATTCACC
GCCGGGGTCTGCGGCTTCATTCCTGGAGTGAGTGAGACCACGAACCCACCAGAAG
GAAGAAACTCTGGACCCATCTGAACAGCTGAAGGAACAAACTCCGGACACACCATG
TTTAAGAACTGTAACACTCACCGGGAGTCTCCGTGGCTTCATTCTTGAAGACAGCGA
GACCAAGAACCCACCAGAAGGAATGAATTCCGCACACAGCAACAGCACAAAGTTAAA
CCAGGAAGTCCCTCTGCCTTGCTAGGGATCCAGGTTTGCCTTCCTGTTGAGGTATCC
CATTTCATTACAGTTGACCTAAGTTTGAACAAACACTGCCACCTGATGCATGAAAGCT
CTACTGTGACCTACGTTAAAAGGAGCTGACACTCCCTCAGGCTACCTTAGTCAGTGG
GGGCTTACTGCAGCATACCTGTGGCGATGAGAGAGAGAGGCACATCACAGGAGCAT
CTGGCACCAGTGGCATCCTGAATTTAAGATGAAACAATAGAGAAAGAACCAAGAAGT
TACATACATTCATCAGAATTGCTGGAGAGTCCTGACCTCTGGCCATCGATCAAAGGGA
AGCGTTCACTACTGAAGGTTTGTCTTCACTGTACTGGGTATTCAACTTCCTTGAAATT

AAAAGGAAGAAGGATAAAAAGTGGTATGCTGAATGGATTAAAGGTAATATTTTGATTAT
ATCAATAGTTTTCAAACTTTTATAACTCATGAGCTGTTTGGGAATATTTGAGCATATGGT
CAATCCACATCTGAATTATCCTGCCCACAAAAATGTCAAGGAAATACTTCTACTGCCC
CTTCTGAAGCCATCTTAATTCCAGGAGTTGAATCAATTTCAAAGTCATTGATAACTGCA
TCAGCCAAAATTTGTCCAAATGTTTTGAAATGCATTTCTATTTCCTGTCACACCTACCT
CTTTGGCTAATGCATTCATTTTATGAGTTTCAAAAATTACCATCTCCCTGTCCCAGGTC
TTTAAAGTTGTTGAATAAGCAAATCTCTGTTCACTTTATTTGTACTATTTATGGTTATATA
GATTTAATTACTTCTAATTAGATTTCCATATTGGAAGTACAAATCTAACCTTAAACAAAAA
ATTCTTTTTATAATTCTCAATATCTCCAATTATTTTGAGCTTGTGCTCTCTGGATCTTTTC
AAGTTATGGCAAACTTGGTTTTGAGGCATAGCAGCAAGAACTACATAAATCTTTTCAAA
CAGAGATATACCAGTATAAAGCTTGCTTTCCAGTATAGTCCTTAATGATTTTCTTCATTT
TCTAGGTCTTTTTGCCTGATGCAGAATATTGGTACATATGCTGGGGTCAACATTTAATG
ACTCTGGGTCTTTTTCTTGAGCAGAATCTAAGGGATAGTCTTTCATTTTATAGATGTGT
TTTAGATTACTCATAAATTCATTACTTTTTCCTCACACACATTATAACATCTCTTAAGGCT
CTGCCCATTGACACGAATCTCAGGATTATTCTATAATGTCTCTCTTCTCTGGGGTGTCT
TCTTTCTGGGGAGATTTGTATATCTTGGAGTCTGAGACTTCACTATGTACTCCTTCCTT
ATCATCATTTATAAACCTATTCAACAGACTCTGCCCCAGAATGGATTCTTGAGCAATCT
TGAATAATTACACGAGTATCCAAAGATACTGACTAGAAATGTCCTGTTTCCAACTTTATA
TTTTCATCAACTTCTTTTTCTATGATGTGTGAGAAACTAGAATATTCAGTGTGCTTTCTT
GAATACCAGCCTTGTTTCAACTCTTTAATGAGTGGACTATTCTCTGAAGCTGGCCCTC
AGTCTTACTCTGGGTTCATCAACCAAGGTCAAGATCTGTCCACATGCACGTAACAGG
AGCACTTTTCCGAGAATTGTAAAGGAGCCACGGTGCAAAGCCTTCTGGACCTGGGT
CTCATGTGAAAACTCAGCAATGAGCCTCCTGGCCTGAGATGAGCCTGCGGAGCACC
TTGTTACAGCACGCATATGATGTATATAAAAAATGAACACATGTATTCCAATTACACTGA
TTTGATCTTTACAAACTATATGGATGTATTAAATTGTCACATGTACCCTCAAAATATGTAC
ATCTATTATGTATCAATAAAATAATTAACA

4.LINC00624-isoform4 (1745nt)

AGCTGCTGCAACCCGCTGCCCTCTGGTGTCCTGCTGTGGGAGCTTTGTTCTTTCAC
TCTCGTAATAAGTCTTGCTGCTGCTCACTCTTTGGGTCCGCACTGTCTCTGTGAGCT
GTAACACTCACCGCGAGGTTCTGTGCCTTCGTTCTTTAAGTCAGGGAGACCACGAAC
CCACCGGGAGGAACAAACAACTGTGATGCGCCATCTTTAAGAGCTGTAACATTCACC
GCCGGGGTCTGCGGCTTCATTCCTGGAGTGAGTGAGACCACGAACCCACCAGAAG
GAAGAAACTCTGGACCCATCTGAACAGCTGAAGGAACAAACTCCGGACACACCATC
TTTAAGAACTGTAACACTCACCGGGAGTCTCCGTGGCTTCATTCTTGAAGACAGCGA
GACCAAGAACCCACCAGAAGGAATGAATTCCGCACACAGCAACAGCACAAAGTTAAA
CCAGGAAGTCCCTCTGCCTTGCTAGGGATCCAGGTTTGCCTTCCTGTTGAGGTATCC
CATTTCATTACAGTTGACCTAAGTTTGAACAAACACTGCCACCTGATGCATGAAAGCT
CTACTGTGACCTACGTTAAAAGGAGCTGACACTCCCTCAGGCTACCTTAGTCAGTGG
GGGCTTACTGCAGCATACCTGTGGCGATGAGAGAGAGAGGCACATCACAGGAGCAT
CTGGCACCAGTGGCATCCTGAATTTAAGATGAAACAATAGAGAAAGAACCAAGAAGT
TACATACATTCATCAGAATTGCTGGAGAGTCCTGACCTCTGGCCATCGATCAAAGGGA
AGCGTTCACTACTGAAGGTTTGTCTTCACTGTACTGGGTATTCAACTTCCTTGAAATT
AAAAGGAAGAAGGATAAAAAGTGGTATGCTGAATGGATTAAAGGTCTTTTTGCCTGAT

GCAGAATATTGGTACATATGCTGGGGTCAACATTTAATGACTCTGGGTCTTTTTCTTGA
GCAGAATCTAAGGGATAGTCTTTCATTTTATAGATGTGTTTTAGATTACTCATAAATTCA
TTACTTTTTCCTCACACACATTATAACATCTCTTAAGGCTCTGCCCATTGACACGAATC
TCAGGATTATTCTATAATGTCTCTCTTCTCTGGGGTGTCTTCTTTCTGGGGAGATTTGT
ATATCTTGGAGTCTGAGACTTCACTATGTACTCCTTCCTTATCATCATTTATAAACCTAT
TCAACAGACTCTGCCCCAGAATGGATTCTTGAGCAATCTTGAATAATTACACGAGTAT
CCAAAGATACTGACTAGAAATGTCCTGTTTCCAACTTTATATTTTCATCAACTTCTTTTT
CTATGATGTGTGAGAAACTAGAATATTCAGTGTGCTTTCTTGAATACCAGCCTTGTTTC
AACTCTTTAATGAGTGGACTATTCTCTGAAGCTGGCCCTCAGTCTTACTCTGGGTTCA
TCAACCAAGGTCAAGATCTGTCCACATGCACGTAACAGGAGCACTTTTCCGAGAATT
GTAAAGGAGCCACGGTGCAAAGCCTTCTGGACCTGGGTCTCATGTGAAAACTCAGC
AATGAGCCTCCTGGCCTGAGATGAGCCTGCGGAGCACCTTGTTACAGCACGCATAT
GATGTATATAAAAAATGAACACATGTATTCCAATTACACTGATTTGATCTTTACAAACTAT
ATGGATGTATTAAATTGTCACATGTACCCTCAAAATATGTACATCTATTATGTATCAATAA
AATAATTAACA

5.LINC00624-Segment 3 (S3)

GATACTGATTTTAGGAGAACAAGGTTGTTGGGTACAGGTAGTTAATTATTCCTAAAACT
GAATATGTCCAATACCTATGTCTTGAGAAGCTCTAAGAGAGTAACAGAAGAGCAACAA
TGGAATGTGACAATTGCCTGCACTGTCTTTCTAGGTTGAAAATCCAAGAAATTTACAT
GCACTGAATTTTATTTCCTTTATTTGCCTATTTATTCACACCAAGAATTCAGGGTCCATG
TTGCTGTAGTGGAAATTGGTTATTTCTGTTTTAGTCTTGAATTGTCTAATTTTGTTCAAC
TTGCCTGGTACGGAGGGGAGATTCACCAGTGGGCCTCACCTGTAAGTGAGGGTCAC
ATCTGTAATTCTCTGATCTCGTGATGCAGAAGTAGGCCACATCTTCCATTTTCATCCTT
GGATTCCTGTGGAATTTACAGATGCACAGATAGAAGTCATTTAGTCTTAGATAGATACC
TTCATCTGCTTTGTCAATTGATGATGAATAAGACTGAGTTGAATGTATTTAGAATGTCTT
GGCTATAAATTCCTCCATATAGCTTAACCCACTGTTTCCTGCAGTATGCACCCCTTTAC
CAAGAGAGAGAAAGAGAGAAAGAATTTCATGTTTCTGTGGGTTTTAGAAGGCTATAG
GAAGGGATTTTTGTTTGCTCATTTTCAGAACTTATTAATAGACAGTTATTGAATACCTAC
CTTGGGCACAGAAATAATCACATTCTCTCCTGAGAATTTTCAACCCACAGCCAAGTAC
AGGTGTGGAAATTTGATGATAGAATTAATACCAATGGAAAAAGGGGCCCACAGAACTG
AAAAAGTGGCCACTGGTGATGACAGTGACCTGGGAGGGAGCGAGGCAACCTAGAG
AGACAATGTGGGGAATCATCACGTTCCATTACAGCGCCCTTCTCTTACTCTCTTGGAG
CTTCTCAAGCCACAGGTGTCAGTCATATTGGTTTTAGAGATTATTAGTAACTACCCAAA
CCCAACAATTTTGTTTTCCTGAAACTAGAAATG

* AER was highlighted

6.LINC00624 S3-AER

GAAAATCCAAGAAATTTACATGCACTGAATTTTATTTCCTTTATTTGCCTATTTATTCACA
CCAAGAATTCAGGGTCCATGTTGCTGTAGTGGAAATTGGTTATTTCTGTTTTAGTCTT
GAATTGTCTAATTTTGTTCAACTTGCCTGGTACGGAGGGGAGATTCACCAGTGGGCC
TCACCTGTAAGTGAGGGTCACATCTGTAATTCTCTGATCTCGTGATGCAGAAGTAGG
CCACATCTTCCATTTTCATCCTTGGATTCCTGTGGAATTTACAGATGCACAGATAGAAG
TCATTTAGTCTTAGATAGATACCTTCATCTGCTTTGTCAATTGATGATGAATAAGACTGA

GTTGAATGTATTTAGAATGTCTTGGCTATAAATTCCTCCATATAGCTTAACCCACTGTTT
CCTGCAGTATGCACCCCTTTACCAAGAGAGAGAAAGAGAGAAAGAATTTCATGTTTCT
GTGGGTTTTAGAAGGCTATAGGAAGGGATTTTTGTTTGCTCATTTTCAGAACTTATTAA
TAGACAGTTATTGAATACCTACCTTGGGCACAGAAATAATCACATTCTCTCCTGAGAAT
TTTCAACCCACAGCCAAGTACAGGTGTGGAAATTTGATGATAGAATTAATACCAATGG
AAAAAGGGGCCCACAGAACTGAAAAAGTGGCCACTGGTGATGACAGTGACCTGGGA
GGGAGCGAGGC

7.LINC00624 A-to-C

AGCTGCTGCAACCCGCTGCCCTCTGGTGTCCTGCTGTGGGAGCTTTGTTCTTTCAC
TCTCGTAATAAGTCTTGCTGCTGCTCACTCTTTGGGTCCGCACTGTCTCTGTGAGCT
GTAACACTCACCGCGAGGTTCTGTGCCTTCGTTCTTTAAGTCAGGGAGACCACGAAC
CCACCGGGAGGAACAAACAACTGTGATGCGCCATCTTTAAGAGCTGTAACATTCACC
GCCGGGGTCTGCGGCTTCATTCCTGGAGTGAGTGAGACCACGAACCCACCAGAAG
GAAGAAACTCTGGACCCATCTGAACAGCTGAAGGAACAAACTCCGGACACACCATC
TTTAAGAACTGTAACACTCACCGGGAGTCTCCGTGGCTTCATTCTTGAAGACAGCGA
GACCAAGAACCCACCAGAAGGAATGAATTCCGCACACAGCAACAGCACAAAGTTAAA
CCAGGAAGTCCCTCTGCCTTGCTAGGGATCCAGGTTTGCCTTCCTGTTGAGGTATCC
CATTTCATTACAGTTGACCTAAGTTTGAACAAACACTGCCACCTGATGCATGAAAGCT
CTACTGTGACCTACGTTAAAAGGAGCTGACACTCCCTCAGGCTACCTTAGTCAGTGG
GGGCTTACTGCAGCATACCTGTGGCGATGAGAGAGAGAGGCACATCACAGGAGCAT
CTGGCACCAGTGGCATCCTGAATTTAAGATGAAACAATAGAGAAAGAACCAAGAAGT
TACATACATTCATCAGAATTGCTGGAGAGTCCTGACCTCTGGCCATCGATCAAAGGGA
AGCGTTCACTACTGAAGGTTTGTCTTCACTGTACTGGGTATTCAACTTCCTTGAAATT
AAAAGGAAGAAGGATAAAAAGTGGTATGCTGAATGGATTAAAGGTAATATTTTGATTAT
ATCAATAGTTTTCAAACTTTTATAACTCATGAGCTGTTTGGGAATATTTGAGCATATGGT
CAATCCACATCTGAATTATCCTGCCCACAAAAATGTCAAGGAAATACTTCTACTGCCC
CTTCTGAAGCCATCTTAATTCCAGGAGTTGAATCAATTTCAAAGTCATTGATAACTGCA
TCAGCCAAAATTTGTCCAAATGTTTTGAAATGCATTTCTATTTCCTGTCACACCTACCT
CTTTGGCTAATGCATTCATTTTATGAGTTTCAAAAATTACCATCTCCCTGTCCCAGGTC
TTTAAAGTTGTTGAATAAGCAAATCTCTGTTCACTTTATTTGTACTATTTATGGTTATATA
GATTTAATTACTTCTAATTAGATTTCCATATTGGAAGTACAAATCTAACCTTAAACAAAAA
ATTCTTTTTATAATTCTCAATATCTCCAATTATTTTGAGCTTGTGCTCTCTGGATCTTTTC
AAGTTATGGCAAACTTGGTTTTGAGGCATAGCAGCAAGAACTACATAAATCTTTTCAAA
CAGAGATATACCAGTATAAAGCTTGCTTTCCAGTATAGTCCTTAATGATTTTCTTCATTT
TCTAGGTCTTTTTGCCTGATGCAGAATATTGGTACATATGCTGGGGTCAACATTTAATG
ACTCTGGGTCTTTTTCTTGAGCAGAATCTAAGGGATAGTCTTTCATTTTATAGATGTGT
TTTAGATTACTCATAAATTCATTACTTTTTCCTCACACACATTATAACATCTCTTAAGGCT
CTGCCCATTGACACGAATCTCAGGATTATTCTATAATGTCTCTCTTCTCTGGGGTGTCT
TCTTTCTGGGGAGATTTGTATATCTTGGAGTCTGAGACTTCACTATGTACTCCTTCCTT
ATCATCATTTATAAACCTATTCAACAGACTCTGCCCCAGAATGGATTCTTGAGCAATCT
TGAATAATTACACGAGTATCCAAAGATACTGATTTTAGGAGAACACGGTTGTTGGGTA
CAGGTAGTTAATTATTCCTCCCCCTGAATCTGTCCCATACCTCTGTCTTGCGCCGCTC
TACGAGAGTAACAGAAGAGCAACAATGGAATGTGACCCTTGCCTGCACTGTCTTTCT

AGGTTGAAAATCCAAGAAATTTACATGCACTGAATTTTATTTCCTTTATTTGCCTATTTA
TTCACACCAAGAATTCAGGGTCCATGTTGCTGTAGTGGAAATTGGTTATTTCTGTTTTA
GTCTTGAATTGTCTAATTTTGTTCAACTTGCCTGGTACGGAGGGGAGATTCACCAGTG
GGCCTCACCTGTAAGTGAGGGTCACATCTGTAATTCTCTGATCTCGTGATGCAGAAG
TAGGCCACATCTTCCATTTTCATCCTTGGATTCCTGTGGAATTTACAGATGCACAGATA
GAAGTCATTTAGTCTTAGATAGATACCTTCATCTGCTTTGTCAATTGATGATGAATAAGA
CTGAGTTGAATGTATTTAGAATGTCTTGGCTATAAATTCCTCCATATAGCTTAACCCACT
GTTTCCTGCAGTATGCACCCCTTTACCAAGAGAGAGAAAGAGAGAAAGAATTTCATG
TTTCTGTGGGTTTTAGAAGGCTATAGGAAGGGATTTTTGTTTGCTCATTTTCAGAACTT
ATTAATAGACAGTTATTGAATACCTACCTTGGGCACAGAAATAATCACATTCTCTCCTG
AGAATTTTCAACCCACAGCCAAGTACAGGTGTGGAAATTTGATGATAGAATTAATACC
AATGGAAAAAGGGGCCCACAGAACTGAAAAAGTGGCCACTGGTGATGACAGTGACC
TGGGAGGGAGCGAGGCAACCTCGCGAGACAATGTGGGGAATCATCACGTTCCATTA
CAGCGCCCTTCTCTTCCTCTCTTGGAGCTTCTCCCGCCACCGGTGTCCGTCATATTG
GTTTTAGAGATTATTAGTAACTACCCAAACCCAACAATTTTGTTTTCCTGAAACTAGAA
ATGTCCTGTTTCCAACTTTATATTTTCATCAACTTCTTTTTCTATGATGTGTGAGAAACT
AGAATATTCAGTGTGCTTTCTTGAATACCAGCCTTGTTTCAACTCTTTAATGAGTGGAC
TATTCTCTGAAGCTGGCCCTCAGTCTTACTCTGGGTTCATCAACCAAGGTCAAGATCT
GTCCACATGCACGTAACAGGAGCACTTTTCCGAGAATTGTAAAGGAGCCACGGTGC
AAAGCCTTCTGGACCTGGGTCTCATGTGAAAACTCAGCAATGAGCCTCCTGGCCTG
AGATGAGCCTGCGGAGCACCTTGTTACAGCACGCATATGATGTATATAAAAAATGAAC
ACATGTATTCCAATTACACTGATTTGATCTTTACAAACTATATGGATGTATTAAATTGTCA
CATGTACCCTCAAAATATGTACATCTATTATGTATCAATAAAATAATTAACA

7.LINC00624 A-to-G

AGCTGCTGCAACCCGCTGCCCTCTGGTGTCCTGCTGTGGGAGCTTTGTTCTTTCAC
TCTCGTAATAAGTCTTGCTGCTGCTCACTCTTTGGGTCCGCACTGTCTCTGTGAGCT
GTAACACTCACCGCGAGGTTCTGTGCCTTCGTTCTTTAAGTCAGGGAGACCACGAAC
CCACCGGGAGGAACAAACAACTGTGATGCGCCATCTTTAAGAGCTGTAACATTCACC
GCCGGGGTCTGCGGCTTCATTCCTGGAGTGAGTGAGACCACGAACCCACCAGAAG
GAAGAAACTCTGGACCCATCTGAACAGCTGAAGGAACAAACTCCGGACACACCATC
TTTAAGAACTGTAACACTCACCGGGAGTCTCCGTGGCTTCATTCTTGAAGACAGCGA
GACCAAGAACCCACCAGAAGGAATGAATTCCGCACACAGCAACAGCACAAAGTTAAA
CCAGGAAGTCCCTCTGCCTTGCTAGGGATCCAGGTTTGCCTTCCTGTTGAGGTATCC
CATTTCATTACAGTTGACCTAAGTTTGAACAAACACTGCCACCTGATGCATGAAAGCT
CTACTGTGACCTACGTTAAAAGGAGCTGACACTCCCTCAGGCTACCTTAGTCAGTGG
GGGCTTACTGCAGCATACCTGTGGCGATGAGAGAGAGAGGCACATCACAGGAGCAT
CTGGCACCAGTGGCATCCTGAATTTAAGATGAAACAATAGAGAAAGAACCAAGAAGT
TACATACATTCATCAGAATTGCTGGAGAGTCCTGACCTCTGGCCATCGATCAAAGGGA
AGCGTTCACTACTGAAGGTTTGTCTTCACTGTACTGGGTATTCAACTTCCTTGAAATT
AAAAGGAAGAAGGATAAAAAGTGGTATGCTGAATGGATTAAAGGTAATATTTTGATTAT
ATCAATAGTTTTCAAACTTTTATAACTCATGAGCTGTTTGGGAATATTTGAGCATATGGT
CAATCCACATCTGAATTATCCTGCCCACAAAAATGTCAAGGAAATACTTCTACTGCCC
CTTCTGAAGCCATCTTAATTCCAGGAGTTGAATCAATTTCAAAGTCATTGATAACTGCA

TCAGCCAAAATTTGTCCAAATGTTTTGAAATGCATTTCTATTTCCTGTCACACCTACCT
CTTTGGCTAATGCATTCATTTTATGAGTTTCAAAAATTACCATCTCCCTGTCCCAGGTC
TTTAAAGTTGTTGAATAAGCAAATCTCTGTTCACTTTATTTGTACTATTTATGGTTATATA
GATTTAATTACTTCTAATTAGATTTCCATATTGGAAGTACAAATCTAACCTTAAACAAAAA
ATTCTTTTTATAATTCTCAATATCTCCAATTATTTTGAGCTTGTGCTCTCTGGATCTTTTC
AAGTTATGGCAAACTTGGTTTTGAGGCATAGCAGCAAGAACTACATAAATCTTTTCAAA
CAGAGATATACCAGTATAAAGCTTGCTTTCCAGTATAGTCCTTAATGATTTTCTTCATTT
TCTAGGTCTTTTTGCCTGATGCAGAATATTGGTACATATGCTGGGGTCAACATTTAATG
ACTCTGGGTCTTTTTCTTGAGCAGAATCTAAGGGATAGTCTTTCATTTTATAGATGTGT
TTTAGATTACTCATAAATTCATTACTTTTTCCTCACACACATTATAACATCTCTTAAGGCT
CTGCCCATTGACACGAATCTCAGGATTATTCTATAATGTCTCTCTTCTCTGGGGTGTCT
TCTTTCTGGGGAGATTTGTATATCTTGGAGTCTGAGACTTCACTATGTACTCCTTCCTT
ATCATCATTTATAAACCTATTCAACAGACTCTGCCCCAGAATGGATTCTTGAGCAATCT
TGAATAATTACACGAGTATCCAAAGATACTGATTTTAGGAGAACAGGGTTGTTGGGTA
CAGGTAGTTAATTATTCCTGGGGCTGAATGTGTCCGATACCTGTGTCTTGGGGGGCT
CTAGGAGAGTAACAGAAGAGCAACAATGGAATGTGACGGTTGCCTGCACTGTCTTTC
TAGGTTGAAAATCCAAGAAATTTACATGCACTGAATTTTATTTCCTTTATTTGCCTATTT
ATTCACACCAAGAATTCAGGGTCCATGTTGCTGTAGTGGAAATTGGTTATTTCTGTTTT
AGTCTTGAATTGTCTAATTTTGTTCAACTTGCCTGGTACGGAGGGGAGATTCACCAGT
GGGCCTCACCTGTAAGTGAGGGTCACATCTGTAATTCTCTGATCTCGTGATGCAGAA
GTAGGCCACATCTTCCATTTTCATCCTTGGATTCCTGTGGAATTTACAGATGCACAGA
TAGAAGTCATTTAGTCTTAGATAGATACCTTCATCTGCTTTGTCAATTGATGATGAATAA
GACTGAGTTGAATGTATTTAGAATGTCTTGGCTATAAATTCCTCCATATAGCTTAACCCA
CTGTTTCCTGCAGTATGCACCCCTTTACCAAGAGAGAGAAAGAGAGAAAGAATTTCAT
GTTTCTGTGGGTTTTAGAAGGCTATAGGAAGGGATTTTTGTTTGCTCATTTTCAGAAC
TTATTAATAGACAGTTATTGAATACCTACCTTGGGCACAGAAATAATCACATTCTCTCCT
GAGAATTTTCAACCCACAGCCAAGTACAGGTGTGGAAATTTGATGATAGAATTAATAC
CAATGGAAAAAGGGGCCCACAGAACTGAAAAAGTGGCCACTGGTGATGACAGTGAC
CTGGGAGGGAGCGAGGCAACCTGGGGAGACAATGTGGGGAATCATCACGTTCCATT
ACAGCGCCCTTCTCTTGCTCTCTTGGAGCTTCTCGGGCCACGGGTGTCGGTCATATT
GGTTTTAGAGATTATTAGTAACTACCCAAACCCAACAATTTTGTTTTCCTGAAACTAGA
AATGTCCTGTTTCCAACTTTATATTTTCATCAACTTCTTTTTCTATGATGTGTGAGAAAC
TAGAATATTCAGTGTGCTTTCTTGAATACCAGCCTTGTTTCAACTCTTTAATGAGTGGA
CTATTCTCTGAAGCTGGCCCTCAGTCTTACTCTGGGTTCATCAACCAAGGTCAAGATC
TGTCCACATGCACGTAACAGGAGCACTTTTCCGAGAATTGTAAAGGAGCCACGGTGC
AAAGCCTTCTGGACCTGGGTCTCATGTGAAAACTCAGCAATGAGCCTCCTGGCCTG
AGATGAGCCTGCGGAGCACCTTGTTACAGCACGCATATGATGTATATAAAAAATGAAC
ACATGTATTCCAATTACACTGATTTGATCTTTACAAACTATATGGATGTATTAAATTGTCA
CATGTACCCTCAAAATATGTACATCTATTATGTATCAATAAAATAATTAACA

Supplementary Methods

Patients and tumor samples

Core needle biopsy samples were collected before treatment from 20 patients diagnosed with HER2+ invasive breast carcinoma, receiving paclitaxel + carboplatin + trastuzumab neoadjuvant chemotherapy followed by surgical resection at Fudan University Shanghai Cancer Center (FUSCC). The 100 tumor tissue cohort is built from another HER2+ breast cancer project in our lab, and used for verification. Patients received chemotherapy + trastuzumab with or without pyrotinib. Samples were collected before treatment. RNA-seq data of LINC00624 were extracted from this cohort. The prognosis cohort samples were collected from 319 patients with early breast cancer receiving surgical resection and adjuvant treatment from 2010 to 2011. The clinical data were collected, and the patients were followed as shown in the Figures. Tumor samples were collected and stored in the liquid nitrogen. The survival analysis was performed by using Kaplan-Meier methods. Patients were analyzed (*All types*) or divided into subgroups according to ER, PR and HER2 expression. *HER2* were defined as IHC HER2 3+ or HER2 2+ with HER2 FISH amplification with ER and PR negative. TNBC were defined as IHC ER, PR and HER2 negative. *Luminal* were defined as IHC ER+ or PR+. This study was approved by the ethics committee of FUSCC and informed consent for the use of sample for research purposes was obtained by participants. TCGA data were extracted and analyzed by GEPIA[1].

Expression plasmids, reagents

LINC00624 full length cDNA were synthesized (Genewiz) according to 5' and 3' RACE results and cloned into pCDH-CMV-Puro vector. Isoforms with A-to-C or A-to-G mutations were synthesized according to the editing results from Sanger sequencing of LINC00624 in ADAR1 overexpressed SK-BR-3 cells. Isoform3 and S1, S2, S3 segments were cloned from the full length LINC00624. The full sequences of isoforms were listed in Supplementary file 1. The ORF of human ADAR1-p110, ADAR1-p150 were cloned from SK-BR-3 cDNA and inserted into pCDH-CMV-Puro with N-terminus 3×FLAG tag. ADAR1-p110 was used for overexpression experiments unless noted otherwise. Serial mutations of ADAR1-p110 were subcloned and constructed with N-terminus 3×FLAG tag. The ORF of mouse ADAR1-p110 was cloned from NF639 cell and inserted into pCDH-CMV-Puro with N-terminus 3×FLAG tag. The plasmids used in this study are available upon request.

The pharmacological reagents lapatinib (S2111, Selleck), trastuzumab (A2007, Selleck), MG132 (C2211, Sigma), Cycloheximide (C7698, Sigma), DMSO (D8418, Sigma), poly(I:C)(HMW) (tlrl-pic, InvivoGen), human IFN-α (C006, Novoprotein), human IFN-γ (300-2, Peprotech), murine IFN-α (CK83, Novoprotein), murine IFN-γ (315-05, Peprotech), 8-azaadenosine (HY-115686, MCE) purchased and used according to the manufacturer's instructions.

ASOs for LINC00624 *in vitro* use were synthesized from Ribobio. ASOs with 5'cholesterol modification for *in vivo* use were synthesized from Hippobio, sequences were listed in Supplementary Table 4.

Cell culture, transfections, and infections

HEK293T, SK-BR-3, BT-474, MCF-7, MDA-MB-231, NF639, and B16 cells were obtained from the ATCC. The cell lines were tested for mycoplasma contamination every month. Human cell lines were authenticated by STR determination. BT-474, NF639, and B16 were cultured in RPMI-1640 medium (L210KJ, BasalMedia) supplemented with 10% FBS (10099141, Gibco). SK-BR-3 which were cultured in McCOY's 5A (L630KJ, BasalMedia) + 10% FBS. HEK293T, MCF-7 and MDA-MB-231 cells were cultured in DMEM (L110KJ, BasalMedia) + 10% FBS. All cells were maintained at 37 °C under 5% CO_2. LINC00624 was deleted in BT-474 and SK-BR-3 cells using transient transfection of GFP and mCherry tagged Cas9 sgRNA plasmids (derived from pX459, Addgene) with the lipofectamine 3000 transfection reagent (L3000150, Invitrogen). Two sgRNAs were transfected at the same time targeting the promoter of LINC00624. Transfected cells were sorted by flow cytometry with GFP and mCherry. For monoclonal selection, sorted cells were plated in 96-well plates with an average of 1-3 cells in a well. Clones were expanded and verified by PCR. Human and mouse ADAR1 were deleted with transfection of GFP tagged Cas9 sgRNA plasmids as described above. Clones were expanded and verified.

For poly(I:C) transfection assays, 1×10^6 cells were plated 24h before transfection. 1 μg/ml poly(I:C) (HMW) (tlrl-pic, InvivoGen) were transfected with Lipofectamine 2000 (11668500, Invitrogen). Cells were harvested or used for downstream analysis after 24h. ASOs and siRNAs for in vitro use were synthesized by RiboBio as listed in Supplementary Table 5**.** Cells were plated 24h before transfection. 0.1 nmol siRNA or ASO were transfected with RNAiMAX (13778150, Invitrogen) and harvested 72h after transfection.

For overexpression cell lines, lentivirus was produced by co-transfecting HEK293T

cells with desired plasmids together with psPAX2 and pMD2.G (Addgene). After 72 h, virus was harvested by passing through a 0.45 mm filter. Collected lentivirus was used directly to infect cells with the addition of 8 mg/ml polybrene (H9268, Sigma) or stored in -80℃. Infected cells were selected with puromycin (ant-pr-1, InvivoGen) at 2 μg/ml.

Immunoblot

Cells were lysed and homogenized by RIPA (89901, Thermo) containing Protease Inhibitor cocktail (B14001, Bimake) and phosphatase inhibitor cocktail. and Pierce BCA Protein Assay kit (23225, Thermo) was used for protein quantification. Cell lysates were separated by 10% SDS–PAGE and fractionated proteins were transferred to PVDF membranes (ISEQ00010, Millipore). After blocking with TBS, 0.1% Tween-20 and 5% skim milk, the membranes were probed with antibodies signals were enhanced by secondary antibodies (anti-mouse, 111-035-144, Jackson; anti-rabbit, 111-035-046, Jackson). Chemiluminescent detection (180-5001, Tanon) was used. The monoclonal anti-β-TrCP (4394S; 1:1,000 dilution), anti-ADAR1(81284S; 1:1,000 dilution), anti-STAT1 (9172S; 1:1,000 dilution), anti-pSTAT1(T701) (9167S; 1:1,000 dilution), anti-IRF3 (11904S; 1:1,000 dilution), anti-pIRF3(S396) (29047S; 1:1,000 dilution), anti-TBK1 (3504S; 1:1,000 dilution), anti-pTBK1(S172) (5483S; 1:1,000 dilution), and anti-HA (3724S; 1:1,000 dilution) antibodies were purchased from Cell Signaling Technology. The monoclonal HRP-anti-GAPDH (60004-1-Ig; 1;10,000 dilution) were purchased from Proteintech. The mouse monoclonal anti-ADAR1 (sc-73408; 1:1,000) were purchased from Santa Cruz Biotechnology (used in immunoblot of mouse cell lines).

RNA isolation, RT-PCR and RT-qPCR

Total RNAs from cultured cells were extracted with TRIzol (15596026, Invitrogen) according to the manufacturer's protocol. Clinical samples were stored in RNAlater (AM7024, Invitrogen) and extracted with TRIzol with the facilitation of rotor-stator homogenizer. cDNAs were reverse transcribed with Hiscript III Reverse Transcriptase (R312, Vazyme) with oligo (dT) and random hexamers followed by qRT-PCR analysis and applied for PCR/qPCR analysis. Real time quantitative PCR was performed with ChamQ SYBR qPCR Master Mix (Q311, Vazyme) and QuantStudio 7 (4485701, Applied Biosystems). The relative expression of different sets of genes was quantified to GAPDH or ACTB mRNA. Primer sequences for RT-qPCR and RT-PCR used were listed in

Supplementary Table 4.

Cell proliferation and viability assay

For proliferation assay, cells were seeded in 96-well flat-bottomed plates with each well containing 3000 cells in 200 µl of culture medium and cultured in ambient environment described above. Plates were imaged by using IncuCyte ZOOM System (Essen Bioscience) at 12-hour interval. The growth rate was measured according to confluence change analyzed by IncuCyte software.

For cell viability studies, 3500 of SK-BR-3 or BT-474 cells were plated in each well of 96 well plates and treated with the indicated agents 24 hours later at the concentrations shown. For viability assays assessing the effect of lapatinib and trastuzumab, cells were treated for 120 hours before measuring viability. Cell viability was measured using the Cell Counting Kit 8 (CK04, Dojindo) according to manufacturer's instructions. Plates were read at 450nM absorbance. Technical replicates were performed 3 times for each condition, and biological replicates were performed 2-3 times per experiment.

Cell death assays

SK-BR-3 or BT-474 were plated in 6-well plates at a concentration of 1 million cells per well 24 h before poly(I:C) transfection. Cells were transfected with 1 µg/ml poly(I:C) and incubated for 24h with ambient culture environment. Following trypsinization and washes in PBS + 2% FBS, cells were stained for 30 min on ice using the manufacturer's recommended concentrations of Annexin-V PE and 7-AAD from the PE Annexin V Apoptosis Detection Kit 1(559763, BD Pharmingen). Staining of cell surface markers was then analyzed using an Accuri C6 flow cytometry system. Analysis was carried out using CytoExpert 2.3 software.

RNA-seq and AEI score calculation

For clinical sample analysis, the core needle biopsy specimens were immediately stored into RNAlater according to the manufacturer's instruction. Samples were extracted with RNAeasy mini kit (74106, Qiagen) according to the manufacturer's instruction. The RiboMinus Eukaryote Kit (A1083708, Invitrogen) was used to eliminate rRNAs. Libraries were prepared using NEBNext Ultra Directional RNA Library Prep Kit (E7775, NEB). Transcript expression was analyzed using StringTie (version 1.2.3) and quantified by

FPKM (fragments per kilobase of exon per million fragments mapped).

For AEI score analysis or GSEA analysis, the total RNA samples of cell lines were treated with VAHTS mRNA Capture Beads (Vazyme) to enrich polyA+ RNA before constructing the RNA-seq libraries. RNA-seq libraries were prepared using VAHTS mRNA-seq v3 Library Prep Kit for Illumina (NR611, Vazyme) following the manufacturer's instructions. Sequencing reads from RNA-seq data were aligned using the spliced read aligner HISAT2, which was supplied with the Ensembl human genome assembly (Genome Reference Consortium GRCh38) as the reference genome. Gene annotation and analysis was conducted by metascape (http://metascape.org/). Gene expression levels were calculated by the FPKM. Gene Set Enrichment Analysis (GSEA) was conducted according to the instructions from the Broad Institute using the pre-ranked method. After gene expression was quantified by FPKM, log2 scaled fold change of all expressed genes was calculated. Graphic representations of results were generated using the cluster Profiler package in R (https://www.r-project.org/).

The analysis of Alu Editing Index (AEI) was following the protocol detailed in Roth et al. with default parameters[2].

Rapid Amplification of Cloned cDNA Ends (RACE)

The 3' and 5' RACE was performed using the RLM-RACE kit (AM1700, Invitrogen) following the manufacturer's instruction. RNA was extracted from SK-BR-3 cells. Primers used for 3' and 5' RACE were listed in Supplementary Table 4.

RNA fluorescence in situ hybridization (FISH) and Subcellular Location

LINC00624 RNA FISH was performed using Ribo FISH Kit (C10910, Ribobio) according to the manufacturer's protocol. FISH probes were synthesized by Ribobio (18S, lnc110102; LINC00624, lnc1CM001). Briefly, cells were grown on coverslips in a 24-well culture plate. Cells were fixed with 4% (w/v) paraformaldehyde in 1×PBS for 10 min. Fixed cells were permeabilized for 5 min at 4℃. The coverslips were washed three time with PBS for 5 min at room temperature and then blocked with pre-hybridization Buffer at 37℃ for 30 min. Cy3 labeled-LINC00624 or 18S RNA probes were hybridized at 37℃ overnight. The coverslips were then washed three times with Wash Buffer I, once with Wash Buffer II and once with Wash Buffer III. Cover slides were stained with DAPI and then mounted. Images were acquired with Leica confocal microscope.

For nuclear and cytoplasmic RNA separation, 1×10^6 cells were collected and extracted using PARIS™ kit according to the manufacturer's instructions (AM1921, Invitrogen). RNAs were reverse transcribed and analyzed with quantitative PCR. The proportion of genes expressed in nuclear and cytoplasmic fraction was calculated.

RNA pull-down assay and mass spectrometry

RNA pull-down was performed as previously described[3]. Briefly, LINC00624 isoforms were in vitro transcribed (E2040S, NEB) and labeled with Biotin-16-UTP (11388908910, Roche). SK-BR-3 cells were used for RNA pull-down/MS analysis. HEK293T cells transfected with ADAR1 truncation plasmids were used for binding analysis. Cells lysates were prepared with modified RIPA (50mM Tris-HCl pH 7.4, 150mM NaCl, 1% Igepal 630, 0.5% sodium deoxycholate). For each sample, 3 µg RNA was mixed with 1×10^7 cell extract and incubated at 4℃ for 4h, followed by incubating with Dynabeads C1 (65002, Invitrogen) at 4℃ for 1h. After elution, the samples were detected by immunoblot or proceed to mass spectrometry. For MS, samples were separated by SDS-PAGE and stained with Fast Silver Stain Kit (P0017S, Beyotime) according to the manufacturer's instructions. Specific bands were cut and analyzed by LC-MS/MS (Shanghai Applied Protein Technology, Shanghai, China). Protein identification was retrieved in the human RefSeq protein database (National Center for Biotechnology Information), using Mascot version 2.4.01 (Matrix Science, London, UK).

In vitro RNA editing assay

Editing of a synthetic Glut-B B11 RNA was assayed in vitro with purified ADAR1 proteins. The standard editing reaction mixture contained 0.2 ng of ADAR1 protein, 0.02 M HEPES (pH 7.0), 0.1 M NaCl, 10% glycerol, 5 mM EDTA, 1 mM DTT, and 4 U of RiboLock RNase inhibitor (EO0384, Thermo) in a 20 µl reaction volume. The synthetic LINC00624 or Alu from 3'UTR of PHACTR4 RNA (Alu-PHAC) was added into the mixtures and pre-incubated at 30℃ for 15 minutes. Then, 50 ng of a synthetic Glut-B11 RNA substrate was added and incubated for 5 or 15 minutes. The reaction was terminated by 70℃ 5min. 6 µl of reaction was reverse transcribed with specific primer and HiScript III (Vazyme) at 37℃ 15min, 45℃ 15min, and then 50℃ 15min. PCR and sanger sequencing of Glut-B11, LINC00624, and Alu-PHAC template was performed and quantified with Snapgene.

Recombinant ADAR1 Expression

ADAR1 was codon optimized, synthesized, and then subcloned into target vector for insect cell expression. DH10Bac strain was used for the recombinant bacmid (rbacmid) generation. The positive rbacmid containing ADAR sequence gene was confirmed by PCR. Sf9 cells were grown in Sf-900 II SFM Expression Medium (10902-088, Life Technologies). The cells were maintained in Erlenmeyer Flasks at 27 °C in an orbital shaker. One day before transfection, the cells were seeded at an appropriate density in 6 wells. On the day of transfection, DNA and Transfection Reagent (E2691, Promega) were mixed at an optimal ratio and then added into the plate with cells ready for transfection. Cells were incubated in Sf-900 II SFM for 5-7 days at 27 °C before harvest. The supernatant was collected after centrifugation and designated as P1 viral stock. P2 was amplified for later infection. The expression was analyzed by Western blot. The 0.1 L SF9 cell culture were infected by P2 virus. Cells were incubated in Sf-900II SFM(1X) for 3 days at 27 °C before harvest. The expression was analyzed by Western blot. Cell pellets were harvested and lysed by proper cell lysis buffer. The cell lysate supernatant was incubated with Anti-Flag column to capture the target protein. Higher purity fractions were pooled and followed by 0.22 μm filter sterilization. The purified protein was dialyzed and stored in 50 mM Tris-HCl, 500 mM NaCl, 20% Glycerol, pH 7.5. Proteins were analyzed by SDS-PAGE by using standard protocols for molecular weight and purity measurements. The concentration was determined by Bradford protein assay with BSA as a standard.

RNA EMSA

The AER region was cloned, in vitro transcribed, and labeled with biotin-16-UTP (11388908910, Roche). Recombinant ADAR1 and AER was incubated in a 10μl reaction volume with editing buffer (0.02 M HEPES (pH 7.0), 0.1 M NaCl, 10% glycerol, 5 mM EDTA, 1 mM DTT, and 4 U of RiboLock RNase inhibitor (EO0384, Thermo)) at 30℃ for 15min. Native PAGE was performed for separating components followed by transferring to Nylon membrane (AM10102, Invitrogen). After ultraviolet cross-linking, HRP-conjugated streptavidin was added according to manufacturer's instruction with LightShift® Chemiluminescent RNA EMSA Kit (20158, Thermo).

OT-I cells isolation and co-culture with B16-OVA cells

C57BL/6-Tg(TcraTcrb)1100Mjb/J (OT-I) mice (JAX stock, 003831) were purchased

from the Jackson Laboratory. The spleen was homogenized, and single cells were suspended in 3 ml ACK buffer (0.15M NH_4Cl, 1mM $KHCO_3$, 0.1mM EDTA, pH 7.4) for 1 min. Cells were pelleted and washed with Wash Buffer (PBS+0.5%BSA+2mM EDTA). CD8+ cells were negatively selected with CD8a+ T cell Isolation Kit, mouse (130-104-075, Miltenyi) as manufacturer's instruction. Purified cells were washed, stained with anti-CD3e and anti-CD8a, and analyzed with flow cytometry for verification.

B16-OVA-pCDH and B16-OVA-LINC00624 cells were pre-incubated with 40 μg/mL of anti-H-2Kb-SIINFEKL (130-096-810, Miltenyi) or isotype control (130-106-545, Miltenyi) for 1 h at 37°C. CD8+ T cells were washed with T cell culture media (RPMI 1640+5%FBS+55 μM 2-Mercaptoethanol (21985023, Gibco)). 1.6×10^5 $CD8^+$ T cells were co-cultured with 2×10^4 tumor cells in a final concentration of 10 μg/mL of the anti-H-2Kb-SIINFEKL or isotype control with 2.5 ng/mL IL-7 (217-17-2, Peprotech), 50 ng/mL IL-15 (210-15-2, Peprotech), and 2 ng/mL IL-2 (212-12-5, Peprotech) for 72 h at 37°C in the dark. At the experimental endpoint, cytokines in conditioned media were analyzed by ELISA with Mouse Interferon-gamma ELISA kit (BE45201, IBL) according to the manufacturer's instruction. Three technical replicates were used for analysis each time.

Tumor immune cell profiling

Tumors were dissected from the surrounding fascia, weighed, mechanically minced, and treated with collagenase I (1 mg/ml, LS004197, Worthington) and DNase I (1 mg/ml, 11284932001, Roche) for 30 min at 37 °C. Cells were passed through a 70μm filter to remove clumps, washed in D-PBS. Live or dead staining were performed with Fixable Viability Stain 780 (565388, BD Biosciences) at 4℃ for 30 min. After washing twice with Stain Buffer FBS (554656, BD Biosciences), blocked with CD16/CD32 (1 μg per 1 million cells in 100 ul, 553141, BD biosciences), antibodies for surface staining were added. Cells were stained for 30 min at 4℃. Cells were washed twice with Stain Buffer and then resuspended in 1 ml of freshly prepared Fix/Perm solution (554714, BD biosciences) for intracellular staining. After fixation and washes, antibodies for intracellular staining were added. Cells were stained for 30 min at 4℃. After washes, analysis was performed using an Accuri C6 flow cytometry system. CytoExpert 2.3 software was used for data analysis. Gating strategy was indicated in Supplementary Fig 8. Antibodies used were listed as below.

Antigen presentation analysis

1×10^6 B16-OVA pCDH or LINC00624 cells were seeded per well in 6-well plate 24 h before stimulation. Murine IFN-α (5 ng/ml) or IFN-γ (10 ng/ml) were added to the culture media. Following trypsinization and washes in PBS + 2% FBS, cells were stained for 30 min on ice with anti-SIINFEKL-$H2K^b$ (1:100, 141605, Biolegend). For *in vivo* analysis, digested tumor cells were stained with Live/Dead first as described above. Then cells were stained with anti-SIINFEKL-$H2K^b$ for 30 min on ice. The analysis was using an Accuri C6 flow cytometry system and CytoExpert 2.3 software.

Immunohistochemistry

Tissue or tumors were fixed in 4% paraformaldehyde overnight. Dehydration and embedding in paraffin were performed following routine methods. These paraffin blocks were cut into 5 mm slides and adhered on the slides glass. Paraffin sections were deparaffinized in xylene and then rehydrated in 100%, 95%, 75% alcohol successively. Antigen was retrieved by critic acid buffer (pH 6.0) in the 100℃ water bath for 15 min. Endogenous peroxidase was inactivated by incubation in 3% H_2O_2 for 15 min. Following a preincubation with 10% normal goat serum to block nonspecific sites for 30 min, the sections were incubated with primary antibodies in a humidified chamber at 4℃ overnight. After the sections were washed with PBS three times, HRP-conjugated secondary antibodies were applied. Staining was performed with DAB or AEC system as indicated. anti-CD8α (1:400, 98941S, CST), anti-ADAR1 (1:400, 81284S, CST), anti-mouse secondary antibody (1:1000, 111-035-144, Jackson), anti-rabbit secondary antibody (1:1000, 111-035-046, Jackson).

Animal treatment

The designs of animal studies and procedures were approved by the Fudan University Shanghai Cancer Center (FUSCC) IACUC committees. Ethical compliance with IACUC protocols and institute standards was maintained. All mice were maintained under pathogen-free conditions. The animal room has a controlled temperature (18-23°C), humidity (40–60%) and a 12 h-12 h light-dark cycle. In each experiment, animals were randomly assigned into each group. No blind was used in this study.

For B16-OVA xenograft model, six-week-old wild-type female C57BL/6J mice were used. 1×10^5 B16-OVA-pCDH or B16-OVA-LINC00624 were subcutaneously injected on

the flank. For ADAR1 KO B16 tumors, 5×10^5 cells were injected. For BT-474 xenograft model, 17b-estradiol pellet 0.72mg (SE-121, IRA) was implanted subcutaneously into 6-week-old nude mice one week before inoculation. 2.5×10^6 BT-474 pCDH or LINC00624 cells were resuspended in D-PBS solution (Gibco), mixed 1:1 by volume with BME (3632-010-02, Cultrex) and subcutaneously injected into the fourth mammary fat pat. 100μg anti-HER2/neu (BE0277, BioXcell) or isotype control (BE0085, BioXcell) was intraperitoneally injected as indicated. For ASO treatment assay, 17b-estradiol pellet 0.72mg (SE-121, IRA) was implanted subcutaneously into 6-week-old nude mice one week before inoculation. 2.5×10^6 BT-474 pCDH or LINC00624 cells were resuspended in D-PBS solution (Gibco), mixed 1:1 by volume with BME (3632-010-02, Cultrex) and subcutaneously injected into the fourth mammary fat pat. ASO2 and ASO3 were mixed 1:1. 10nmol ASO 2 & 3 mixture (5 nmol each) or ASO control were intravenously injected each time for each mouse as indicated. For PD-1 treatment assay, six-week-old wild-type female C57BL/6J mice were obtained from Jackson laboratories. B16-OVA cells were transfected with poly(I:C) at 1 μg/ml for 4 hr and irradiated by a UVC500 UV crosslinker at 120 mJ/cm^2 followed by 24 h incubation. For anti-tumor effects, mice were injected intraperitoneally (I.P.) with UV irradiated B16 OVA cells (1 x 10^6 cells / mouse) 7 days before inoculation. 1×10^5 B16-OVA-pCDH or B16-OVA-LINC00624 were subcutaneously injected on the flank. At 0 and 6 days, mice were I.P. with UV irradiated B16 OVA cells again. Antibodies were administered subcutaneously at day 5, 8, and 12 at 100 μg/mouse using isotype control IgG (BE0089, BioXcell) or anti PD-1 (BE0146, BioXcell).

The tumor volume was measured using calipers and calculated with the formula Volume=(length×width×width)/2. Animals were randomized before treatment and no blinding was performed.

Statistics and Reproducibility

Statistical analyses were performed using SPSS v.23.0 (SPSS) or Prism GraphPad 9.0. For most of the experiments, independent sample t-tests were used to calculate the *P* values. Survival curves were plotted using the Kaplan–Meier method and compared using log-rank tests. All statistical analyses were performed using two-tailed *P* values. Statistical details and methods used are indicated in the Figure legends, text or methods.

1. Tang Z, Li C, Kang B, *et al*. GEPIA: a web server for cancer and normal gene expression profiling and interactive analyses. *Nucleic Acids Res* 45, W98-W102 (2017).
2. Roth SH, Levanon EY, Eisenberg E. Genome-wide quantification of ADAR adenosine-to-inosine RNA editing activity. *Nat Methods* 16, 1131-1138 (2019).
3. Xiu B, Chi Y, Liu L, *et al*. LINC02273 drives breast cancer metastasis by epigenetically increasing AGR2 transcription. *Mol Cancer* 18, 187 (2019).